

# POLITECNICO DI TORINO

**Corso di laurea magistrale  
in Ingegneria Energetica e Nucleare**

Master Degree Thesis



## **Study on the use of a parabolic dish collector to drive a small-scale organic Rankine cycle**

**Relatore**  
Prof. Davide Papurello

**Candidato**  
Marco Coppola

Academic year 2023-2024

# ABSTRACT

This thesis work has analysed the behaviour of an Organic Rankine Cycle powered by a Parabolic dish collector.

In the first three chapters, a basic overview of the solar collector technology, the Organic Rankine Cycle and the storage systems are given.

Then, in Chapter 4, the definition of the base system and its components has been done. As a working fluid, it has been chosen the R123, which is a refrigerant that is widely used also in ORC applications, and as heat transfer fluid it has been chosen the Dowtherm. All of the working conditions of the components have been properly calibrated according to the thermo-chemical characteristics of the R123.

In chapter 5 it has been conducted a thermodynamic and economic analysis of the plant. From the thermodynamic analysis, it has emerged that the cycle operates with a relatively high value of electrical production efficiency (if compared to the average values for the ORC), that arrived up to 12%, and at a good value of efficiency of combined production of heat and power, that arrived up to 80 %. On the other hand, from the economic analysis, it has emerged that the cost of solar collectors represented the bottleneck of this type of technology because it constitutes more than 50 % of the total CAPEX. Moreover, the OPEX constituted a minimal part if compared to the CAPEX. The revenues are mainly made by selling the thermal energy generated in the condenser, the NPV at the end of the life of the plant is positive, but the return on investment is relatively low (around 18%). The payback time happens after more than 20 years and the levelized costs are not competitive if compared to other technologies, especially for the one of the electricity. Economic incentives are necessary for the success of this technology

In Chapter 6, several possible improvements have been analysed, including the use of a different working fluid, the implementation of superheating and the implementation of the heat recuperator within the cycle. The best working fluid analysed is N-pentane, which is an isotropic form of pentane. The superheating, if implemented together with an optimisation of the heat exchange inside the evaporator (in terms of reduction of the logarithmic mean temperature difference), can give contrasting results from a thermodynamic point of view, while it always gives positive results from an economic point of view, due to the increased generation of both electrical and thermal power. In conclusion, the installation of a recuperator increases the thermodynamic performances, but gives contrasting results from an economic point of view, because the effect of the reduction of the CAPEX (related to the reduction of the thermal power input inside the evaporator linked to the presence of the recuperator) is offset by the reduced thermal power output of the condenser.

In any case, the best performance was obtained by an ORC with N-pentane as working fluid, with superheating up to 250 °C and regeneration.

## INDEX

Index of figures .....	5
Index of tables .....	9
Introduction.....	12
<b>Chapter 1: An Overview on the CSP technology.....</b>	<b>14</b>
Chapter 1.1: Classification of the main CSP technologies .....	15
1.1.1: Parabolic Trough Technology .....	17
1.1.2: Linear Fresnel Technology.....	21
1.1.3: Solar Tower Technology .....	24
1.1.4: Parabolic Dish Technology .....	28
Chapter 1.2: Other applications of CSP .....	30
1.2.1: Solar Cooling.....	30
1.2.2: Desalination.....	33
1.2.3: Usage of the waste heat for heating purposes .....	35
1.2.4: Hydrogen Production .....	36
<b>Chapter 2: Power production – Organic Rankine Cycle (ORC) .....</b>	<b>38</b>
Chapter 2.1: Basic overview of the Rankine Cycle.....	38
Chapter 2.2: Organic Rankine Cycle (ORC) .....	42
Chapter 2.3: Types of working fluids utilized in ORC powerplants .....	43
2.3.1: Type of ORC fluid basing on the slope of the saturated fluid on the T-s diagram .....	44
2.3.2: Thermodynamic properties requirements.....	46
2.3.3: Chemical properties requirements .....	47
2.3.4: Transport properties requirements .....	48
Chapter 2.4: Types of expanders utilized in ORC powerplants .....	48
2.4.1: Turbo-expanders .....	49
2.4.2: Volumetric Machines .....	52
Chapter 2.5: Efficiency improvement techniques for an ORC.....	57
2.5.1: Superheated ORC .....	57
2.5.2: Recuperated ORC .....	57
2.5.3: Reheated ORC .....	58
2.5.4: Regenerated ORC .....	59
<b>Chapter 3: Energy Storage Systems .....</b>	<b>61</b>
Chapter 3.1: Sensible TES.....	62
Chapter 3.2: Latent TES .....	63
3.2.1: Organic PCM .....	64
3.2.2: Inorganic PCMs.....	65

3.2.3: Eutectic mixtures .....	65
3.2.4: Choice of the optimal PCM for latent TES .....	66
Chapter 3.3: Reversible Thermochemical TES .....	66
<b>Chapter 4: Modelling of an ORC on Aspen Plus .....</b>	<b>70</b>
Chapter 4.1: Case study introduction .....	70
4.1.1: Details on the solar collector .....	70
4.1.2: Temperature values .....	71
Chapter 4.2: Choice of the working fluid.....	72
Chapter 4.3: Definition of the base components of the system.....	73
4.3.1: Pump .....	73
4.3.2: Evaporator .....	74
4.3.3: Turbine .....	74
4.3.4: Condenser .....	74
<b>Chapter 5: Results obtained .....</b>	<b>75</b>
Chapter 5.1: Thermodynamic analysis .....	75
Chapter 5.2: Economic analysis .....	77
5.2.1: Cost of the plant .....	78
5.2.2: Operating expenditures of the plant .....	83
5.2.3: Revenues .....	83
5.2.4: Economic indexes .....	84
<b>Chapter 6: Improvements .....</b>	<b>87</b>
Chapter 6.1: Usage of different working fluids .....	87
6.1.1: Operational characteristics of the ORC implemented with the two fluids chosen.....	88
6.1.2: Comparison of the results.....	89
Chapter 6.2: Implementation of the superheating strategy .....	95
6.2.1: Implementation of the superheating in the cycle .....	95
6.2.2: Comparison of the results.....	96
Chapter 6.3: Implementation of the heat recuperation strategy .....	114
6.3.1: Implementation of the recuperator .....	115
6.3.2: Comparison of the results.....	115
<b>Chapter 7: Conclusions .....</b>	<b>122</b>
<b>Bibliography .....</b>	<b>124</b>

# Index of Figures

- Figure 1.1: General working scheme of a CSP plant
- Figure 1.2: General diagram of a CSP plant with integrate Thermal Energy Storage
- Figure 1.3: Main CSP technologies
- Figure 1.4: Geometry of a Parabolic Trough Collector
- Figure 1.5: Image of a real Parabolic Through collector
- Figure 1.6: Image that shows how the focal length is actually the only parameter needed to define the shape of the parabola
- Figure 1.7: Geometrical parameters used to describe a Parabolic Trough collector
- Figure 1.8: Typical layout of a parabolic through solar field
- Figure 1.9: Difference between a standard curved mirror and a Fresnel mirror
- Figure 1.10: Image of a real Linear Fresnel collector
- Figure 1.11: Structure of the receiver of the Linear Fresnel Technology
- Figure 1.12: Another image used to show up the receiving methodology of a Linear Fresnel System
- Figure 1.13: Image of a real Solar Tower power plant
- Figure 1.14: Shape of Heliostats used in the Solar tower power plants
- Figure 1.15: Some of the receivers used for the Solar Tower technology. (a) Direct absorption receiver, (b) External tube receiver, (c) Cavity receiver
- Figure 1.16: Image of the two types of air receiver, (a) Open air receiver, (b) Pressurized air receiver
- Figure 1.17: Schematic image (a) and real image (b) of a parabolic dish collector
- Figure 1.18: Scheme of a single effect Absorption Chiller
- Figure 1.19: Scheme of an Adsorption Chiller
- Figure 1.20: Examples of coupling of Multi-Effect Desalination (MED) and Reverse Osmosis (RO) processes with a CSP power plant
- Figure 2.1: Basic scheme of a Rankine Cycle
- Figure 2.2: Image of an ideal Rankine Cycle
- Figure 2.3: Image of a real Rankine Cycle
- Figure 2.4: Base ORC subcritical cycle, (a) Working scheme, (b) typical T-s diagram
- Figure 2.5: Base ORC cycle realized with a dry fluid
- Figure 2.6: Base ORC cycle realized with an isentropic fluid
- Figure 2.7: Base ORC cycle realized with a wet fluid

- Figure 2.8: Effect of the latent heat on the formation of irreversibility during the heat exchange phase
- Figure 2.9: Image of axial (left) and radial (right) turbines
- Figure 2.10: Representation of a Radial Inflow Turbine
- Figure 2.11: Representation of a Radial Outflow Turbine
- Figure 2.12: Representation of a Scroll Expander
- Figure 2.13: Representation of a Screw Expander
- Figure 2.14: Representation of a Piston Expander
- Figure 2.15: Representation of a Rotary Vane Expander
- Figure 2.16: Schematics of a recuperated ORC: (A) system schematic and (B) T-s diagram
- Figure 2.17: Schematics of a reheated ORC: (A) system schematic and (B) T-s diagram
- Figure 2.18.: Schematics of a regenerative ORC: (A) system schematic and (B) T-s diagram
- Figure 3.1: Sketches of the possible TES technologies
- Figure 3.1: Representation of the scheme of a sensible TES system
- Figure 3.3: Summary of the possible materials used as PCM for latent TES
- Figure 3.4: Graphical representation of a eutectic mixture
- Figure 3.5: Generic scheme of a latent TES system
- Figure 3.6: Heat and Entropy fluxes in TES technologies with direct heat exchange
- Figure 3.7: Heat and Entropy fluxes in TES technologies with indirect heat exchange
- Figure 3.8: Comparison between the energy storage density of the various TES technologies
- Figure 4.1: Solar collector used for the study
- Figure 4.2: medium temperature on the solar collector as function of the time of the day for each season
- Figure 4.3: T-s diagram of R-123 calculated with Aspen Plus
- Figure 4.4: Base scheme of the ORC
- Figure 5.1: Average number of hours for which the temperature of the collector is equal or greater than the one requested by the inlet hot fluid of the evaporator
- Figure 5.2: NPV as function of the year
- Figure 6.1: T-s diagram of R-245fa calculated with Aspen Plus
- Figure 6.2: T-s diagram of N-isopentane calculated with Aspen Plus
- Figure 6.3: Graphic Comparison of the generated electrical and thermal power in the three cases
- Figure 6.4: Graphic Comparison of the electrical efficiency and the efficiency of combined electrical and thermal generation for the three fluids

- Figure 6.5: Graphic comparison of the number of collectors required for the three different fluids
- Figure 6.6: Graphical comparison of the CAPEX values for the three different fluids
- Figure 6.7: Graphical comparison of the OPEX values for the three different fluids
- Figure 6.8: Graphical representation of the trend of the NPV along the years for the three different fluids
- Figure 6.9: Graphic representation of the Evolution of the produced electricity and thermal power as function of the turbine inlet temperature for the R123
- Figure 6.10: Graphic representation of the evolution of the electrical efficiency and of the efficiency of combined generation of heat and power as function of the turbine inlet temperature
- Figure 6.11: Evolution of the CAPEX as function of the turbine inlet temperature for the R123
- Figure 6.12: Evolution of the NPV as function of the turbine inlet temperature for the R123
- Figure 6.13: Graphical representation of the evolution of the levelized costs as function of the turbine inlet temperature for the R123
- Figure 6.14: Graphic representation of the evolution of the produced electricity and thermal power as function of the turbine inlet temperature for the R245fa
- Figure 6.15: Graphic representation of the evolution of the electrical efficiency and of the efficiency of combined generation of heat and power as function of the turbine inlet temperature for the R245fa
- Figure 6.16: Evolution of the CAPEX as function of the turbine inlet temperature for the R245fa
- Figure 6.17: Evolution of the NPV as function of the turbine inlet temperature for the R245fa
- Figure 6.18: Graphic representation of the evolution of the levelized costs as function of the turbine inlet temperature for the R245fa
- Figure 6.19: Graphic representation of the evolution of the produced electricity and thermal power as function of the turbine inlet temperature for the N-pentane
- Figure 6.20: Graphic representation of the evolution of the electrical efficiency and of the efficiency of combined generation of heat and power as function of the turbine inlet temperature for the N-pentane
- Figure 6.21: Evolution of the CAPEX as function of the turbine inlet temperature for the N-isopentane
- Figure 6.22: Evolution of the NPV as function of the turbine inlet temperature for the N-pentane
- Figure 6.23: Graphical representation of the evolution of the levelized costs as function of the turbine inlet temperature for the N-pentane
- Figure 6.24: Graphical representation of the comparison of the produced electricity and thermal power for the three fluids with the superheating

- Figure 6.25: Graphic representation of the comparison of the electrical efficiency and of the efficiency of combined generation of heat and power for the three fluids with the superheating
- Figure 6.26: Graphic representation of the comparison of the required number of collectors for the three fluids with the superheating
- Figure 6.27: Graphic representation of the comparison of the CAPEX required for the three fluids, with and without superheating
- Figure 6.28: Graphic representation of the comparison of the NPV for the three fluids, with and without superheating
- Figure 6.29: Graphic representation of the comparison of the Levelized cost of electricity for the three fluids, with and without superheating
- Figure 6.30: Graphic representation of the comparison of the Levelized cost of heat for the three fluids, with and without superheating
- Figure 6.31: Graphic representation of the comparison of the thermal power produced for the three fluids, with and without recuperator
- Figure 6.32: Graphical representation of the comparison the electrical efficiency for the three fluids, with and without recuperator
- Figure 6.33: Graphic representation of the comparison of the efficiency of combined generation of heat and power, with and without recuperator
- Figure 6.34: Graphic representation of the comparison of the CAPEX for the three fluids, with and without recuperator
- Figure 6.35: Graphic representation of the comparison of the Net Present Value for the three fluids, with and without recuperator
- Figure 6.36: Graphic representation of the Comparison of the levelized cost of electricity for the three fluids, with and without recuperator
- Figure 6.37: Graphic representation of the comparison of the levelized cost of heat for the three fluids, with and without recuperator



# Index of Tables

- Table 1.1: General table of most important CSP plants
- Table 3.1: Volumetric thermal capacity of various materials
- Table 4.1: General operating characteristics of the parabolic disk
- Table 5.1: Main power flux associated to each component
- Table 5.2: Working time of the powerplant for each season
- Table 5.3: Average daily value of irradiance for each season
- Table 5.4: Expense of all the components
- Table 5.5: CAPEX of the plant
- Table 5.6: Total revenues
- Table 5.7: Levelized costs for the different types of energy considered
- Table 6.1: Comparison of the generated electrical and thermal power for the three different fluids
- Table 6.2: Comparison of the electrical efficiency and the efficiency of combined electrical and thermal generation for the three fluids
- Table 6.3: Comparison of the needed number of collectors for the three different fluids
- Table 6.4: Comparison of the CAPEX and OPEX for the three different fluids
- Table 6.5: Comparison of the Net Present Value and of the Payback Time for the three different fluids
- Table 6.6: Comparison of the values of ROI for the three different fluids
- Table 6.7: Comparison of the Levelized costs for the three different fluids
- Table 6.8: Levelized cost of electricity for the different Renewable Technologies
- Table 6.9: Levelized cost of heat for the different Renewable Technologies
- Table 6.10: Evolution of the produced electricity and thermal power as function of the turbine inlet temperature for the R123
- Table 6.11: Evolution of the electrical efficiency and of the efficiency of combined generation of heat and power as function of the turbine inlet temperature for the R123
- Table 6.12: Evolution of the required number of collectors as function of the turbine inlet temperature for the R123
- Table 6.13: Evolution of the Return on the investment as function of the temperature for the R123
- Table 6.14: Evolution of the Levelized costs as function of the turbine inlet temperature for the R123
- Table 6.15: Evolution of the produced electricity and thermal power as function of the turbine inlet temperature for the R245fa

- Table 6.16: Evolution of the electrical efficiency and of the efficiency of combined generation of heat and power as function of the turbine inlet temperature for the R245fa
- Table 6.17: Evolution of the required number of collectors as function of the turbine inlet temperature for the R245fa
- Table 6.18: Evolution of the Return on investment as function of the turbine inlet temperature for the R245fa
- Table 6.19: Evolution of the Levelized costs as function of the turbine inlet temperature for the R245fa
- Table 6.20: Evolution of the produced electricity and thermal power as function of the turbine inlet temperature for the N-pentane
- Table 6.21: Evolution of the electrical efficiency and of the efficiency of combined generation of heat and power as function of the turbine inlet temperature for the N-pentane
- Table 6.22: Evolution of the required number of collectors as function of the turbine inlet temperature for the N-pentane
- Table 6.23: Evolution of the Return on Investment as function of the turbine inlet temperature for the N-pentane
- Table 6.24: Evolution of the Levelized costs as function of the turbine inlet temperature for the N-pentane
- Table 6.25: Comparison of the produced electricity and thermal power for the three fluids in the superheating
- Table 6.26: Comparison of the electrical efficiency and of the efficiency of combined generation of heat and power for the three fluids with the superheating
- Table 6.27: Comparison of the required number of collectors for the three fluids with the superheating
- Table 6.28: Comparison of the CAPEX required for the three fluids, with and without superheating
- Table 6.29: Comparison of the NPV for the three fluids, with and without superheating
- Table 6.30: Comparison of the Payback time for the three fluids, with and without superheating
- Table 6.31: Comparison of the Return on Investment for the three fluids, with and without superheating
- Table 6.32: Comparison of the Levelized cost of electricity for the three fluids, with and without superheating
- Table 6.33: Comparison of the Levelized cost of heat for the three fluids, with and without superheating

- Table 6.34: Comparison of the Levelized cost of energy for the three fluids, with and without superheating
- Table 6.35: Comparison of the thermal power produced for the three fluids, with and without recuperator
- Table 6.36: Comparison of the electrical efficiency for the three fluids, with and without recuperator
- Table 6.37: Comparison of the efficiency of combined generation of heat and power, with and without recuperator
- Table 6.38: Comparison of the number of collectors for the three fluids, with and without recuperator
- Table 6.39: Comparison of the CAPEX for the three fluids, with and without recuperator
- Table 6.40: Comparison of the Net Present Value for the three fluids, with and without recuperator
- Table 6.41: Comparison of the PBT for the three fluids, with and without recuperator
- Table 6.42: Comparison of the Return on Investment for the three fluids, with and without recuperator
- Table 6.43: Comparison of the levelized cost of electricity for the three fluids, with and without recuperator
- Table 6.44: Comparison of the levelized cost of heat for the three fluids, with and without recuperator
- Table 6.45: Comparison of the levelized cost of energy for the three fluids, with and without recuperator

# Introduction

One of the most important challenges nowadays regards how to deal with the increase in energy demand (that is, the natural consequence of the technological progress that modern society is undergoing, which leads to an increase in the demand for goods and services per capita) with one of the biggest sources of concern of the 21st century: the climate change. Today, most of the electricity comes from fossil fuels, such as coal, oil and natural gas. The combustion process of fossil fuels releases significant quantities of greenhouse gases into the atmosphere, with the consequent rising of global temperatures and creation of destructive phenomena such as: drastic changes in the ecosystems of some vegetable and animal species, melting of the global icebergs and increased of the frequency of the extreme weather events. In light of these concerns, it becomes immediate to understand why the theme of the shift from fossil based powerplants to more sustainable solutions (i.e. renewable sources) is widely discussed nowadays.

The fossil fuels need to be replaced with renewable energy systems also for another reason: concerning energy sources such as sun and wind, which are almost evenly distributed all over the countries and easily accessible to everyone, fossil fuels are physically present only in some specific areas of the world. As a consequence, if the energy consumption of a nation primarily relies on energy sources produced by other states and sold by them, any instability in these supplier nations could potentially create significant problems for the buyers. Examples of that are:

-The "First Big Oil Crisis" of 1973, during which Arab members of the OPEC (Organization of the Petroleum Exporting Countries) decided to impose an embargo on the USA, as a consequence of their decision to extend increased support to the Israeli military. The oil price skyrocketed and led to a period of significant inflation, that had direct repercussions on both consumers and industries.

-The conflict in Ukraine, lead to an increase of the price of natural gas. This situation has caused significant issues for Europe, as its energy consumption has been heavily dependent on the import of natural gas.

In this scenario full of risk and challenges, the Renewable Energies are taking place. Renewable Energy Systems (RES) are a kind of technologies used to generate energy without the significant emissions of greenhouse gases that characterize the fossil based powerplants and, as anticipated before, they are almost homogeneously distributed throughout the globe and easily accessible to all countries. Nowadays, the renewable energies are mainly used to generate electricity and, in a minor part, domestic heating. Wind, solar, hydro, wave, ocean, geothermal, and biomass energy can contribute to diminish the greenhouse emissions associated to the energy production and also to create an energy mix that can lead each country to be energetically independent, at least from the electricity production point of view<sup>1</sup>.

---

<sup>1</sup> It has to be kept in mind that the electricity consumption represents only a part (usually around 20%) of the total consumption of energy of a country and that there are some sectors (like the transport sector) in which, even if there are some attempts to reduce the fossil fuel consumption (for example, the spread of electrical cars like Tesla) they are very difficult to decarbonize.

The penetration of the renewable energies until the last year (2022) can be represented by the following figures of merit, extrapolated by a study conducted by Hannah Ritchie, Max Roser and Pablo Rosado [1].

For what regards the Global Scenario, the renewables represent:

- The 11.3% of the global energy consumption
- The 26.3% of the global electricity consumption

For what regards the Italian Scenario, the renewables represent:

- The 16.6% of the Italian energy consumption
- The 36.4% of the Italian electricity consumption

It can be seen that the Italian situation is slightly better than the global situation, even if is still not enough to consider Italy as an energetically independent country.

For what regards the installed power, in can be seen from the Terna<sup>2</sup> site [2], that in Italy the renewable capacity installed is 61,1 GW and it is divided as it follows:

- The hydroelectric turbines account of 23.2 GW (37.9 %)
- The Photovoltaic panels account of 25.1 GW (41.1%)
- The wind turbines account of 11.3 GW (18.5%)
- The geothermal energy accounts of 0.8 GW (1,3%)
- The other minor renewables account for the remaining 0.8 GW (1,3%)

Among these options, hydroelectric capacity has almost saturated, as the cumulative installed power is almost constant since 2007 [3] and wind power is well-suited for large-scale power generation, relying on areas with coastal or hilly terrain and high wind speeds. Biomass and tidal energy are better suited for smaller, individual purposes; however, the widespread use of biomass energy is constrained by the limited availability of organic waste and vegetation. In contrast, solar energy stands out as having the biggest potential to address the ongoing energy crisis while preserving the environment.

The two main types of solar energy technologies are: solar photovoltaic (PV, which represents 41.1% of the cumulative installed capacity in Italy) and concentrated solar power (CSP, which belongs to the group of 1.3% that includes "other minor renewable technologies").

CSP is a renewable technology that, like solar panels, is based on the sun. There are currently a few CSP plants in the world: the largest is the 'Noor Complex Solar Power Plant' in the Sahara (Morocco), with a capacity of 580 MW, but the total installed capacity of CSP is much lower than that of photovoltaics because it is a less competitive technology. For this reason, CSP technology is currently the subject of very in-depth studies aimed at testing and eventually improving its competitiveness.

The aim of this Master's thesis is to study an Organic Rankine Cycle developed using Concentrated Solar Power (CSP) technologies at the Energy Centre of the Politecnico di Torino, using commercial software for system modelling.

---

<sup>2</sup> TERNA is the official Italian Transmission System Operator (TSO)

# CHAPTER 1: An overview on the CSP technology

As just anticipated, the CSP is a renewable energy technology that exploits the sun to generate electricity. While the solar PV system can occupy up to 10m<sup>2</sup> of roof space, for the CSP instead only 3m<sup>2</sup>-4m<sup>2</sup> are required [4]. Moreover, CSP can transform about 90% of solar radiation into heat, while solar photovoltaic has an efficiency that goes from 15% to 20% [4].

In CSP technology, lenses and panels are used to concentrate the sun's direct normal irradiation (DNI) on a Heat Transferred Fluid (HTF) which is then passed through a series of heat exchangers to produce superheated steam, that flows inside a conventional steam turbine to finally produce electricity.

The main components of a CSP plant are then the following [5]:

- The concentrator: a system composed of mirrors that are aligned in such a way to concentrate the light on a receiver. They are therefore curved to reach an appropriate concentration factor depending on the desired maximum temperature that the thermodynamic cycle has to reach. Since the mirrors work with the direct radiation coming from the sun, there is a control system that is implemented to follow the path of the sun during the whole day.

- The solar receiver: it is the surface that receives all the solar radiation reflected by the concentrator and it transfers the heat to the Heat Transfer Fluid

- Heat Transfer Fluid: it is the fluid that receives the heat from the solar receiver and then it may directly drive a heat engine, or it also be used to transfer the heat to another fluid. Another possibility is to use it as an energy storage system to store the heat for moments in which there is no sun (for example, during the night). There are different types ranging from water to the more modern molten salts;

- The thermal machine: this is usually a steam or organic-fluid turbine (for low operating temperatures), but also Stirling engines can be used.

The general working scheme of a CSP power plant and the structure are then represented in the figures 1.1 and 1.2, reported below:

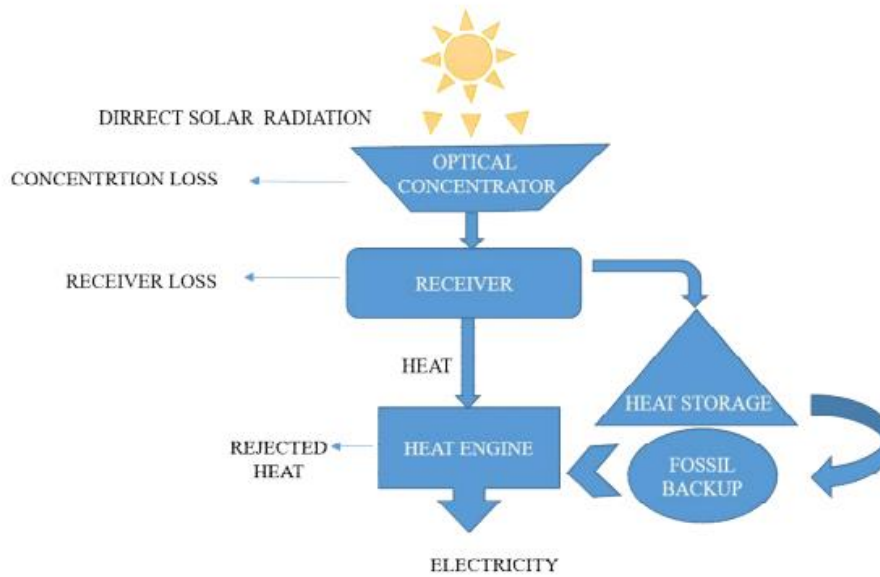


Figure 1.1: General working scheme of a CSP plant [4]

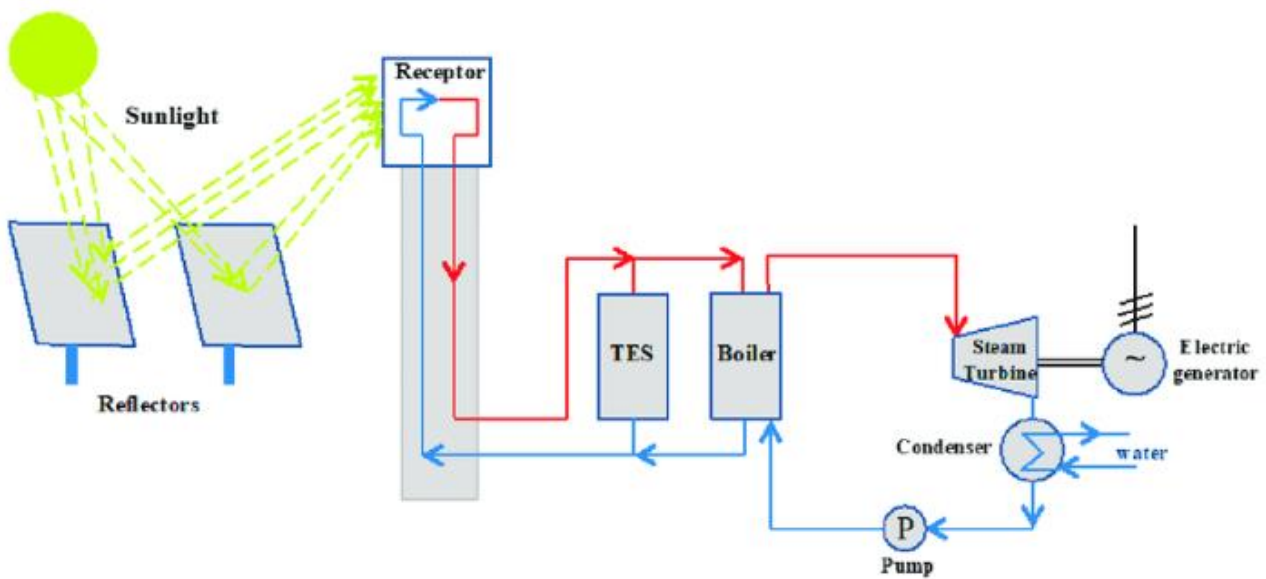


Figure 1.2: General diagram of a CSP plant with integrated Thermal Energy Storage [6]

## Chapter 1.1: Classification of the main CSP technologies

The CSP power plants are mainly divided into two categories, based on the way that the sun's beams are focused to heat the HTF: line-focusing systems and point focusing systems.

-Line focusing systems concentrate the solar radiation onto a linear absorber tube (or series of tubes). The range of working temperatures shifts between 350 °C and 550 °C. The two main line focusing technologies used are the "Parabolic Trough Collectors" (PTC) and the "Linear Fresnel Collectors" (LFC).

-Point focusing systems use all the panels to concentrate the sun radiation onto a central point (called “focal point”). The temperatures reached are much higher (up to  $>1000\text{ }^{\circ}\text{C}$ ). The two main technologies used are the “Solar Tower Concentrator” (STC) and the “Parabolic Dish Concentrator” (PDC).

The figure 1.3 and the table 1.1 reported below can be used to sum up the main CSP technologies:

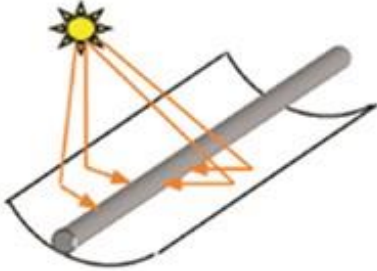
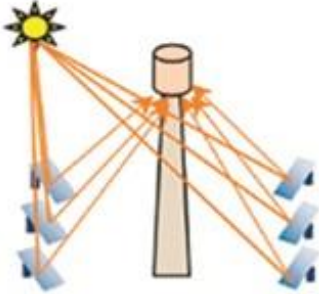
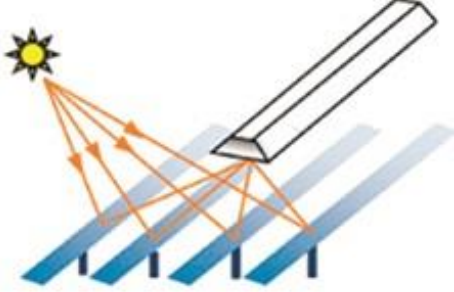

	Line Focus	Point Focus
Dominant technologies	<p><b>Parabolic trough</b></p> 	<p><b>Solar tower</b></p> 
Emerging technologies	<p><b>Linear Fresnel reflector</b></p> 	<p><b>Parabolic dish</b></p> 

Figure 1.3: Main CSP technologies [7]



Technology	Short description	Typical Capacity (MW)	Operating Temperature (°C)	Peak Efficiency (%)	Annual Efficiency	Concentration Ratio
Parabolic trough	Long, curved mirror Parabolic sheet of reflective material	100-300	250-550	20-25	14-22	30-80
Linear Fresnel	Flat mirror instead of curved mirror of the parabolic trough	10-200	150-550	18-20	13-18	30-80
Solar tower	It contains large heliostat field with tall tower in its centre	10-200	500-1200	22-24	15-23	1000-3000
Parabolic Dish	Parabolic mirror is used to focus heat directly on a Stirling engine	0.01-0.025	600-1500	28-32	18-25	200-1000

Table 1.1: General table of most important CSP plants

### 1.1.1 Parabolic Trough Technology

As the name suggests, in the Parabolic Trough technology the collector is a [8] symmetric section of a parabola around its vortex. Parabolic troughs have a focal line, which consists of the focal points of the parabolic sections. Radiation entering a plane parallel to the optical plane is reflected in such a way that it passes through the focal line.

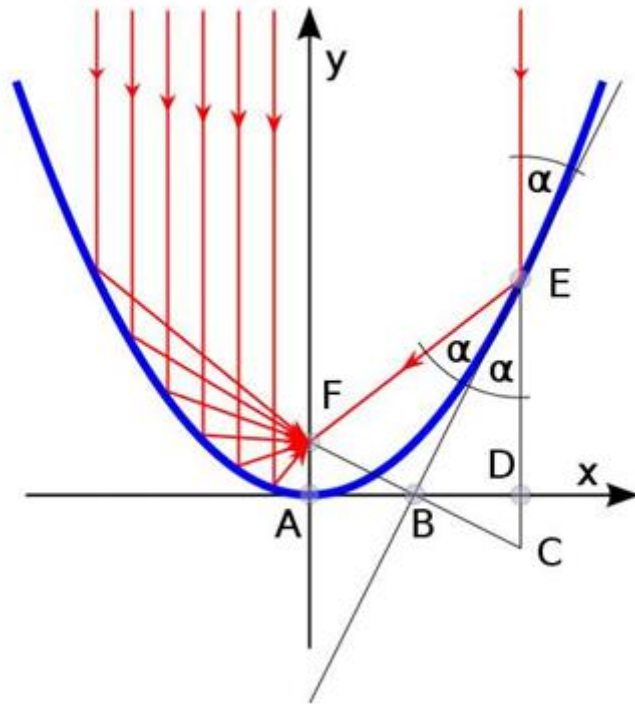


Figure 1.4: Geometry of a Parabolic Trough Collector [6]

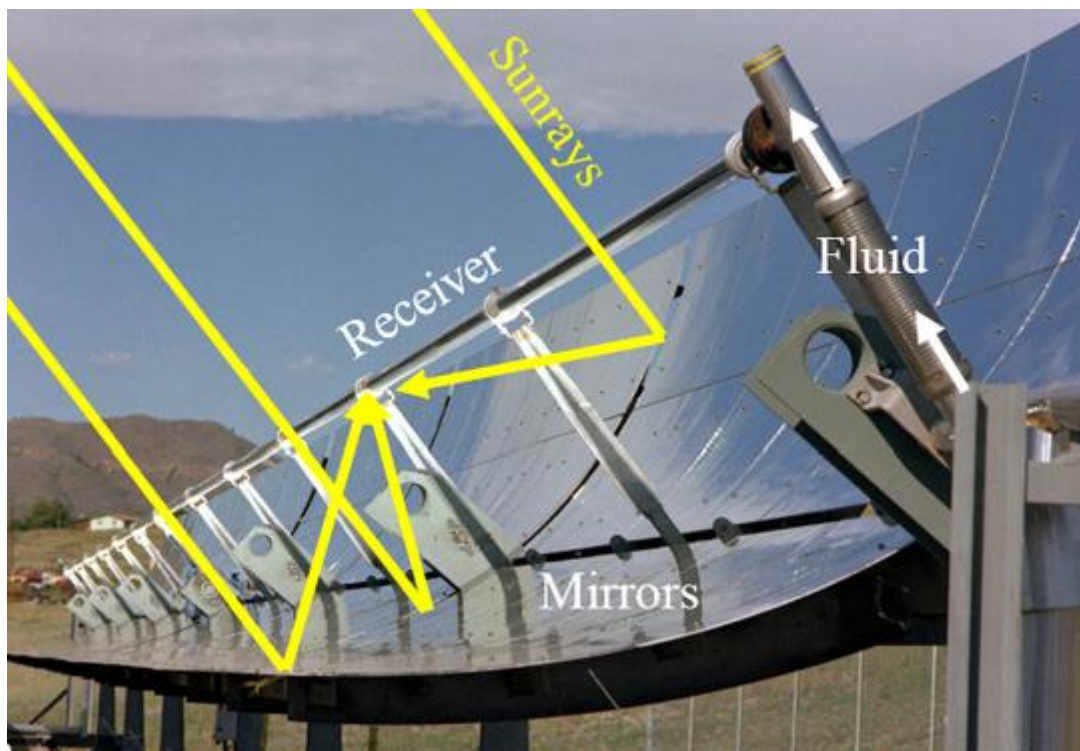


Figure 1.5: Image of a real Parabolic Through system [9]

The following parameters are usually required to determine all of the geometry involved in the parabolic through technology:

-Trough length: it is the length of the trough collector, and it is the only parameter that does not deal with the definition of the size and shape of the parabola.

-Focal length: it is the distance between the focal point and the vertex of a parabola. It is important to remember that it is possible to define completely the shape of a parabola by only defining the focal length. In fact, given that “f” is the focal length, the shape of the parabola on a x-y diagram is represented by the following equation:

$$y = \frac{1}{4f} \cdot x^2 \quad (1.1)$$

A graphical representation of this equation is represented in the figure 1.5

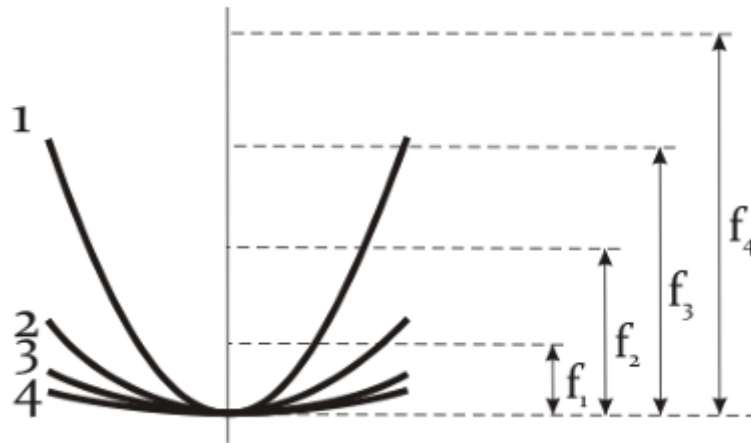


Figure 1.6: Image that shows how the focal length is the only parameter needed to define the shape of the parabola [8]

-Aperture width: it is the distance between one rim and the other

-Rim angle: it is the angle between the optical axis and the line between the focal point and the mirror rim). The rim angle alone determines the shape of the cross-section of a parabolic trough. This means that the cross-sections of two parabolic troughs with the same rim angle are similar, and so as a consequence, the cross-sections of one parabolic trough with a given rim angle can be made congruent to the cross-section of another parabolic trough with the same rim angle by a uniform scaling). To determine the shape of the cross section of a parabolic collector (without having interest on its absolute size), then it is sufficient to indicate the rim angle.

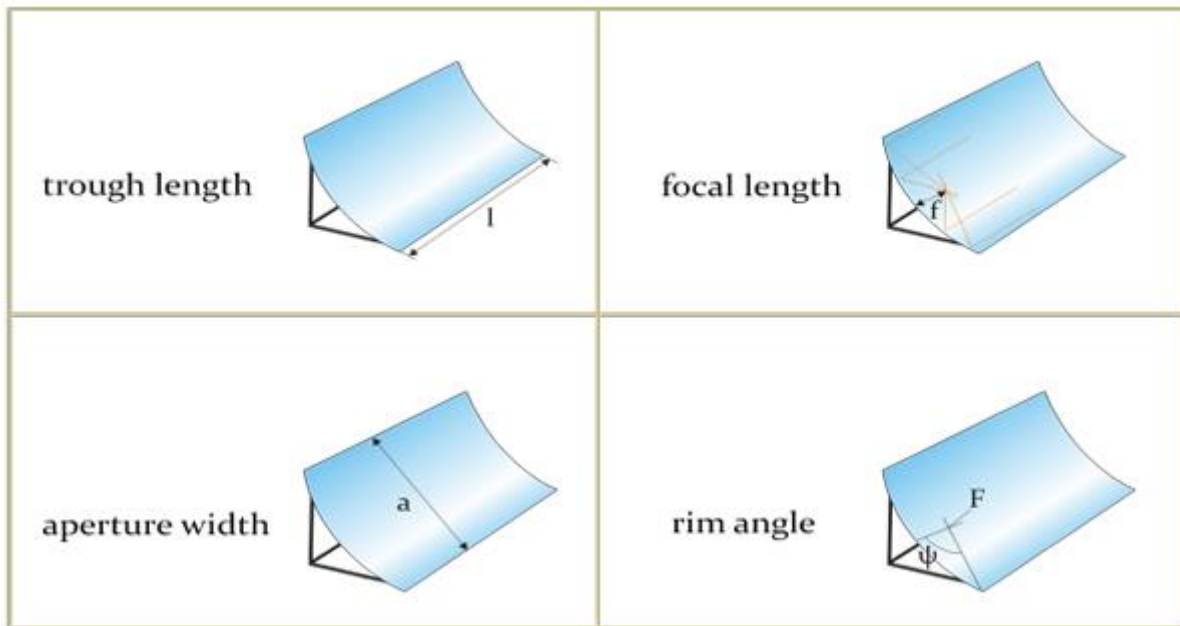


Figure 1.7: Geometrical parameters used to describe a Parabolic Trough collector [8]

As already anticipated, to define completely the geometry of the parabolic trough (size and shape), the focal length, the aperture width and the rim angle are used. It is possible to state that only 2 out of these 3 parameters need to be defined to set the geometry of the parabolic trough, and the third one can be expressed as a function of the other two.

For what regards the materials used for the collector, the ones with high reflectivity<sup>3</sup> are used. One of the most common choices are the silver-coated glass mirrors.

The receiver has the shape of a tube. More precisely, it is an absorber tube at which some different coatings can be applied to increase its performance. The coating typically includes 3 layers, defined as it follows:

- At the bottom, there is a reflection layer made out of a metal that is highly reflective in the infrared range (like aluminium or molybdenum) to avoid high heat losses
- In the middle, there is the cermet (ceramic+ metallic) layer
- On the top there is an antireflection ceramic layer

The whole absorber tube is then placed inside a glass tube, used to reduce the conductive and convective heat losses. Vacuum tubes are used because they help with thermal insulation.

The HTF used is usually a synthetic oil, a mineral oil or a molten salt. The steam generation may be both direct (in which the HTF is used directly to drive a Rankine Cycle) or indirect (in which the HTF is used to warm up water to drive a Rankine Cycle).

<sup>3</sup> Since the reflectivity of a material changes with the wavelength of the incoming wave, the reflectivity must be high in the spectrum of the visible light

For what regards the solar field, the north-south alignment is usually preferred, with respect to the east-west alignment. The reason is that the north-south alignment can grant a more equilibrate collector irradiance over the day and a higher peak irradiance at noon. The solar field, shown in the figure 1.7 has typically a square shape, with the power block located near the centre. Moreover, there are two pipes: one pipe leads the cold heat transfer fluid to the solar field, while the other leads the hot heat transfer fluid from the solar field to the central power block

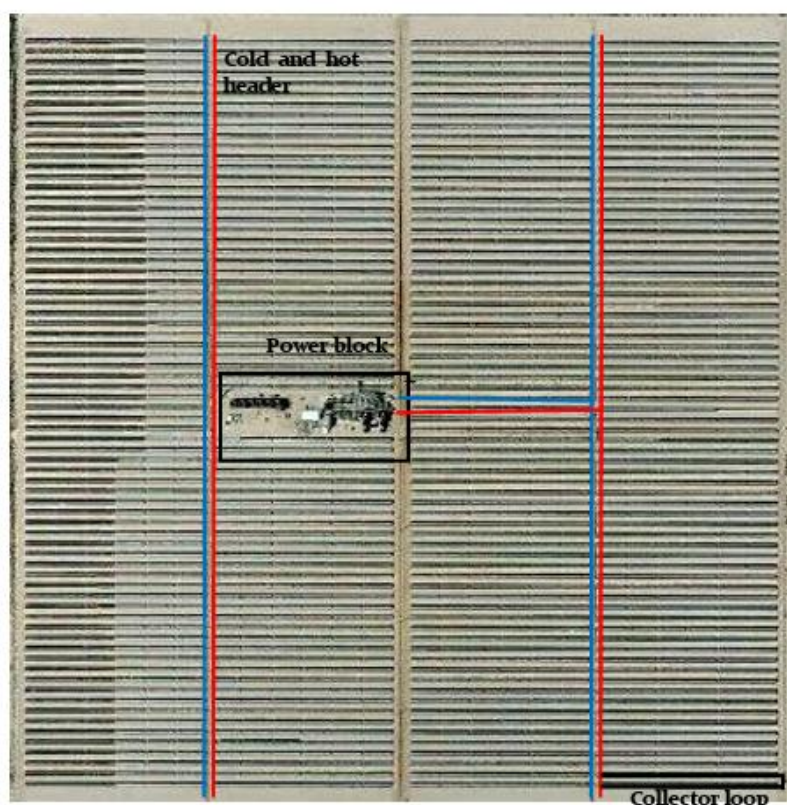


Figure 1.8: Typical layout of a parabolic trough solar field [8]

The Solar field of the parabolic trough systems usually presents series of collector loops (typically comprising 4, 6, or 8 collectors), interconnected in a comb-like fashion to the main heat transfer fluid pipelines. The cold fluid is conveyed through the main supply pipeline and, as it flows through the receiver tubes, it undergoes heating before returning in a heated state through the main return pipeline. The main pipelines are subdivided into several branches to form distinct subfields, each centred around the power generation block.

The parabolic trough technology is the most used CSP technology and, as previously said, the temperatures reached are between 50 and 400°C.

### 1.1.2: Linear Fresnel Technology

The Fresnel Collectors consist in [10] multiple flat or slightly curved primary mirrors with a fixed receiver. The working principle of the Fresnel Collectors [11] is the chopping of the continuous surface of a standard mirror into a set of surfaces with discontinuities between them. This allows a

substantial reduction in thickness (and thus weight and volume) of the mirror itself, at the expense of the creation of optical losses.

In the figure 1.8 it is reported the difference between a standard curved mirror and a Fresnel mirror

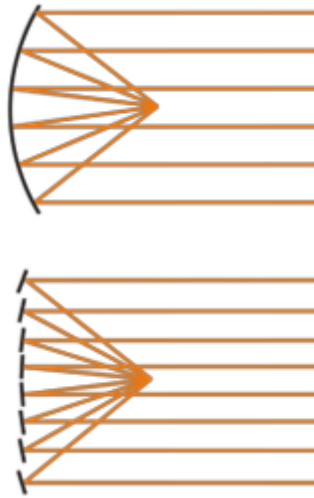


Figure 1.9: Difference between a standard curved mirror and a Fresnel mirror [10]



Figure 1.10: Image of a real Linear Fresnel system [12]

For what regards the collectors, as just said, they are flat mirror stripes, which receive a small curvature by mechanical bending. The material that is used is usually the same of the parabolic trough collectors: silver coated glass mirrors.

The design phase of the linear Fresnel collectors requires the definition of the following parameters

-Width of the entire collector: it should not be too narrow, as this would increase the number of mirror strips required to cover a given aperture area, and it should not be too wide, as this would reduce the effectiveness of the operating principle of the Fresnel mirror type.

-Number of parallel mirror strips

-Height of the absorber above the plane of the primary mirrors: it should not be too small because there may be a stronger effect of shading and blocking between the primary mirrors and as a consequence the incidence angles on the receiver will be very large, and it should not be too large because very distant mirrors contribute less to the radiation concentration and the effect of tracking inaccuracies will be stronger.

-Gap between the mirror strips: it should not be too small, because small gaps imply higher shading and blocking between the mirror rows, and it should not be too large, because large gaps imply a large collector width with distant mirrors without aperture area gains.

-The curvature of the mirrors: It should have a radius that is neither too large nor too small, as in either case a large part of the radiation would miss the receiver.

As far as the receiver is concerned, it has a completely different structure to that of the parabolic dish receiver. In fact, it is made up of a secondary collector (concentrator) and an absorber tube, as shown in Figures 1.11 and 1.12.

Two main components:

- secondary concentrator
- absorber tube(s)



Figure 1.11: Structure of the receiver of the Linear Fresnel Technology [10]

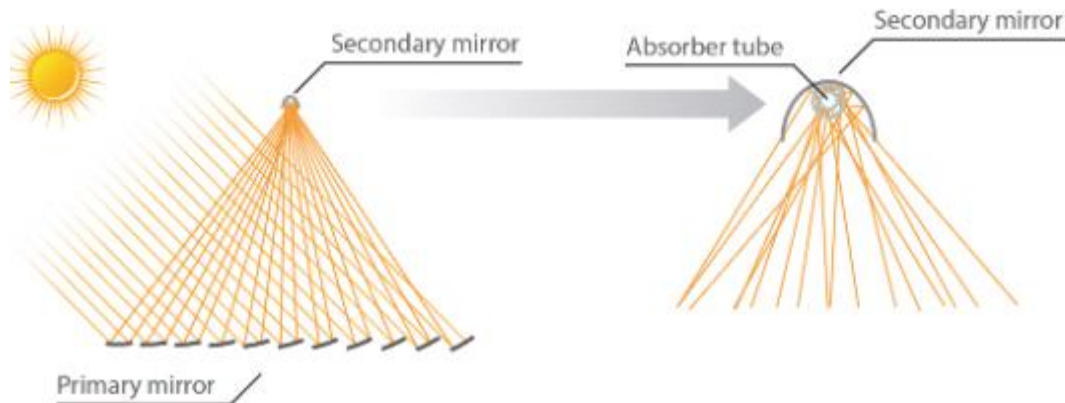


Figure 1.12: Another image used to show up the receiving methodology of a Linear Fresnel System [13]

The use of a secondary collector is done because a Fresnel mirror system alone cannot reach continuously the same radiation concentration like a parabolic trough. The reason is that, contrary to the parabolic trough technology, the Sun is not always situated in the optical axis plane. And so, in order to mitigate the optical inaccuracy and to increase the intercept factor, a secondary concentrator is implemented.

The absorber tubes of the Linear Fresnel technology present some differences from the ones of the Parabolic Trough. First of all, since the secondary collector acts also (as a secondary function) as a thermal insulator, the use of vacuum tubes is not common nowadays (even if some attempts are currently under development). The main tube is in stainless steel and, like in parabolic troughs, it is applied a selective coating that has a high absorptance at short wave lengths and a low emittance for infrared radiation. Cermet materials are used as coating, and their stability has been proved for temperatures until 450 °C.

The types of Heat Transfer Fluid used are typically [14]: Thermal oil, pressurized water, or steam.

With respect to the Parabolic Trough Technology, the Linear Fresnel presents some advantages and disadvantages that can be summed up as it follows:

For the Advantages,

- Presence of a fixed receiver: it permits to have a quite constant distribution of radiation over the absorber tube.
- The configuration is made in such a way that most of the radiation hits the absorber tube from below, and this represents an advantage in case of direct steam generation because the liquid phase flows rather in the lower part of the absorber tube.
- The use of flat mirrors allows a cost reduction compared to curved mirrors. Moreover, the cleaning process also becomes simpler
- The Absorber tubes used for the Fresnel systems, as already mentioned before, are simpler because they don't need the presence of a vacuum tube for thermal insulation.

For the Disadvantages,



- With respect to the parabolic trough collectors, Fresnel collectors do not suffer only of longitudinal cosine losses, but they are affected also by transversal cosine losses.
- There are shading problems at high transversal incidence angles

### 1.1.3: Solar Tower Technology

The solar tower technology is [15] essentially a CSP technology in which a large number of sun-tracking mirrors are used to focus highly concentrated solar irradiation on an absorber device, called receiver, which is located top of a tower. The receiver then transforms the concentrated radiation into heat and transfers the heat to a working fluid. Again, as seen before, a direct steam generation cycle or an indirect steam generation cycle can be implemented.



Figure 1.13: Image of a Solar Tower power plant [11]

The collectors, also called “heliostats” represent the biggest part of the CAPEX of a solar tower power plant (roughly 50%) and the differences between one from another can be very vary. The first difference regards the material used to build the mirrors: typically, a combination of two materials is used to increase the to maximize the coefficient of reflection, such as “Glass with a layer of aluminium” or “Teflon with a layer of silver”. Another main difference regards the shape of the Heliostats. A lot of different shapes can be used, and the most important are the following:

- Canted glass mirror Heliostat: it is a single large heliostat that has been divided into a number of sub-mirrors.
- Stretched-membrane focused and non-focused Heliostat: in this case, the reflector is made of either stretched polymer (plastic) or metallic foil and it has a curve shape
- Flat or nearly flat single or multiple mirror heliostats: in this case the Heliostats are flat and they assume often a rectangular (or square) shape.

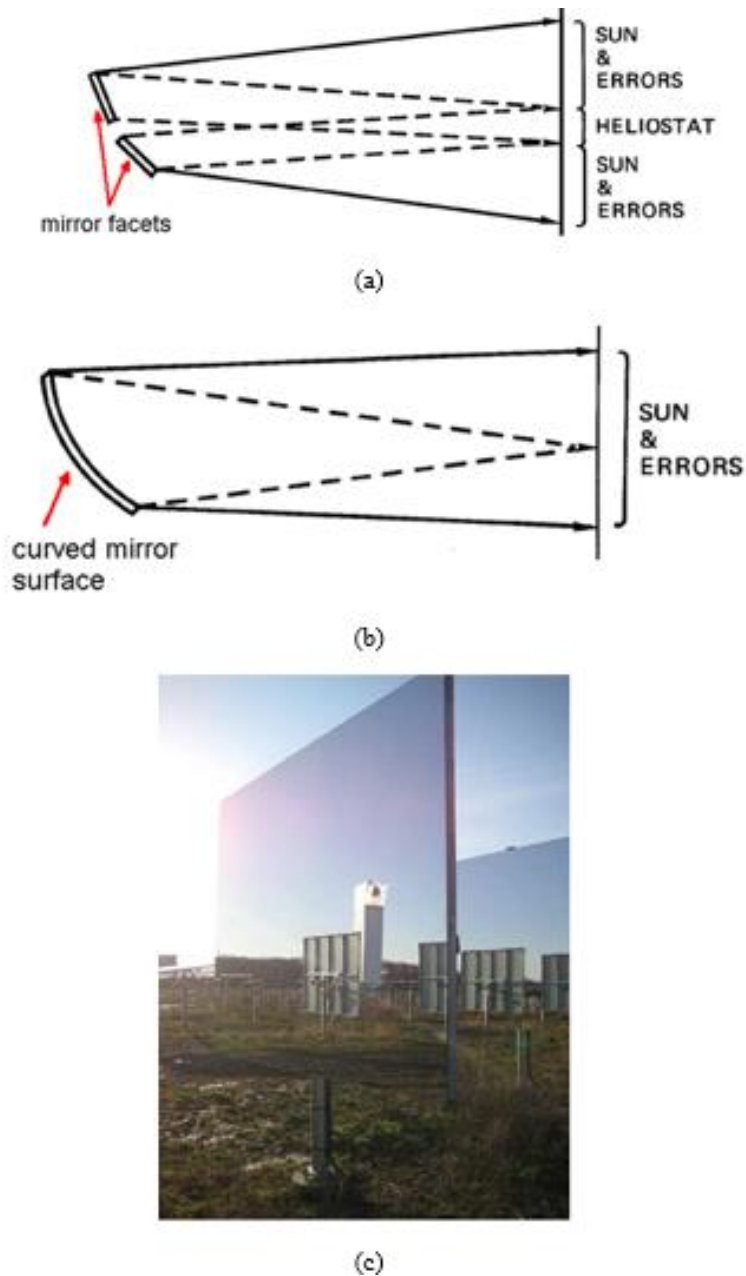


Figure 1.14: Shape of Heliostats used in the Solar tower power plants: (a) Canted glass mirror Heliostat, (b) Stretched membrane Heliostat, (c) Flat or nearly flat Heliostat [15]

Another source of differences between the heliostats regards their size: it can vary from only 1 m<sup>2</sup> to roughly 150 m<sup>2</sup>. The advantage of using bigger heliostats is that less collectors will need to be installed and, as a consequence, fewer step motors will be required. The disadvantage, however, is the more difficult installation and maintenance problems (for example, the replacement of actuators or broken mirrors).

For what regards the receiver, on the contrary from what it has been seen until now for the linear CSP plants, there is not only one technology used (absorption tube) but, different concepts, that are reported below, has been developed over the time.

-Direct Absorption Receivers: in this case, the (point) concentrated solar irradiation directly hits the HTF, without entering in contact with the layer of an absorption tube. As a first advantage of this technique, the direct heat transfer from the sun to the heat transfer fluid allows the system to reach much higher temperatures (until 2000 °C) because there is not the problem of the reaching of the technological limit of the material of the tube. The HTF used are falling particles or molten salts.

-External tube receiver: it consists of a large number of vertically arranged pipes through which the HTF is pumped in upward direction. The HTF used in this case are molten salt, water for direct steam generation, and sodium.

-Cavity receiver: It is a cavity with a small opening (inlet aperture) at which the concentrated solar irradiation is aimed. Inside this small opening there are the tubes carrying the working fluid, that are typically the same used for external tube receivers (even if also fluids in gaseous form can be used). Since from the radiation entering the inlet aperture, only small amounts are reflected back into the atmosphere through the inlet aperture, the radiation losses are diminished.

-Air receiver: As the name suggests, in this case the fluid that receives the solar radiation is the air. Two different kind of air receiver exists: the “Open volumetric receiver” and the “Pressured volumetric receiver”.

The Open volumetric receiver, typically consists in a porous material receiver in which air is let passed by. The heat is transferred from the heliostats to the porous receiver, and the porous receiver passes it to the air that flows inside. The use of a porous material is done because, with respect to the air, thanks to its porosity it can give a very high absorption area and so it counter-balances the effect of the low heat transfer coefficient of the air.

In the Pressurized volumetric receiver, the use of compressed air (up to 15 bar) is done. This concept is under study and development for Solar Hybrid Gas Turbine and CC Systems.

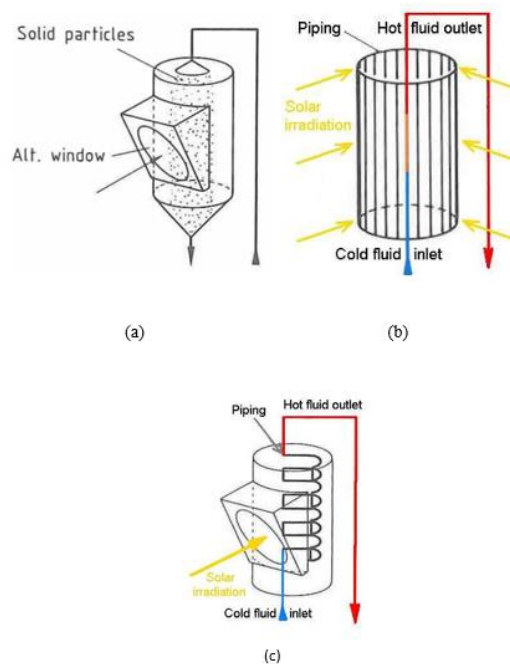
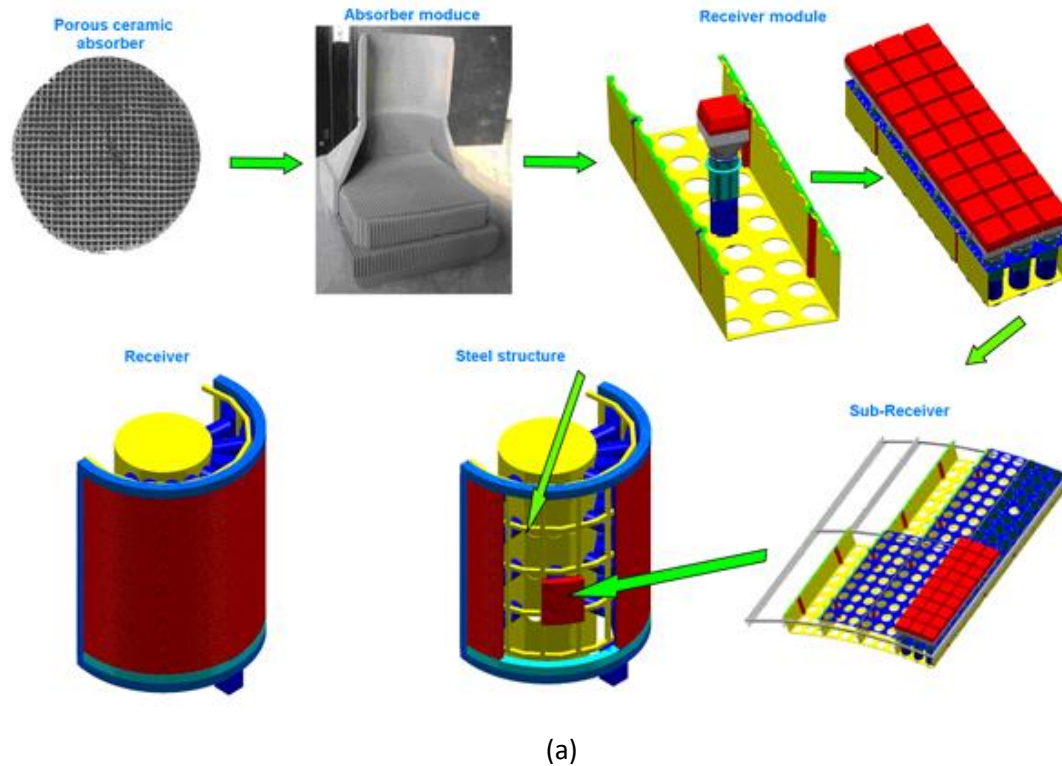
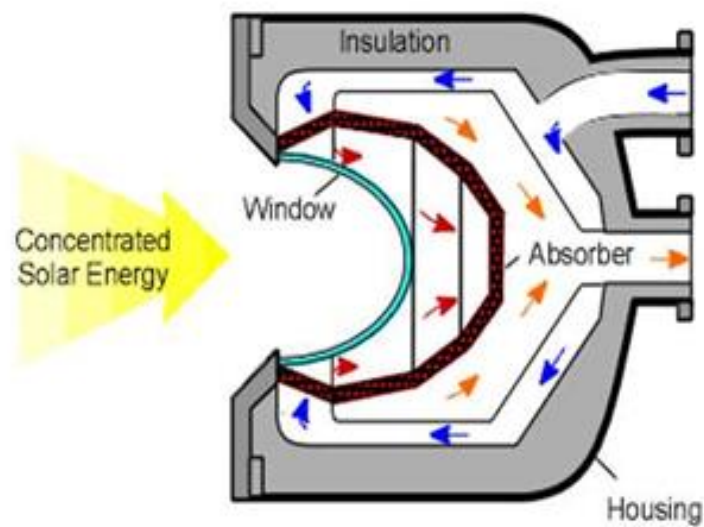


Figure 1.15: Some of the receivers used for the Solar Tower technology. (a) Direct absorption receiver, (b) External tube receiver, (c) Cavity receiver [15]



(a)



(b)

Figure 1.16: Image of the two types of air receiver, (a) Open air receiver, (b) Pressurized air receiver [15]

### 1.1.4: Parabolic Dish Technology

A Parabolic Dish Concentrator is a system that uses [12] a parabolic dish-shaped or concave mirror to concentrate sunlight on to a receiver situated at the focal point of the mirror. The paraboloid dish must follow the sun in such a way that it can reflect its rays back to the receiver. For this purpose, the collector is mounted on a support structure capable of rotating about two axes.

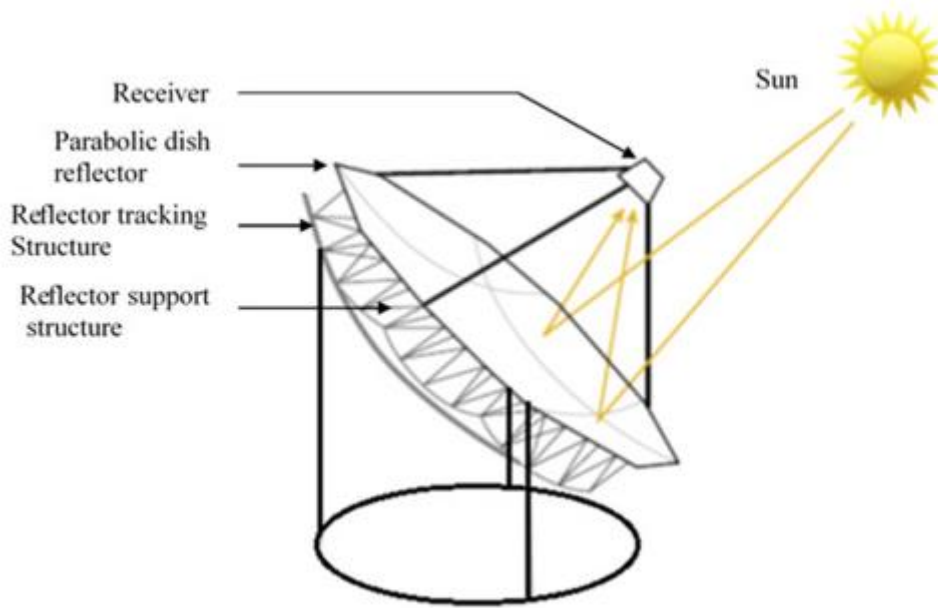


Figure 1.17: Schematic image (a) [16] and real image (b) of a parabolic dish collector [17]

For what regards the collector, the shape of a parabolic concentrator and the location of its focal point can be defined either using the dish focal distance to diameter ratio or the rim angle. The relationship between the focal distance and the rim angle is the following equation

$$f = \frac{D_d}{4 \cdot \tan\left(\frac{\psi_{rim}}{2}\right)} \quad (1.2)$$

Moreover, the distance “Q” between the surface of the concentrator and the focal point of the aperture at any angle ( $\psi$ ) between 0 and the rim angle can be calculated as it follows

$$Q = \frac{2 \cdot f}{1 + \cos(\psi)} \quad (1.3)$$

For what regards the receiver, it is located usually at the focus of the paraboloid shape and in is the place where the majority of thermal losses in a Solar dish system happen.

The thermal losses that are present are the following:

- Conduction losses through the walls of the receiver
- Convection losses from the cavity
- Radiation losses through the opening of the aperture

The best way to reduce the losses (and hence increase the thermal input captured by the receiver) is a correct design of the aperture of the collector. The aperture must not be too big because in this case there will be an increase of the convection and radiation losses, and it must be not too small so that a significant fraction of the reflected solar irradiance will be transmitted onto the absorber. Very precise systems that take in to account a lot of factors (such as: the irregularities in the slope of the parabolic mirror created during manufacturing, receiver alignment discrepancies, tracking error from the tracking sensors, variations in the mirror specular reflectance, and the tracking drives not being in a uniform position [18]) are used nowadays to estimate the correct size of the aperture.

The main advantages of the Parabolic Dish Collectors are the following:

- Because they are always pointed directly at the sun, they are the most efficient solar collectors between the CSP technologies discussed. The electricity conversion efficiency is up to 30% [18]
- The high concentration ratios reached (between 600 and 2000) allow them to have very high temperatures and thus high efficiencies of energy transformations.
- Their modular structure allows them to operate individual units independently.

## **Chapter 1.2: Other possible applications for the CSP technologies**

Until now, the only possible application discussed for the CSP systems is the possibility of the production of electricity. Even if the power generation is the main task for which CSP systems are used, other secondary uses are interesting for this technology.

### **1.2.1: Solar Cooling**

As the name suggests, the solar cooling is a technique that aims to cool down a closed environment by using as the sun as energy source. The cooling process can be electrically or thermally driven. With respect to CSP technology, in general, both solutions are technically feasible [19]. Two of the most important thermally driven cooling technologies for cold production are: absorption and adsorption chillers<sup>4</sup>.

The Absorption chiller [20] is a system that uses the solar-thermal energy to drive a vapour compression cycle. The number of heat exchangers within the absorption chiller distinguishes the system as either single-effect, double-effect or even triple-effect absorption chillers.

The Single-effect absorption chiller uses only one heat exchanger, and it is composed by the following parts: an absorber, a generator, a separator, a condenser and an evaporator. A graphical representation

---

<sup>4</sup> Normally, Absorption and Adsorption Chillers use a low-temperature solar thermal source (<100 °C), that can be supplied by a simple flat-plate collector, and so it does not strictly require the presence of a CSP system (that can produce temperatures up to 200 °C or more). Even though, the CSP systems can be still used to run absorption and adsorption chillers, of course not as a “primary” goal, but rather as a by-product of the high temperatures obtained with the solar concentration.

of a single-effect absorption chiller is available in the figure 1.18, and the working principle of its components is reported below.

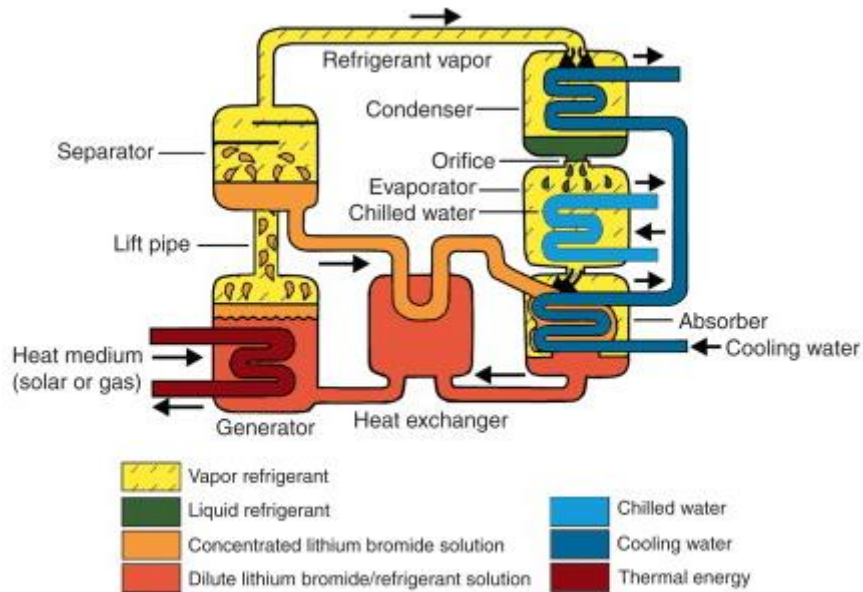


Figure 1.18: Scheme of a single effect Absorption Chiller [21]

-The components called respectively “Absorber” and “Generator” constitutes the compressor block; hence, they are the responsible of the compression phase. In a usual refrigerant cycle, this stage is done by using a compressor machine fed by electricity in order to compress a vapour that exits from the evaporator. This method has two main drawbacks: the use of a mechanical compressor can generate a non-indifferent source of noise and in can be very costly, especially nowadays with the price of the electricity that is continuously fluctuating. In an absorption chiller, this mechanism is replaced by a “thermal compression”, that is divided in two steps represented by the two blocks (absorber and generator) that exploit a liquid refrigerant/sorbent solution and a heat source in order to make the working fluid (the refrigerant) a hot high-pressure vapour. More in depth, in the absorber there is a sorbent material that is in contact with a refrigerant in vapour form. The absorber material absorbs the vapour and becomes a low concentration liquid solution. Cooling water is used to cool down this process. Then, this solution is compressed thanks to a mechanical pump, that is not represented in the scheme. The reason is that this process is energy saving because it is widely known that the compression of a liquid is much less energy-expensive with respect to the compression of a vapour. Then, the low concentration refrigerant/sorbent solution arrives into the generator. In this component, an external heat source (that can be, the heat generated from the CSP system) heats up this solution causing the physical separation of the absorbent material from the refrigerant and, as final result, there are: the refrigerant, that is a hot high-pressure vapour, and the absorbent material as concentrated solution.

-Then there is the separator, that is a component in which no thermodynamic transformations are done. More in depth, this component is only used to physically separate all of the refrigerant (that is in vapour form), from the concentrated absorbent solution (that is in liquid or solid form). The refrigerant is sent to the next component (that is, the condenser), meanwhile the concentrated is collected and sent back to the absorber.

-Then, there is the condenser, in which the refrigerant that leaves the generator passes from the condenses, shifting from vapour phase to a colder liquid phase, and circulates through the system.

-Then, there is an expansion valve in which the refrigerant becomes a low-pressure cold vapour. The shift from a high-pressure condition to a low-pressure condition is necessary because the next component (that is, the evaporator) needs a low-pressure environment to work correctly.

-In the end there is the evaporator, that is the component in which the cooling effect of the Absorption Chiller is obtained. In the evaporator, the cooling fluid (in the figure 1.18 is called “chilled water”) gives heat to the condensed refrigerant, and so it becomes cold and it is consequently used to refrigerate the environment. The low-pressure environment inside the evaporator is used to assure that the refrigerant remains in a vapour form in such a way that it can be sent again to the absorber block and so the whole cycle can start again.

In Double-effect absorption chiller systems, there is a high-temperature generator and a low-temperature generator to improve the thermodynamic efficiency of the absorption cooling cycle. In this case, the use of CSP technology is necessary to drive the high temperature for the heating cycle.

The triple-effect absorption chiller systems are the result of the combination of two single-effect absorption circuits.

For what regards the choice of the absorbent solution, it obviously depends by the refrigerant fluid that has been chosen. Two common refrigerant/absorbent combinations are: water and lithium bromide (LiBr–H<sub>2</sub>O) (used in water-cooled absorption systems) and ammonia and water (NH<sub>3</sub>–H<sub>2</sub>O) (used in air-cooled systems). For a single-effect absorption chiller, the COP ranges from 0.6 to 0.8. For the double-effect absorption chillers, the COP may achieve values up to 1.0-1.2.

The Adsorption chiller is a system that uses the solar-thermal energy to drive a common desiccant cycle. Just like the Absorption chillers, also in this kind of system the refrigerant is paired with a sorption material, that can be solid or liquid. Solid sorption materials typically use water as refrigerant and silica gel (or also zeolites) as adsorbent. The basic scheme of an Adsorption chiller contains: a condenser, an adsorber, an evaporator and a desorber. This scheme is shown in figure 1.19, in which the adsorber is the component marked with the number (2) and the desorber is marked with the number (1). The working principle of each component is discussed below.

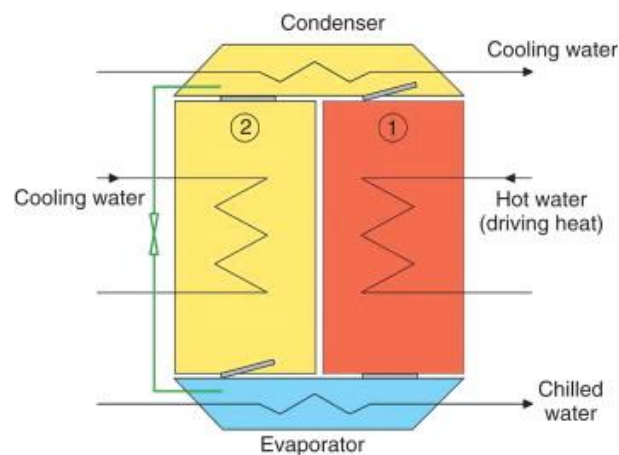


Figure 1.19: Scheme of an Adsorption Chiller [20]



-In the desorber, the adsorbent containing the working fluid is heated, and so the refrigerant is desorbed. As a consequence, the pressure increases and the refrigerant is sent to the condenser. The hot water used to heat the sorbent/refrigerant solution can be obtained using the heat generated from the CSP system.

-In the condenser, the refrigerant, in vapour form, is condensed and so it becomes liquid. To do that, cooling water is used. The liquid refrigerant passes through a throttling valve that decreases its pressure and sends it to the evaporator.

-In the evaporator, the refrigerant takes the heat from the fluid responsible for the cooling effect (that in the figure 1.19 is called “chilled water”). So, the refrigerant absorbs heat and becomes vapour, while the cold water will be used to cool down the environment. Once that the refrigerant has become vapour, it is sent to the adsorber.

-In the adsorber, the refrigerant in vapour form is adsorbed by the sorbent material, and so the refrigerant/sorbent mixture is formed again, ready to perform another cycle. Since the process is exothermic, the heat has to be removed using cooling water.

The COP of an Adsorption chiller assumes typically values between 0.5-0.6. Large heat exchange surfaces permit a mode of operation close to the thermodynamic limits.

For what regards the market possibility for solar cooling technologies, the growing demand for air conditioning in homes and small office buildings is producing a growing market for different types and scales of solar-assisted cooling technologies. Nowadays, the research in this field is worldwide, and it is dominated by Japan and, increasingly, China. For what regards the Europe, it is one of the global leaders in the implementation of solar thermal cooling technology. As the following study [22] states, for the 2030 the contribution of solar thermal to the low temperature heat demand of the European Union (EU 27) will be between 4% (worst case scenario) and 15% (best case scenario), with the corresponding annual solar yields of 198 TWh and 582 TWh. For the 2050, the contribution of the solar thermal cooling is expected to be between 8% and 47%.

### **1.2.2: Desalination**

Another interesting secondary possibility of application of the CSP technology regards the desalination, that is a process that uses thermal or electrical [23] energy to remove salts and other source of impurities from the marine water, in order to obtain clean water.

Along the world, a large number of different desalination techniques are available and applied. Only some of these technologies reached a semi-commercial state and can be applied in large units in order to be effectively combined with CSP plants [24]. The two most important processes are the “Multi-effect Desalination” (MED) and the “Reverse Osmosis” (RO).

The MED is a thermal distillation process and has gained attention due to its relevant thermal performance [25]. The implant for MED is composed of a sequence of cells, or stages, arranged in a decreasing order of pressure (and temperature) from the initial high-pressure cell to the final low-pressure one. Each cell primarily features a bundle of pipes. The upper part of the bundle is sprayed with seawater, which then descends through the tubes due to gravity. Inside the tubes, heating steam is introduced. While the heat runs along the tubes, the seawater warms up and partially evaporates, capturing the heat from condensation (latent heat). The vapor generated through seawater evaporation is cooler than the heating steam. The progressive pressure reduction from one cell to the next facilitates the movement of brine and distillate to subsequent cells. Within these cells, the brine and

distillate undergo a flash process, releasing additional vapor at the lower pressure. This additional vapor then condenses into distillate within the following cell. This sequence of processes is repeated across a series of effects. In the ultimate cell, the steam produced condenses within a traditional shell-and-tube heat exchanger termed the "distillate condenser." This component is cooled by seawater. The warmed seawater exiting this condenser serves partially as the unit's makeup water, while the remaining portion is discharged into the sea. As the process continues through each cell, brine and distillate accumulate and are drawn from one cell to the next until the final cell. From there, they are extracted by centrifugal pumps.

The RO is a water treatment process that works thanks to a membrane separation method. The RO removes contaminants from water by using pressure (greater than the osmotic pressure of the solution) to force water molecules through a semipermeable membrane. Membrane layers hold back the salt ions from the pressurized solution, allowing only the water to pass.

The MED and the RO can be coupled with CSP systems, as shown in the figure 1.20

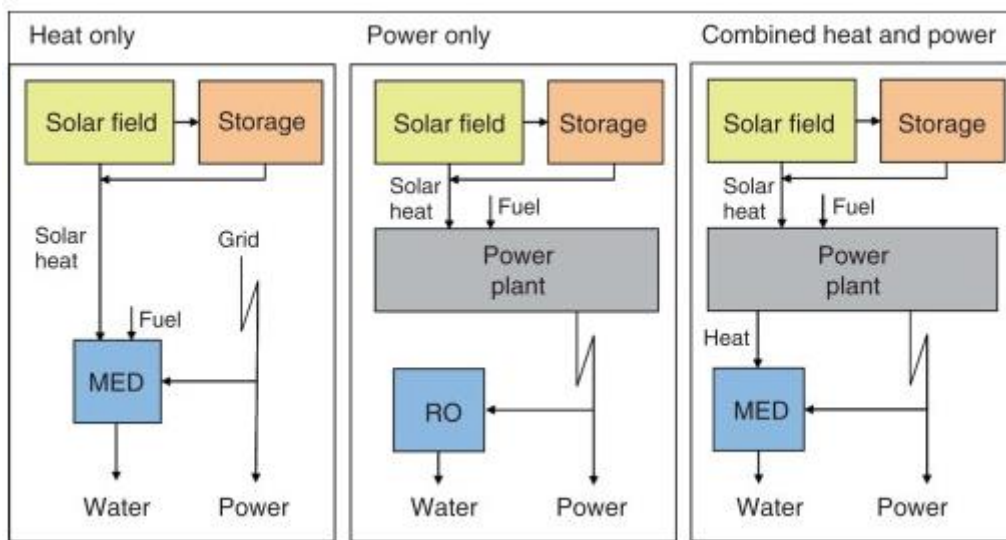


Figure 1.20: Examples of coupling of Multi-Effect Desalination (MED) and Reverse Osmosis (RO) processes with a CSP power plant [26]

With respect to the figure 1.20, as it can be seen, the MED requires both the presence of heat and electricity, while the RO needs only the electricity. More in detail:

- In the first desalination system (MED system), the heat is recovered from the CSP system, while the electricity is taken from the grid.
- In the second system, the CSP system provides only the electricity necessary for the RO.
- In the third system the CSP grants both the heat and the electricity to run the MED.

Since desalination systems usually are designed to work non-stop [27], every CSP powerplant should have a storage system in order to grant also night operation.

### 1.2.3: Usage of the waste heat for heating purposes

Apart from the previously discussed cogeneration applications of desalination and cooling, waste heat can also be profitably used for other applications, such as heating purposes.

The usage of the waste heat for heating purposes is one of the most interesting energy saving technologies because of their simplicity and effectiveness. In fact, the literature is full of cases in which the usage of waste heat increases the overall efficiency of the cycle. As an example of that, the waste heat of a turbogas power plant can be used in a Heat Recovery Steam Generator, in order to heat up a steam power plant and thus creating a combined cycle, or to preheat the air after the compression phase. In both cases it is obtained an efficiency higher than the one of the base thermodynamic cycle of the turbogas powerplant. Moreover, in case of steam-power plants, by reducing the temperature of the waste steam as much as possible, the condensation power required for the recycling of the process steam can be reduced.

The applications suitable for the waste heat are determined by its source temperature: below 100 °C they are called “Low-temperature heat applications”, while, above 100 °C “High-Temperature heat applications”

For what regards the Low-temperature heat applications (<100 °C), they are suitable for hot water production and space heating in residential and commercial buildings, hotels or schools. Another typical use is the crop drying.

For what regards the High-temperature waste heat applications (>100 °C), they can be used for some different industrial processes, such as in the paper and food industries. Another possible application regards the preheating of the working fluid for the power production cycle. This is one of the highest temperature applications of waste heat.

### 1.2.4: Hydrogen Production

The last important alternative application for a CSP powerplant that will be discussed is the production of hydrogen. This topic is facing an increasing relevance since it is widely believed that the hydrogen will be the fuel of the future.

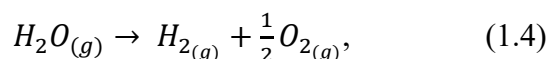
The potential of the hydrogen is witnessed by the two following characteristics, which make it unique [28]:

- Hydrogen is the most abundant element in the universe,
- It is the fuel with highest specific energy and, unlike electricity, it can be easily stored.

One of the most important sectors in which the research has been conducted is the automotive industry.

Of course, the hydrogen production becomes more significant and environmentally friendly if it is realized with carbon-free methods. One of the most important ways to produce hydrogen in a carbon-free way is the “Water splitting process” [29].

The water splitting process is a thermochemical method to produce hydrogen based on the following reaction



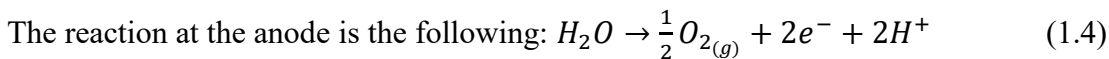
with

$$\Delta H_{298K} = \Delta H^0 = +242 \text{ kJ/mol} \text{ and } \Delta S = \Delta S^0 = +0.045 \text{ kJ/molK}$$

The two most important water splitting methods that can be coupled with the CSP technology are: the water electrolysis and the thermochemical water splitting cycles (Chemical looping).

The water electrolysis is a method that involves two separated reactions to split the water molecule: one at the cathode and one at the anode.

Supposing to use a PEM electrolyser, the reactions would be the following



The theoretical cell voltage is about 1.23 V, but the presence of over-voltages lead to an effective cell voltage usually in the range 1.8–2.2 V.

Typically, the efficiency of the water electrolysis process can reach values up to 60–75%.

The value of the overall efficiency is determined by multiplying the value of the efficiency of the water electrolysis process (that is typically in the range 60-75%), with the efficiency of the powerplant used to feed the electrolysis. This last term has usually a low value and represents the bottleneck of the system. For example, if the heat-to-electricity efficiency of the CSP system is around 20% (that is, the typical value of annual efficiency of a Parabolic Dish), and it is considered a value of efficiency of 60-75% for the electrolysis method, it is possible to obtain overall heat-to-hydrogen efficiencies in the range 12-15%.

The Thermochemical water splitting cycles method consist of a series of “N” chemical reactions whose net effect is represented by the equation 1.3 (that is:  $H_2O_{(g)} \rightarrow H_{2(g)} + \frac{1}{2}O_{2(g)}$ ).

The most famous processes for the hydrogen production are two steps chemical looping processes, in which:

- At the first step, there is the reduction of an oxygen carrier. The heat necessary for this step is taken from CSP
- At the second step there is the oxidation of the oxygen carrier, in which it is added an hydrogen-carrier molecule that has also oxygen (like H<sub>2</sub>O). The hydrogen is extracted from the added molecule while the oxygen is used to oxidise the oxygen carrier

Thanks to the use of chemical intermediate reactants and products, those multiple reactions can occur at low temperatures (< 1500 °C) and without using electrical energy.

The following criteria are generally used to select the thermochemical cycle:

- heat-to-hydrogen thermal efficiency;
- Possibility of the coupling with the primary energy source

- complexity of product separation and heat recovery;
- chemical reaction kinetics (for catalysts and heat transfer issues);
- material corrosion and mechanical resistance;

## CHAPTER 2: Power production – Organic Rankine Cycle (ORC)

In order to produce electrical energy using the heat collected from the sun, it is necessary to implement a thermodynamic (direct) cycle. From the fundamentals of thermodynamics and heat transfer, it is known that the thermodynamic cycles used to produce electricity are essentially of two types: the gas cycles and the steam cycles.

In the power plants based on steam cycles, the working fluid is a liquid (typically water) that shifts from liquid phase to vapour phase. The water is heated up in a boiler, that uses the heat generated typically from the combustion of fossil fuels. The combustion is external of the working fluid and the cycle is closed. Examples of steam cycles are the Rankine cycle or the Hirn cycle.

In the power plants based on gas cycles, the working fluid is a gas (typically air) that remains in gaseous form for the overall duration of the cycle. The air is heated up in a combustion chamber by mixing it with fossil fuels, typically natural gas (methane). The combustion is internal of the working fluid and the cycle is open, since the air is taken directly from the environment and released in it after the cycle is completed. Examples of gas cycles are the Otto cycle, the Diesel cycle or the Sabathé cycle.

### Chapter 2.1: Basic overview on the Rankine cycle

The Rankine cycle is the most used thermodynamic cycle for the electricity production in steam power plants.

The base sketch of a Rankine cycle is represented in figure 2.1, and the basic functioning of its components is discussed below

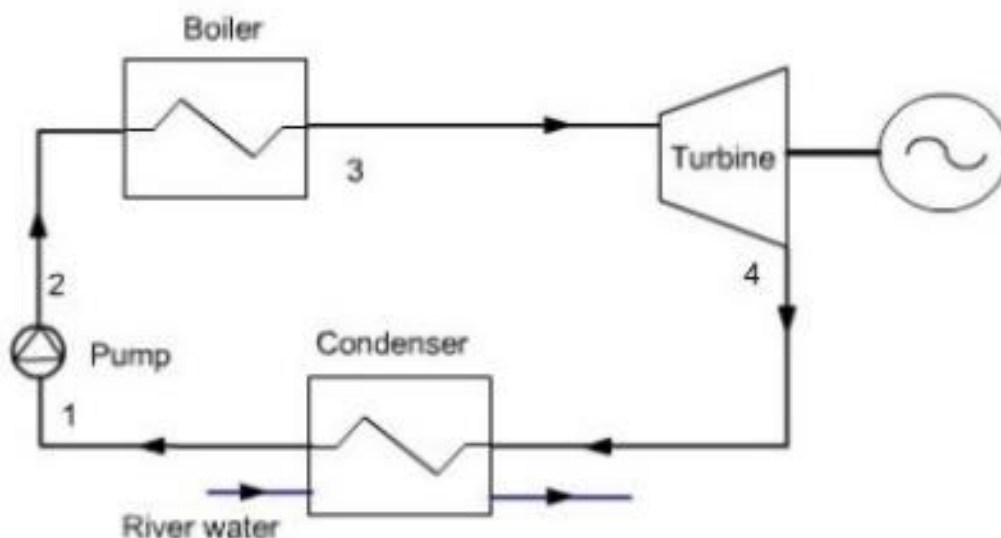


Figure 2.1: Basic scheme of a Rankine Cycle [30]

-The pump takes the liquid from the starting point (1) and increases its pressure up to the level required inside the boiler (point 2). Since the pump works with a liquid, the work required for its functioning is almost negligible

-The boiler heats up the liquid until it becomes vapour and consequently reaches the highest temperature level of all the cycle, represented by point 3.

-The turbine takes the inlet vapour and it expands it until the lower pressure level is reached (point 4). Inside the turbine, the working fluid undergoes an expansion. This expansion generates mechanical work to rotate the shaft, which, being connected to an electric generator by means of a speed reducer, enables the generation of electricity.

-The condenser is a heat exchanger that takes the working fluid at the outlet conditions of the turbine and it condenses it, by extracting heat with a cooling fluid. In such a way, the working fluid is again in the starting conditions and a new cycle can be performed.

If all of the thermodynamic transformations that happen inside the components are made without any source of losses, the cycle is called “ideal”. The ideal Rankine cycle is shown in the figure 2.2, and it is discussed below

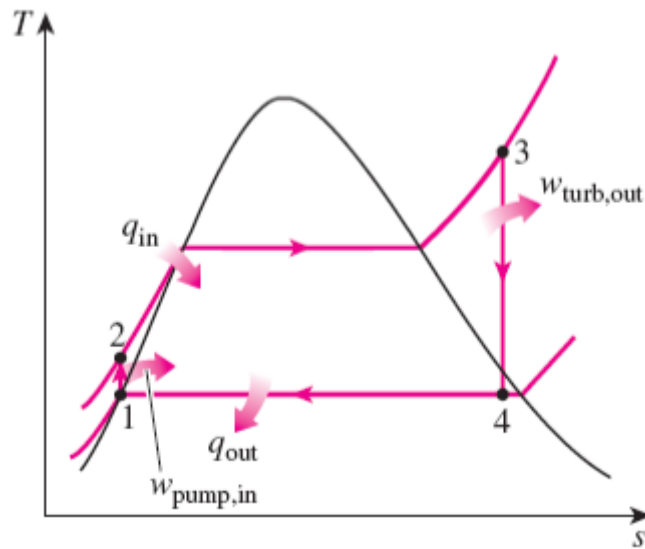


Figure 2.2: Image of an Ideal Rankine Cycle [31]

-The action of the pump is expressed in the line 1-2. The compression, in the ideal case, is isentropic, and so it proceeds on a vertical line on the T-s diagram. The work required can be indicated as  $L_{12}$

-The action of the boiler is represented in the line 2-3. The boiler heats up the fluid in a constant pressure way. Once that the liquid has reached the saturated condition, the phase change occurs at constant temperature<sup>5</sup>. The heat given to the fluid can be indicated as  $Q_{23}$

-The action of the turbine is expressed in the line 3-4. The expansion phase, in the ideal case, is isentropic, and so, in the same way done for the pump, it proceeds on a vertical line on the T-s diagram. The work extracted can be indicated as  $L_{34}$

<sup>5</sup> In the base Rankine cycle, the heating phase finishes when the condition of dry saturated steam is reached. However, for a Rankine cycle, it is very common to reach much higher temperatures and reach conditions in which the fluid, at the inlet of the turbine, is a superheated steam. A Rankine cycle that works in this condition, and that has also been represented in the figure 2.2, is called “superheated Rankine cycle” or also “Hirn cycle”.

-The action of the condenser is represented in the line 4-1. The condensation phase, essential for the pump that must work with a purely liquid material in order to avoid damages due to cavitation, happens at constant temperature. The heat extracted from the fluid can be indicated as  $Q_{41}$

Using the first principle of the thermodynamic for open systems it is possible to obtain the energy quantities that have been just discussed.

$$\text{-Pump: } |L_{12}| = h_2 - h_1 \quad (2.1)$$

$$\text{-Boiler: } Q_{23} = h_3 - h_2 \quad (2.2)$$

$$\text{-Turbine: } L_{34} = h_3 - h_4 \quad (2.3)$$

$$\text{-Condenser: } |Q_{41}| = h_4 - h_1 \quad (2.4)$$

$$\text{The first-law efficiency can be defined as } \eta_{th} = \frac{L_{34} - |L_{12}|}{Q_{23}} \quad (2.5)$$

In the real case, there are some losses that must be considered [32]. These losses, that alter slightly the form of the Rankine cycle in the T-s diagram, are discussed below:

-The pump and the turbine do not undergo isentropic transformations. Hence, two isentropic efficiencies must be considered.

-The boiler and the condenser can undergo some pressure drops. So, two pneumatic efficiencies must be considered.

-The boiler can have some internal losses for which the heat generated is lower than the heat effectively transferred to the working fluid. So, a boiler efficiency must be considered.

-The pump and the turbine can have other source of irreversibility due to the friction on bearings between moving parts. So, two mechanical efficiencies must be considered.

The comparison of the graph of an ideal Rankine cycle with a real Rankine cycle is represented in figure 2.3



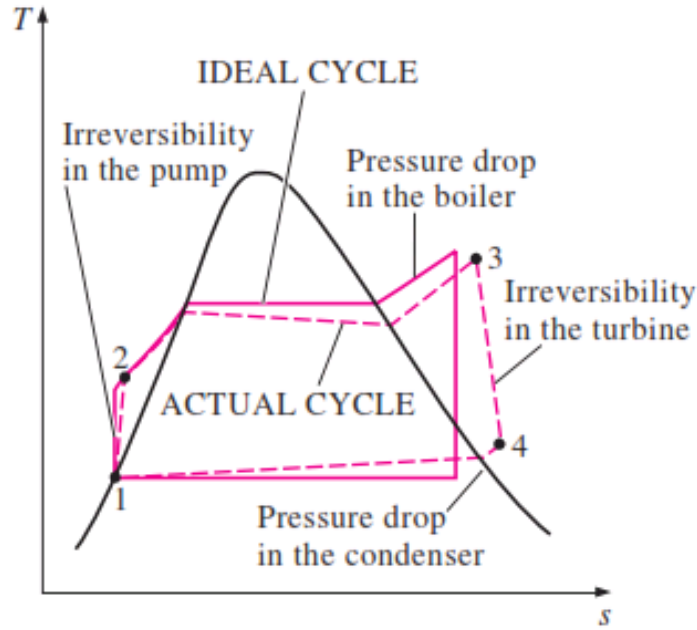


Figure 2.3: Comparison between an ideal Rankine cycle and a real Rankine cycle [33]

During the fluid compression phase (trait 0-1), the irreversibility due to the isentropic efficiency of the pump cause an increase in entropy in the system: in fact, in the ideal cycle the trait 1-2 results vertical (i.e., with constant entropy), while in the real cycle the line is oblique (entropy increases). The same thing happens in turbine expansion (tract 3-4), and for the same reason there is an increase in entropy that causes a decrease in the available enthalpy jump, thus decreasing the work produced.

In order to take these two phenomena into account, the isentropic efficiencies of the pump and of the turbine can be defined as it follows

$$\eta_{is,pump} = \frac{L_{01,id}}{L_{01,re}} = \frac{h_{2,id} - h_1}{h_2 - h_1} \quad (2.7)$$

$$\eta_{is,turbine} = \frac{L_{34,re}}{L_{34,id}} = \frac{h_3 - h_4}{h_3 - h_{4,id}} \quad (2.8)$$

The pressure drops inside the boiler and the condenser cause a gap between the ideal line and the real line: in particular, the real transformations occurring in the components are located below the isobaric line (that indicates the ideal transformations).

The heat losses inside the boiler, that cause a reduction of the heat transferred to the working fluid, can be accounted by defining the boiler efficiency as it follows

$$\eta_b = \frac{Q_{12,re}}{Q_{12,id}} \quad (2.9)$$

Using the first principle of thermodynamics and considering the efficiencies of the components, the exchanges of work and heat in the real basic cycle are:

$$\text{-Pump: } |L_{12}| = \frac{h_{2,id} - h_1}{\eta_{mecc,pump} \cdot \eta_{is,pump}} \quad (2.10)$$

$$\text{-Boiler: } Q_{23} = (h_{2,re} - h_1) \cdot \eta_b \quad (2.11)$$

$$\text{-Turbine: } L_{34} = (h_3 - h_{4,id}) \cdot \eta_{mecc,turbine} \cdot \eta_{is,turbine} \cdot \eta_{alternator} \quad (2.12)$$

$$\text{-Condenser: } |Q_{41}| = h_{4, re} - h_1 \quad (2.13)$$

The real first-law efficiency can be defined again as  $\eta_{th} = \frac{L_{34} - |L_{12}|}{Q_{23}}$  and it is surely lower than the ideal first-law efficiency.

## Chapter 2.2: Organic Rankine Cycle (ORC)

The Organic Rankine Cycle (ORC) [34] is essentially a type of Rankine cycle that uses substances with a lower working temperature with respect to water (usually, organic fluids and that's the reason behind the term "organic") as working fluids in order to generate power from relatively low temperature sources. As stated by the book "Organic Rankine Cycle (ORC) Power Systems" [35]: "ORCs are the unrivalled technical solution for generating electricity from low-medium temperature heat sources of limited capacity". This means that, taken a low-temperature source that is potentially exploitable for the energy production, the ORCs represent the best technological solution, much more than conventional Steam Rankine Cycles or Turbogas Cycles, to produce electricity. This feature can assume a key importance nowadays because it becomes a potential solution to convert efficiently low-grade heat renewable sources (such as: waste heat energy from other thermal systems, solar energy, geothermal energy, biomass products, and so on) into electricity.

Since the ORC is a type of Rankine cycle, scheme of its implant is very similar to the ones discussed in the previous paragraph, and it is shown below in figure 2.4

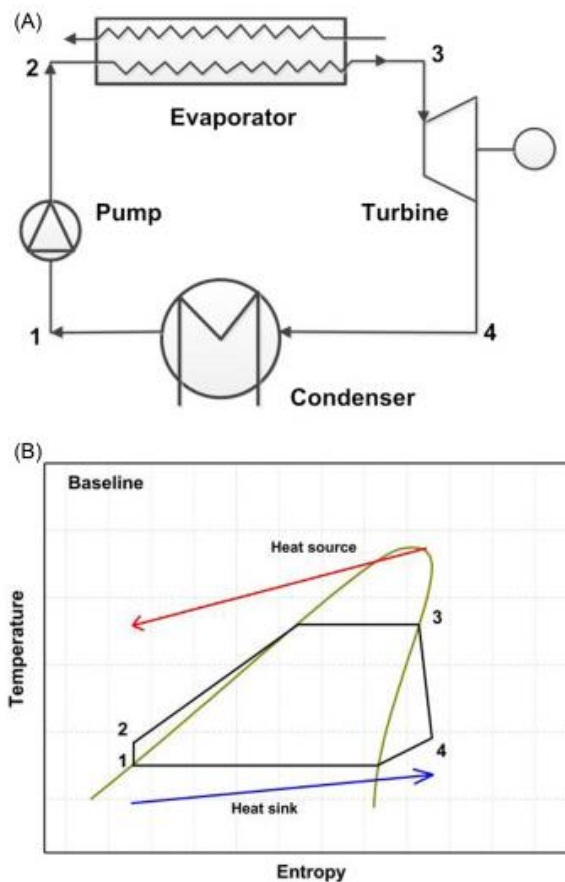


Figure 2.4: Base ORC subcritical cycle, (a) Working scheme, (b) typical T-s diagram [36]

In the system shown in Figure 2.4, the working fluid passes through a pump that increases its pressure, then is heated up in the evaporator (conceptually, it is a component that works in the same way of the boiler, in the sense that it takes a liquid fluid and evaporates it). Then, it expands through a turbine (that is also called “expander”) and finally it is condensed in such a way that returns in a fully liquid form to the pump.

With respect to the steam Rankine cycle, there are some differences. The first main difference can be easily seen by comparing the figure 2.4 with the figure 2.3: even if the fundamentals of the cycle are the same, the shape of the cycle in the T-s diagram is slightly different. The reason behind this diversity is due to the different shape of the lines of the saturated liquid and vapour for the water and the organic fluid. For the last one, it can be seen that the expansion phase (3-4) happens entirely in the superheated vapour zone, and also in the condenser it does not enter a saturated mixture (liquid + vapour), but again a superheated vapour. Other differences are in the working conditions of the components. For the boiler, since it works with lower temperatures, it undergoes less thermal stress and so it can be more compact. This matter can be applied also to the turbine which, having a lower enthalpy jump, does not need all the stages that are used in steam cycles, but only one is sufficient. Moreover, as it can be deduced from the definition of the Carnot efficiency (that is the upper limit that each thermodynamic cycle can reach in terms of efficiency), the usage of lower maximum temperatures inside the cycle implies a reduction of the maximum efficiency that can be reached. Typically, the overall efficiency does not exceed the 15%.

## **Chapter 2.3: Types of organic fluid utilised in the ORC powerplants**

As a starting point, it can be helpful to understand why the usage of air or water is not suitable for ORC powerplants. In fact, when talking about the usage of organic fluids, the first thing that comes to mind is their economic cost, that is much higher if compared to the air and the water, that are relatively free and easily accessible.

The main reason behind the choice of organic working fluids is that in case of usage of low-medium temperature sources, they are much more performance-oriented, if compared to air and water.

For instance, the air is a fluid with a very low “thermodynamic quality” [37]. A gas cycle (that is the one typically used for applications in which the air is the working fluid), with a maximum temperature of 250 °C (that can represent a typical value for low-medium heat renewable sources), an outdoor temperature of 15 °C, under other reasonable assumptions, has an ideal cycle efficiency below 10%.

For what regards the water, the first thing that can be stated is that, every working fluid that undergoes a Rankine cycle in the same conditions previously discussed for the air, gives almost the same value of total efficiency. So, basing only on this statement, it seems that the water should be a reasonable choice. But in the reality, it is not. The problem with the choice of water for ORC systems is that, due to its thermochemical properties, it requires the adoption of capital-intensive multistage turbines with a very complex design. This solution can be used in case of big powerplants that operate with very high temperatures, but not for an ORC in which the use of single stage turbines, that are cheaper and less complex, is strongly desired.

As a matter of fact, for working temperatures of interest ( $>100$  °C), the usage of a single-stage action turbine would result in: high supersonic flows at the stator exit (hence, converging-diverging inter-blade channels must be adopted), high peripheral speed, high liquid content in the fluid discharge and high volumetric flow rate ratio between inlet and outlet conditions. The adoption of a reaction turbine would help with the first two points, but it would give as a result even higher peripheral speed. Hence, since the design of a turbine that works in a limited temperature range with water as working fluid

would require complex and costly solution, it is preferred to use another working fluid (with higher molecular mass, higher molecular complexity and lower critical pressure) that allows to use a single-stage turbine with easy design and low cost.

All of the advantages, for the generation at low temperatures, of an ORC with respect to a conventional Rankine Cycle, can be summed up as it follows [37] [38]:

- Optimal values of enthalpy drop and volume flow rate in the turbine
- Reduced cost of components
- Higher thermal efficiency and power generation

The choice of a working fluid is a very critical point in the ORC systems. Indeed, the working fluid should respect a series of constraints related to the working conditions of the system, to the cycle efficiency, and to some hygiene, biocompatibility and safety matters. For this reason, the main aspects for the choice of an organic fluid for an ORC are now discussed in the following paragraphs.

### 2.3.1: Type of ORC fluid basing on the slope of the saturated fluid on the T-s diagram

Typically, concerning the slope of the saturated fluid on the T-s diagram, three kind of organic fluids can be identified [39]

-Dry fluids ( $\frac{dT}{ds} > 0$ )

The fluids that belong to this category are characterized by the fact that they arrive at the turbine inlet in the form of saturated vapor and become superheated steam after isentropic expansion.

Some examples of dry fluids are: Benzene ( $C_6H_6$ ), Toluene ( $C_7H_8$ ) and Freon (R-113)

An image of a typical T-s diagram of an ORC with a dry fluid is reported below in figure 2.5

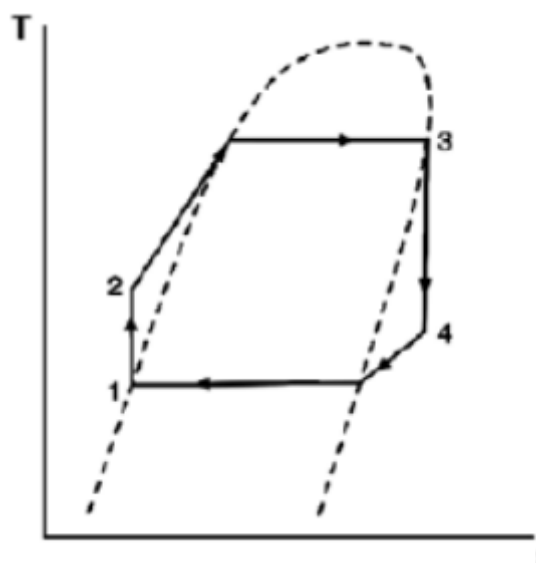


Figure 2.5: Base ORC cycle realized with a dry fluid [40]

-Isentropic fluids ( $\frac{dT}{ds} = 0$ )

An isentropic fluid is characterized by the fact that the upper saturated curve has an almost vertical shape. If an isentropic fluid is implemented in an ORC, it will arrive at the turbine inlet in the form of saturated vapor and it will remain on the upper saturated curve during the whole isentropic expansion of the turbine. Hence, at the condenser inlet it will arrive a saturated vapour.

Some examples of isentropic fluids are: Freon (R-12, R-11 or R-134A)

An image of a typical T-s diagram of an ORC with an isentropic fluid is reported below in figure 2.6

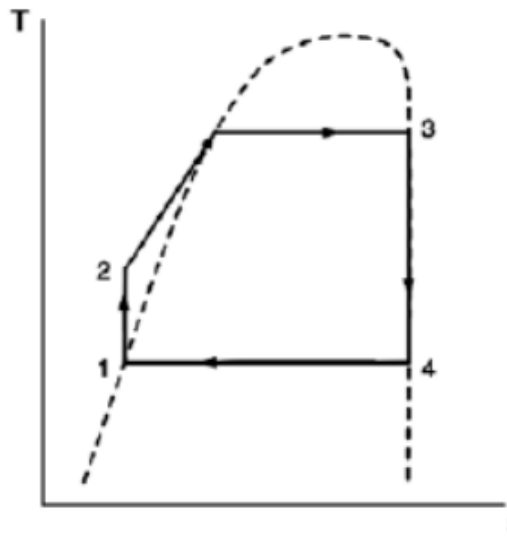


Figure 2.6: Base ORC cycle realized with an isentropic fluid [40]

-Wet Fluids ( $\frac{dT}{ds} < 0$ )

The wet fluids (like water) are typically characterized by a low molecular weight. As it can be easily seen in the figure 2.7, during the expansion phase of a wet fluid, liquid droplets are formed and thus there is the serious risk of damage for the blades of the turbine. One potential solution is to implement a superheating strategy, in such a way to maintain an elevate title at the turbine outlet.

Some examples of wet fluids are: Water (H<sub>2</sub>O), Ammonia (NH<sub>3</sub>) or a mixture of these two.

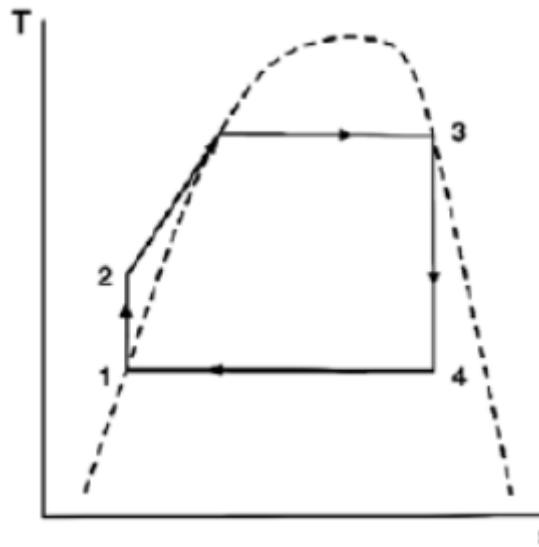


Figure 2.7: Base ORC cycle realized with a wet fluid [40]

The information contained in this section permit to understand better the sentence discussed at the beginning of this paragraph: it is easily understandable that the dry fluids (like water) are not indicated for a use in an ORC. It is generally better to choose a dry or isentropic type of fluid.

### 2.3.2: Thermodynamic properties requirements

The most important chemical properties requirements are for density and latent heat of vaporization.

-Latent heat of vaporization: the latent heat of vaporization is defined as the heat required to change one mole (or one kilogram) of liquid at its boiling point under standard atmospheric pressure. Generally, when working with high-temperature energy sources, it is better to use substances with high latent heat of evaporation since they can absorb more energy during the heating phase. However, when talking about low-temperature resources, substances with low latent heat of evaporation are preferred. The reason is that, thanks to the reduced vaporization heat of the organic fluids, the biggest part of heat exchange in the evaporator involves the sensible heat, thus leading to the reduction of the formation of irreversibility during the heat transfer phase. This result is further shown in figure 2.8

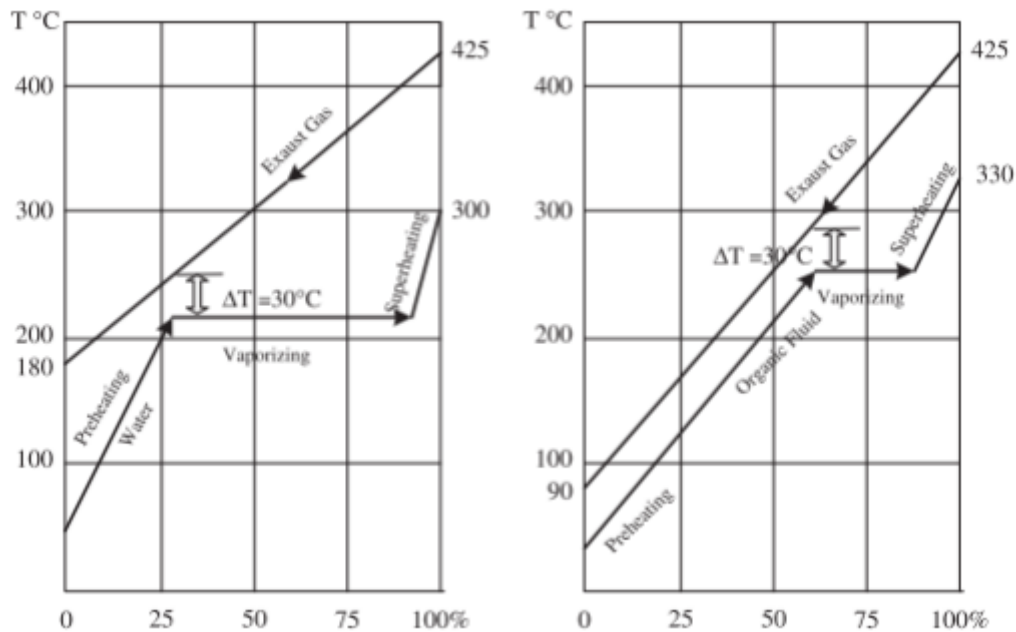


Figure 2.8: Effect of the latent heat on the formation of irreversibility during the heat exchange phase [41]

-Density: for what regards the density, typically the working fluids with high density are preferred. The reason is that a low value of density leads to low volume flow rates and so to high heat exchange areas required

### 2.3.3: Chemical Properties requirements

The most important chemical properties requirements for the working fluid of an ORC regards: the critical temperature and pressure, the molecular weight, the thermal stability and material compatibility.

-Critical temperature: the critical temperature of a liquid, that is the minimum value of temperature for which a liquid cannot be liquified (no matter how much pressure is applied) is a function of the strength of the intermolecular interactions that binds the molecules of a substance together as a liquid [42]. High critical temperatures lead to higher turbine inlet temperatures (and so, high efficiency) but, on the other hand, it produces also lower condensing pressures, that can lead to the infiltration of non-condensable gases. Low critical temperature fluids perform better for supercritical cycles, but they also risk degradation if the temperature reached is too high. However, as a rule of thumb, Henrik & Per [43] clearly stated that higher critical temperature fluids give superior performance.

-Critical pressure: for what regards the critical pressure, its value is also important since, if the evaporation pressure in the evaporator reaches that value, the characteristics of the working fluid can undergo enormous changes: even slight temperature changes generate massive pressure changes, which make the entire system unstable. Moreover, if the evaporation pressure is near the critical pressure, dry organic fluids risk to exit the turbine in a bi-phase condition, that can destroy the turbine's blades. For this reason, the maximum pressure of the cycle must be lower than the critical pressure [44]

-Molecular weight: for what regards the molecular weight, it has been demonstrated [42] that it is inversely proportional to the enthalpy of vaporization. For this reason, it is preferable to use fluids with high molecular weight: in such a way, with a lower enthalpy drop, the usage of single-stage turbines is facilitated

-Thermal stability: Differently from the water, the organic fluids tend to chemically decompose and degrade at high temperatures. For this reason, before using an organic fluid for an ORC, it is of crucial importance to check that the temperature of thermal stability is higher than the maximum temperature reached in the cycle. Hence, the maximum temperature of the heat source is therefore limited by the chemical stability of the working fluid

-Material compatibility: Since the working fluid will flow inside all of the components of the cycle, it is important to check that it will not act as a corrosive material with the objects with which it will come into contact

-Safety and Environmental aspects: Even if the working cycle is closed, the risk of leakages highlights some limits and requirements that the working fluid of the ORC must respect. For what regards the safety aspects, for the security of the people that works in the ORC powerplant, it is necessary that the working fluid is non-toxic and non-flammable. For what regards the environmental aspects, the working fluid must guarantee: zero ozone depletion potential (ODP), minimal global warming potential (GWP) and low atmospheric lifetime (ALT)

### **2.3.4: Transport Properties requirements**

The two main requirements regard the dynamic viscosity and the thermal conductivity

-Dynamic viscosity: As it is known from the fundamentals of fluid dynamics, the dynamic viscosity is proportional to the distributed friction losses by means of the Reynolds number. For this reason, fluids with low dynamic viscosity are chosen.

-Thermal conductivity: it is better to use working fluids with high thermal conductivity because they facilitate the heat transfer and consequently the size of the heat exchangers can be reduced.

It is possible to conclude this paragraph on the requirements of the organic fluid by saying that it is generally desirable to use working fluids that are economic and easy to produce.

## **Chapter 2.4: Types of expanders utilized in ORC powerplants**

For the correct and efficient design of a system, the accurate choice of the components is a crucial aspect that must be carefully studied.

In the design phase of an ORC, this matter regards the correct choice of the pump, evaporator, turbine and condenser. For what regards the evaporator and the condenser, since they are basically two heat exchangers, they can be appositely sized by using the most famous methods known in literature (for example, the  $\epsilon$ -NTU method) and so the design phase can follow some standard procedures. For what regards the pump, again the state of the art is such advanced that its choice does not generally present a big problem. On the other hand, for the turbines the situation is much different.

In an ORC system, the turbine represents the most technically advanced component and, in the comparison between an ORC and the conventional Rankine Cycle, it is the component that mostly changes. Indeed, the turbine of an ORC must be appositely designed to complete the whole expansion of the fluid in only one stage. Depending on the particular configuration of the system, the usage of one kind of turbine with respect to another can greatly change the efficiency of the cycle and so, since the overall efficiency (as previously anticipated) is particularly low due to the exploiting of low-medium temperature resources, the usage of a correct turbine is of fundamental importance in order to avoid some further big reductions of the efficiency. In the following, a list of the most used kind of turbines with their relative range of applications will be presented.



The fluid machines are mainly divided in two groups [45]: turbo-machines and volumetric machines.

-The turbo-machines are instruments that work with a continuous stream of fluid. The dynamic of the power generation is the following: while the stream passes through a series of blades, its dynamic pressure is converted into mechanical energy, that is represented by the rotation of the turbine. Turbomachines are typically used for large-scale applications and boast a high level of efficiency.

-The volumetric machines are instruments that work by insulating finite quantity of fluid. They are also known as “positive displacement machines”. The dynamic of the power generation is the following: the pressurized fluid is introduced into a chamber, that is composed by mechanical elements that are free to move. The pressure of the fluid applies a positive force on the mechanical elements, that so give as a consequence an increase of the chamber volume (positive displacement) and so a generation of mechanical work. For smaller power output (<50 kW), volumetric machines are frequently the preferred choice.

Both turbomachines and volumetric expanders have their own advantages and disadvantages along with several types available for each main category.

In the following two paragraphs (2.4.1 and 2.4.2) both the two categories of turbines will be explored more in detail and the most common machines available on the market will be shortly presented.

### 2.4.1: Turbo-machines

In the turbo-machines, also called “turbo-expanders”, the high static pressure of the fluid that comes out from the boiler is converted into high-flow velocity when it passes through nozzles. The high-velocity fluid passes through an array of blades, by causing their rotation. This rotation is passed through a shaft to the alternator, that exploits this movement to generate electricity.

Turbo-expanders have two main categories: axial turbines and radial turbines. The main difference is that: in axial turbines, the flow of the working fluid is parallel to the shaft, meanwhile, in radial turbines, it is radial to the shaft at the inlet of the turbine and axial at the outlet.

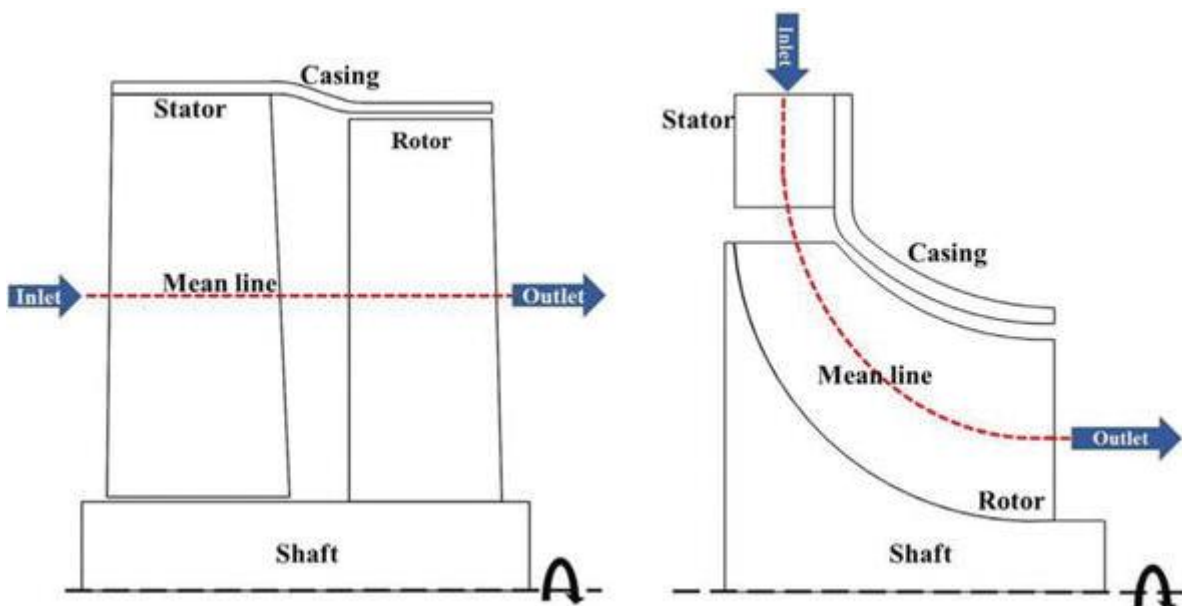


Figure 2. 9: Image of axial (left) and radial (right) turbines [45]

The selection of the appropriate turbine depends by the desiderated operating conditions.

In case of high mass flows and low pressure drops required, the axial turbines represent the preferred choice. The reason is that they can maintain a high efficiency due to the elimination of the flow turning in the meridional plane. Moreover, usually the disc of an axial turbine is protected at high temperatures since only the blades are exposed to the heat. On the other hand, in the radial turbines both the blades and the disc are exposed to the heat. Axial turbines also have better performances in case of off-design conditions

In case of low mass flows and high pressure drops required, the radial turbines represent the preferred choice. In these conditions, the usage of an axial turbine would require very small blades that will produce as a consequence an efficiency drop due to the difficulty of maintaining small tip clearance between the blades and the casing, meanwhile, for the radial turbines, there is lower sensitivity to the blade profile. Another reason to choose a radial turbine instead of an axial one, is the fact that the working conditions of an ORC, the usage of an axial turbine would require more expansion stages, while the usage of a radial turbine requires a unique stage thanks to the radius reduction from the rotor inlet to the exit.

Now, the main types of turboexpanders are rapidly commented

#### -Radial Inflow Turbines (RIT)

In the Radial Inflow Turbines, the high-pressure fluid enters the casing (volute) inlet with a flow that is mainly radial. Then, as the flow enters to the inlet of the rotor, it assumes also a tangential component. Later, as the flow passes through the rotor, the tangential component is gradually lost and the radial component is converted into axial. At the rotor exit, ideally, in a radial inflow turbine, the flow is purely axial.

Radial Inflow machines are often manufactured by using the casting process. The possibility of using this technique represents an advantage since, with respect to the production of axial machines, that often requires that the rotor and the blades undergo separated manufacturing processes, the RIT can be manufactured as single pieces. In such a way, the turbine is stiffer and it has a better rotor-dynamic stability. Then, as already anticipated, while the downsizing of an axial machine to the scale requested an ORC can create different problems that lead to efficiency losses, the radial turbines does not suffer these problems. They can be easily downsized, and also, they support much higher pressure ratios.

The scheme and the section of a Radial Inflow Turbine is represented in figure 2.10.

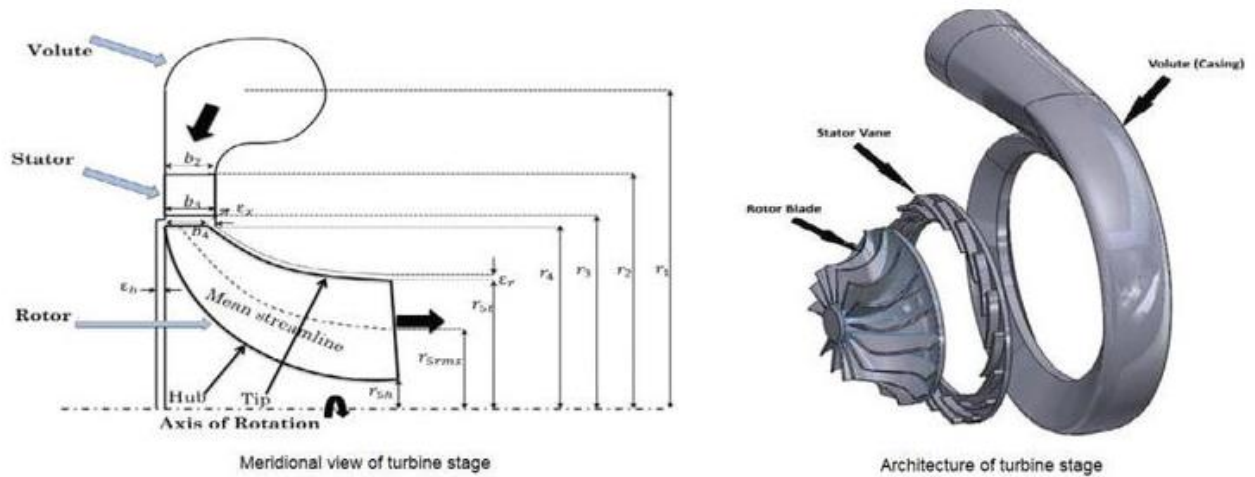


Figure 2.10: Representation of a Radial Inflow Turbine [45]

### -Radial Outflow Turbines (ROT)

In a Radial Outflow Turbine (ROT), the direction of the flow is exactly the opposite to one of the Radial Inflow Turbine. Indeed, in this case, the flow enters at the centre of the turbine, near the axis of rotation, with only an axial component, and then it travels outwards in the radial direction while passing through arrays of rotor and stator blades. The Radial Outflow Turbines have an enlargement in the area as the flow moves in a radial direction which means supersonic flows can be avoided and losses can be reduced to end up with high-efficiency turbines.

A ROT is characterized by multi-stator-rotor ring arrangements in the radial direction. In this way, the machine keeps low peripheral speeds, and so the mechanical and bearing stresses can be easily handled.

As a disadvantage, with respect to the RIT, a ROT has slightly lower efficiencies. Furthermore, for heavy/large-molecule working fluids, the first stage often has insufficient flow passage area and so, therefore, the turbine application is limited only to high-temperature applications.

An image of a Radial Outflow Turbine is represented in figure 2.11

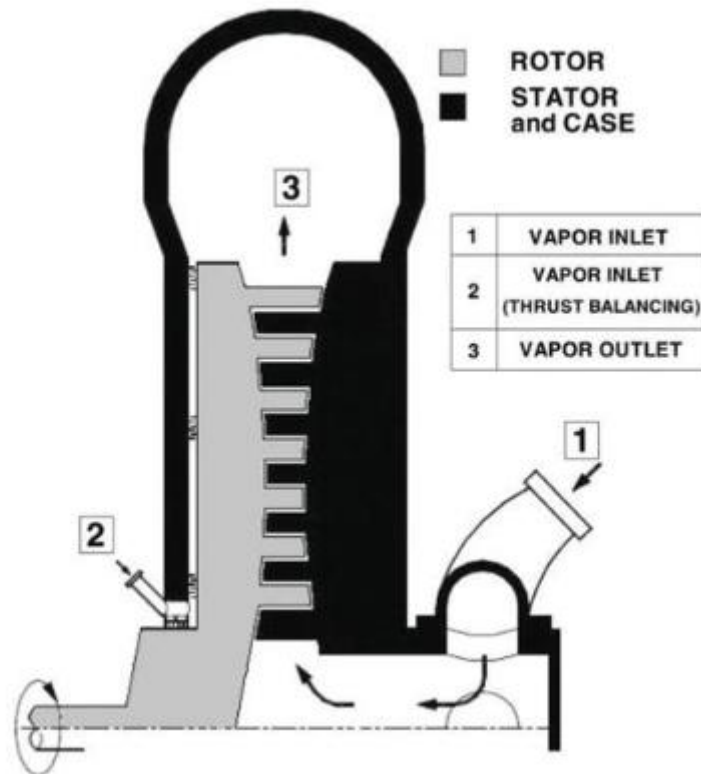


Figure 2.11: Representation of a Radial Outflow Turbine [45]

### -Axial Turbines

In the axial turbines, as previously anticipated, the primary flow of the working fluid is always in axial direction and parallel to the rotational axis.

For the large power generation, they are the most used machines. The most important reason is that, in large scale operation, they present very high values of efficiency. Another reason is that they are a very flexible kind of machines: the operating pressure can go from some bars (last stages of the steam cycle) to 300 bar (supercritical cycle) and the diameters can go from few centimetres to hundred of meters (like in the wind turbine applications).

On the other hand, as previously said, they are not so much used for the ORC because they are limited by the fact that considering large-stage expansion ratios, the axial channel undergoes span-wise enlargements with a consequent creation of losses.

### 2.4.2: Volumetric Machines

The volumetric expanders are machines in which the fluid movement is not continuous (like in the case of the turbo-machines), but cyclic.

One typical characteristic of the volumetric expanders is the fact that they operate with a fixed volume expansion ratio. Because of that, the thermodynamic cycle must be designed for the optimum expansion ratio of the turbine. In fact, even if a higher pressure ratio with respect to the optimal one could give an efficiency increase, it will also generate some over-expansion losses that will limit the overall performance.

The volumetric turbines are also called “displacement expanders” because during their operation, a volume of fluid is trapped and displaced into the discharge of the machine. This pressure drop is the responsible of the generation of mechanical work.

Another peculiarity of volumetric expanders is related to their need of lubrication requirement. Lubrication is needed to prevent the elevate wear that is caused by the high friction generated by the mechanical parts that move to create the volume expansion. The most common solution is to use lubricant oils that go inside the working fluid. Then, the oil can be circulated in the complete ORC cycle or just inserted in the volumetric chamber for the expansion phase. If the last case represents the desired solution, there is the need of using appropriate oil separation systems, that increase the overall system costs and complexity.

In the following, the most important types of volumetric expanders are briefly described

#### -Scroll Expanders

A Scroll Expander is an instrument that consist of two spirals: the first one is an orbiting scroll and the second one is a fixed scroll. The orbiting scroll moves along with the fixed scroll with tight tolerances. The representation of a Scroll Expander is represented in figure 2.12

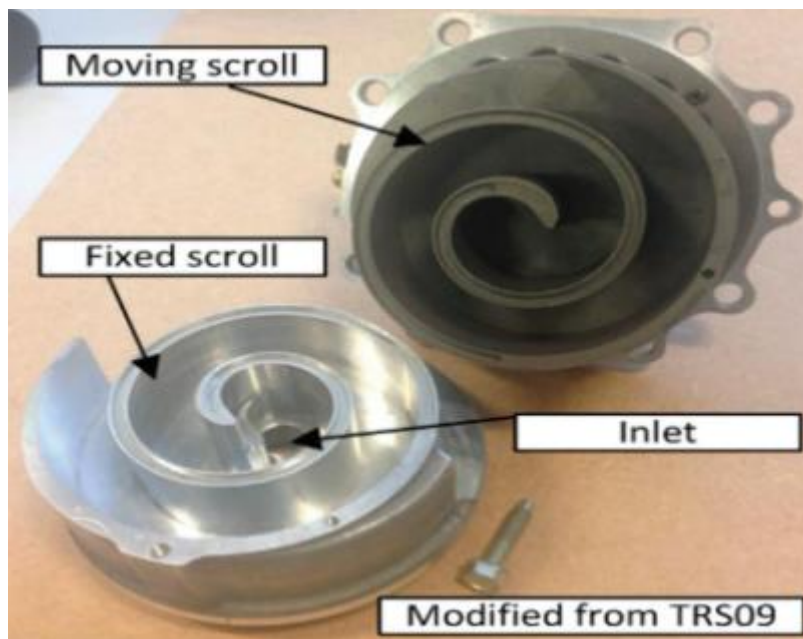


Figure 2.12: Representation of a Scroll Expander [46]

The low parts count feature makes the Scroll Expanders perfect for small-scale applications: their simplicity of design gives high reliability and cost-effectiveness and low noise.

The working fluid enters from the centre and goes out moving inside the space created between the two scrolls. The increase of the fluid volume of the expansion chambers produce the pressure decrease that will generate the work.

Scroll expanders can be divided in two main types: compliant or constrained. In the compliant Scroll Expanders, it is necessary to use a lubrication system in order to reduce the friction between the

contacting sidewalls. On the other hand, in the constrained Scroll Expander, thanks to a linking mechanism between the rotating and the fixed scroll, the lubrication is not required.

Some typical operating values of the Scroll Expanders can be given in order to have some order of magnitude:

The operating speeds are around 3600 RPM. This value is adequate to have a direct coupling with the electric generator.

The typical power output is relatively low: between 0.5 kW and 10 kW.

The volumetric ratio is between 1.5 and 5 and the efficiency is usually around 80%.

Since volumetric ratio is small if compared to other types of expanders, nowadays there are some attempts that lead to increase that coefficient. One of the possible studied solutions seems to be the utilizing variable thickness walls; however, no such commercial unit is available yet.

#### -Screw Expanders

A Screw Expander is an instrument that consist of two helical rotors that are designed with an accurate profile to trap the required amount of the working fluid. The representation of a Scroll Expander is represented in figure 2.13

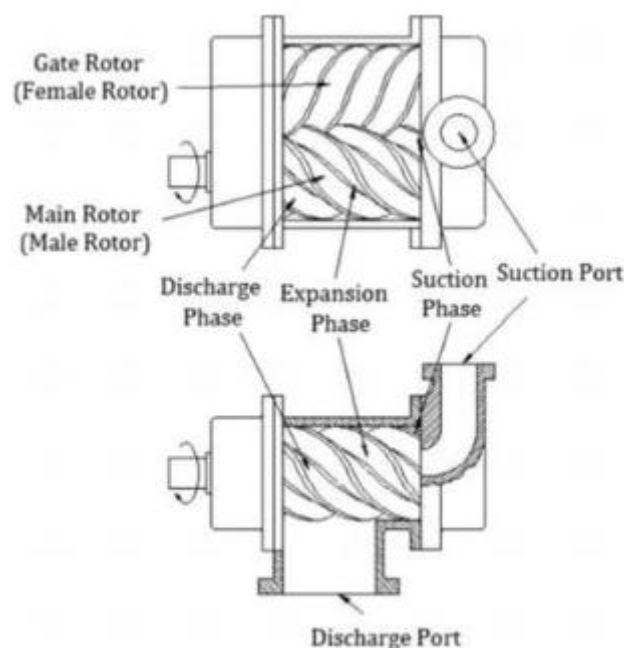


Figure 2.13: Representation of a Screw Expander [45]

The synchronized movement of the two rotors generates volume chambers that start at one end of the rotor and terminate at the other end. In these chambers, the working fluid is expanded. Since the two rotors move with direct contact, in a Screw Expander the lubrication is always needed. However, as previously discussed, one way to avoid to install a lubrication system (that increases the overall complexity and enhances the costs) is to use a fluid with lubrication capacity.

Some typical operating values of the Screw Expanders can be given in order to have some order of magnitude:

The operating speeds in general for screw machines are around 5000 RPM, so higher than the Scroll Expanders. For this reason, the usage of a gearbox can be possible.

The typical power output can range from some kilowatts up to 1 MW.

The volumetric ratio is between 2 and 8 and the isentropic efficiency is usually maximum 70%.

Thanks to the very small rotor clearance (that is below 50  $\mu\text{m}$ ), the leakage losses are comparatively small, thus reducing friction losses.

#### -Piston Expanders

The piston expander is the type of volumetric machines that is most used for ICE. In a piston expander, the working fluid enters when the piston is around the Top Dead Centre (TDC). Then, the fluid expands and mechanically pushes the piston, with the consequent creation of work. This work is transferred to the central crankshaft by connecting rod. After the expansion phase, when the surface of the piston is at the Bottom Dead Centre (BDC), the piston moves again to the TDC and by doing that it pushes the exhaust fluid away. The representation of a Piston Expander is represented in figure 2.14

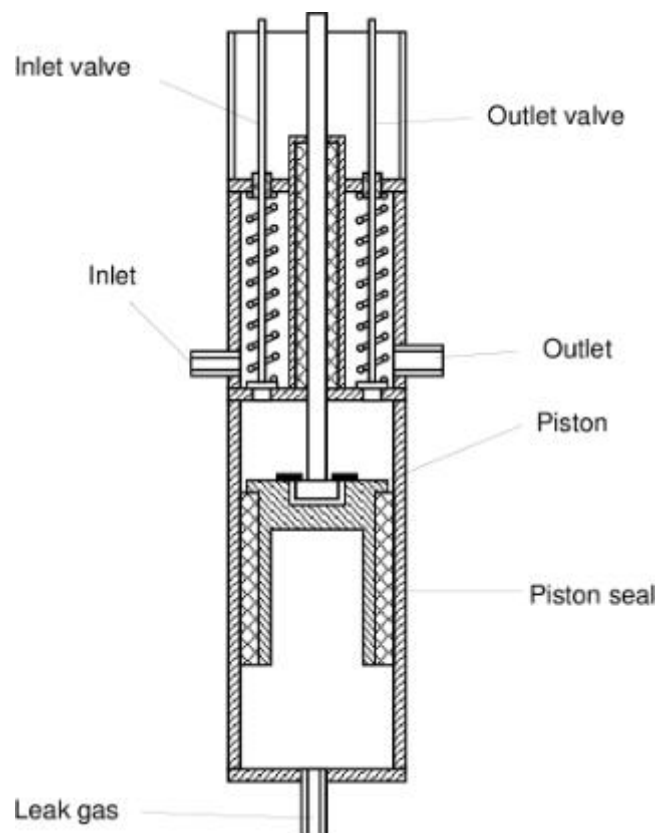


Figure 2.14: Representation of a Piston Expander [47]

As it can be seen from figure 2.14, unlike the previous categories of expanders that has been reported, the piston expanders need an inlet and an outlet valve in order to let the fluid go respectively in and out. Another difference is that the Piston Expanders can operate also under two-phase conditions of the working fluid (liquid + vapour). Like the Screw Expanders, also Piston Expanders need a lubrication system. However, they are heavy and suffer from noise and vibration. The piston expanders mainly suffer from the requirement for weight balancing, torque impulse, heavy weight, precise valve operation, and a large number of parts but they have mature manufacturing technology available.

Some typical operating values of the Screw Expanders can be given in order to have some order of magnitude:

The power output of the Piston Expanders with steam as working fluid is typically low: about a dozen of kilowatts.

The isentropic efficiency of a Piston Expander is generally lower than the one of the turbomachines: 50% as average value

The operating pressure ratios are relatively big: in the range 6-14 bar

-Rotary Vane Expanders

The Rotary vane expanders are machines that operate by exploiting the Wankel concept. The representation of a Rotary Vane Expander is represented in figure 2.15

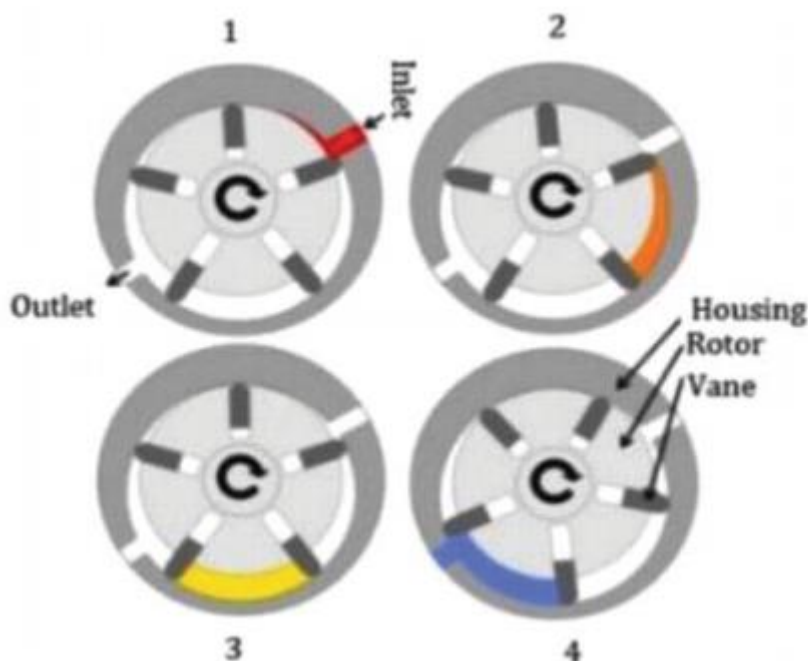


Figure 2.15: Representation of a Rotary Vane Expander [45]

As it can be seen, the machine is composed by a case (called “Housing”) and an internal rotor, that has moveable vanes. First of all, the working fluid (with a very low volume, i.e. in a compressed state) enters by the inlet point. Then, thanks to the rotation of the rotor, it is trapped into the space between two vanes. As the rotation angle increases, also the volume on the chamber in which the



fluid is trapped increases. So, the fluid undergoes an expansion and produces work. Once that the fluid is exhausted, it exits the machine from the outlet port.

The Rotary Vane Expanders are characterized by: by small vibration, low acoustic impact, and simple and reliable structure. Moreover, they have low system costs thanks to the simple design and consequent low manufacturing cost. As all of the other volumetric machines that have been presented, also the Rotary Vane Expanders need a lubrication system, that is useful to minimize wear.

Some typical operating values of the Screw Expanders can be given in order to have some order of magnitude:

The power output is typically very low: it ranges from few Watts to 2.2 kW.

The rotational speed is also very low: for this reason, just like the Scroll Expanders, the Rotary Vane Expanders can be directly attached to the generator.

The isentropic efficiency, with respect to the other types of volumetric expanders, is generally lower due to leakages and higher friction losses.

The volumetric ratio is limited in the range 3-7 and the maximum temperature reached is also very low: often less than 140 °C.

## **Chapter 2.5: Efficiency improvement techniques for an ORC**

When talking about improvement techniques for an Organic Rankine Cycle, since this typology of implant can work with a vast selection of working fluids, an accurate selection of the working fluid, based on the specified characteristics of the plant, might be the most rapid effective solution.

Then, as a second possibility, the base scheme of the ORC (and, as a consequence, the shape of the thermodynamic cycle) can be also modified in order to improve some aspects, such as the net power production or the efficiency (that, as previously remarked in more occasions, is typically very low). In the following, some of the possible layouts available in literature for an ORC are presented [49]

### **2.5.1: Superheated ORC**

The superheated ORC is essentially a superheated Rankine cycle (also called, “Hirn cycle”). So, the base scheme is the same represented in figure 2.4 and, once that the working fluid has reached the dry saturated steam condition inside boiler, it is heated further through isobaric vaporization to reach superheated steam temperatures.

Finally, it has to be said that, analogously for what happens for the base Rankine cycles, since the superheating increases the highest temperature reached by the cycle, also the efficiency of the cycle increases.

### **2.5.2: Recuperated ORC**

In a recuperated ORC cycle, a new component called “regenerator” is added to the base scheme. More precisely, it is placed after the pump before the evaporator. The recuperator is basically a heat exchanger that allows heat transfer between the superheated vapor at the turbine exit and the subcooled liquid at the pump outlet: on one side of the recuperator, it flows the working fluid in liquid form, after it has passed through the pump; meanwhile, on the other side, it passes the vapour that has just left the turbine after the expansion. The residual heat contained in the vapour that exits

from the turbine is transferred to the subcooled liquid at the pump outlet and so, in this way, the working fluid is pre-heated and some energy savings can be done inside the evaporator.

The scheme of a recuperated ORC cycle is shown in figure 2.16

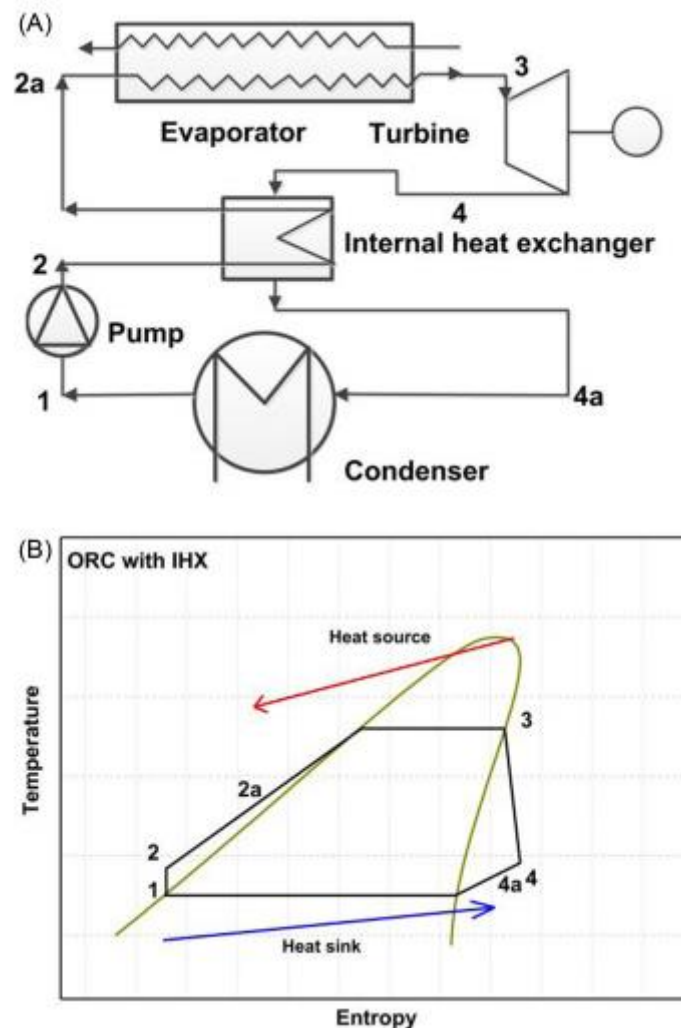


Figure 2.16: Schematics of a recuperated ORC: (A) system schematic and (B) T-s diagram [48]

### 2.5.3: Reheated ORC

In a reheat ORC system, there are two turbines employed: a high-pressure first-stage turbine and a low-pressure second-stage turbine. The expansion on the working fluid is divided in two steps: first of all, the superheated vapor expands in the high-pressure turbine. This expansion does not arrive to the low-pressure level of the cycle (working pressure of the condenser), but it is stopped at an intermediate level called “reheat pressure”. Then, the fluid is delivered back to the evaporator, where it is reheated again up to a certain level of temperature. Then, the re-heated vapour is sent to the second turbine, in which it expands from the intermediate level of pressure reached before to the low-pressure level of the cycle. The reheat technique, if used correctly, allows an increase of the efficiency of the cycle.

The scheme of a reheated ORC cycle is shown in figure 2.17

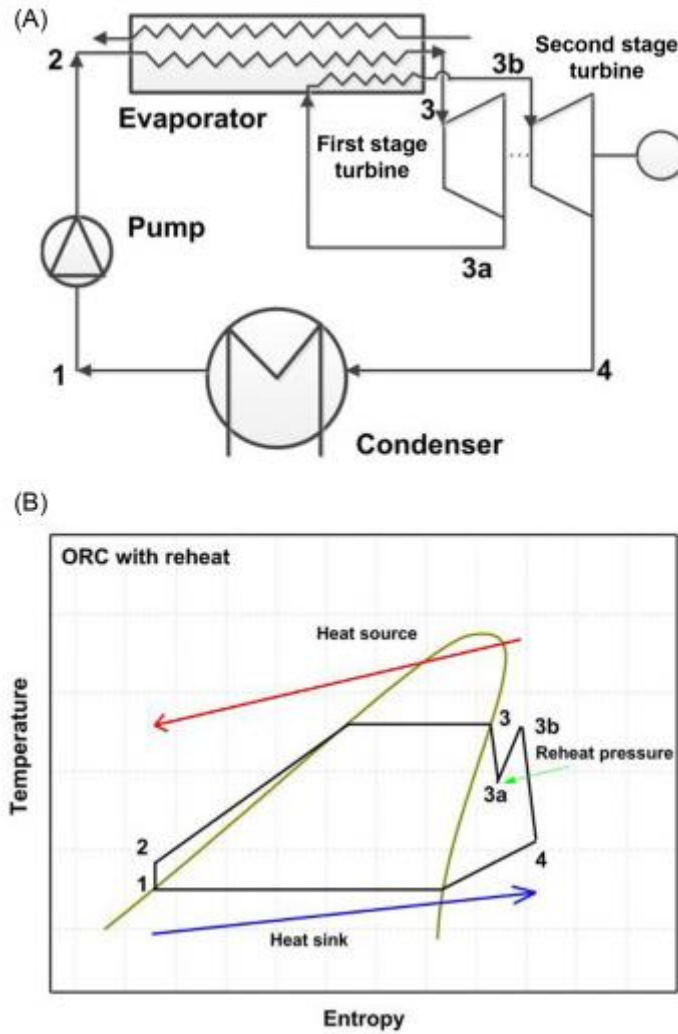


Figure 2.17: Schematics of a reheated ORC: (A) system schematic and (B) T-s diagram [48]

## 2.5.4: Regenerative ORC

In the regenerative ORC cycle, the compression part is split in two stages (hence, two pumps are used) and between these two stages, a new component called “regenerative tank” is added. During the expansion process, part of the working fluid vapor is extracted from the turbine at an intermediate pressure and it is sent to the regenerative tank, where it mixes and exchanges heat with the subcooled liquid pressurized by the first pump. Then, all of the working fluid is pressurized by the second pump and delivered to evaporator. In this way, there is a reduction of the net work (because part of the vapour does not undergo the full expansion but it is stopped at an intermediate pressure level) but some energy savings in the pumping and heating processes are realized.

The scheme of a regenerative ORC cycle is shown in figure 2.18

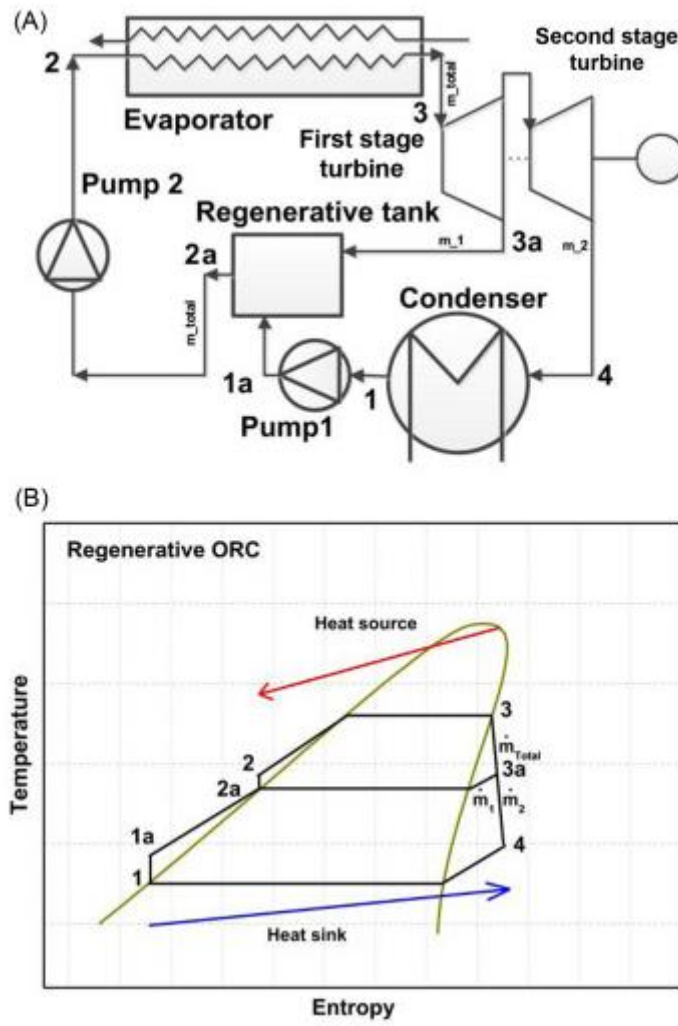


Figure 2.18: Schematics of a regenerative ORC: (A) system schematic and (B) T-s diagram [48]

## CHAPTER 3: Energy Storage Systems<sup>6</sup>

One of the main problems with the renewable energy sources, like the sun or the wind, is that they are intermittent (i.e. the energy cannot be produced arbitrarily at any time). This matter becomes very relevant when talking about grid balancing.

The grid balance is the result of the continuous comparison between the demand of energy by the customers and the available generation made by the suppliers. It is a very complex operation, in which it has to be assured that the amount of electricity produced matches exactly the electricity needed at every moment. The eventual lack of timing between periods of high demand and periods of high supply can create serious problems to the grid. Let's say, as an example, that there is a certain hour during the day in which the renewable sources can produce big amounts of electricity, but the energy demand is very low: if no action is done, all of the energy that could be produced but that will not be used will be unavoidably wasted.

In this scenario, the Energy Storage Technologies are gradually taking place. The possibility of storing energy in periods in which the renewable energy production is higher than the demand, and using that amount of energy in periods in which the energy demand is higher than the production made by the renewables, can generate several benefits such as: energy cost reduction, increase in the flexibility of the energy system and a reduction of the energy consumption.

Currently, the energy can be stored in various forms thanks to the several energy storage technologies that have been developed. Some examples are: mechanical systems, hydraulic systems, electrochemical systems, magnetic storage, hydrogen production etc.

Of course, the choice of the system is strictly dependent by the type of energy that it is requested to store. For example, if in a house with integrated PV panels is necessary to store the electricity produced by the plant in order to use it in the night, it is convenient to use a battery (that is, an electrochemical energy storage system).

In the case of the CSP powerplants, the energy has to be stored as heat that can be used to heat up the working fluids even in periods in which the sun is not present. The energy storage technologies based on the heat storage are often indicated with the acronyms "TES" (Thermal Energy Storage).

The TES [42] are generally classified in three ways: for the duration of the storage, for the operating temperature or for the way in which the thermal energy is stored.

For what regards the duration of the storage, the classification is divided in: short-term TES, medium-term TES and long-term TES. The short-term TES has the duration of some hours and it is used mainly to face peaks of energy demand in a few hours. The efficiency of a short-term TES can reach values up to 90%. The medium-term TES has the duration of some weeks, while the long-term TES can arrive up to several months. The efficiency in these last two cases is slightly lower: maximum 70%.

For what regards the operating temperature, the distinction is between low temperature TES and high temperature TES. The threshold is usually 120 °C. Below that value it is a low temperature TES and above that high temperature TES.

---

<sup>6</sup> Except where specifically indicated, all information in this chapter is referenced to the reference [49]

For what regards the storage technology, it is possible to say that the heat storage systems are typically three: sensible heat storage, latent heat storage and reversible thermochemical heat storage.

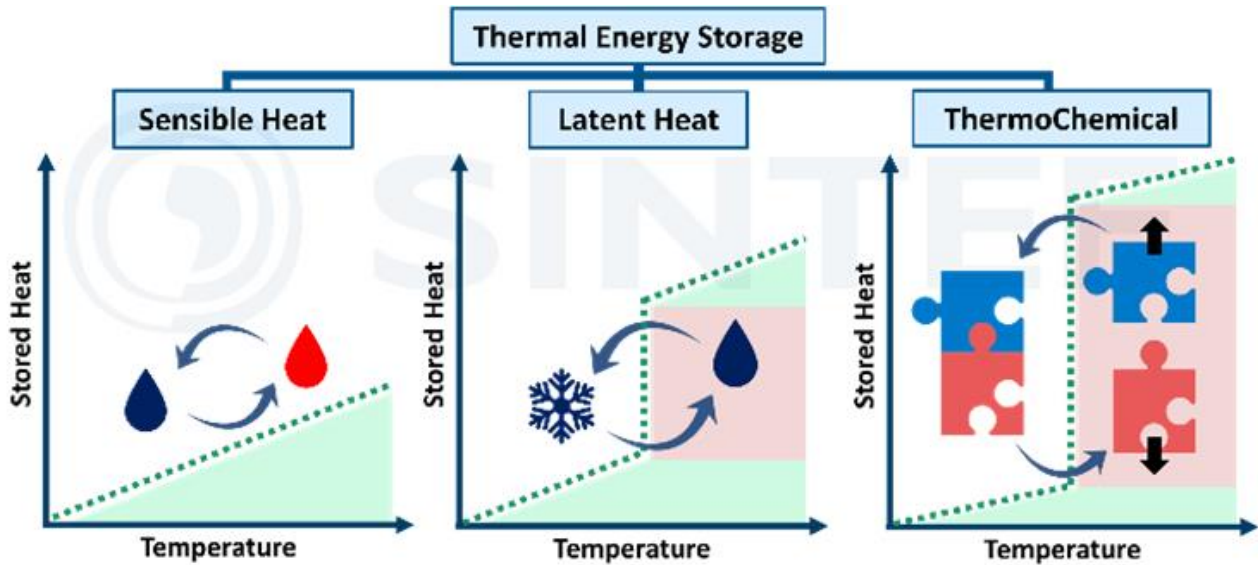


Figure 3.2: Sketches of the possible TES technologies [50]

## Chapter 3.1: Sensible TES

In the sensible TES, the energy is saved by increasing the temperature of a given material.

The energy needed to heat up a storage material with volume “V” from a state 1 to a state 2 is:

$$E = m \cdot c \cdot (T_2 - T_1) = \rho \cdot V \cdot c \cdot (T_2 - T_1) \quad (3.1)$$

It appears clear that the most important quantity for the sensible TES is the product between the density and the specific heat, also called “volumetric thermal capacity”. In the table 3.1 reported below there is a list of the thermal capacity of some materials.

Table 3.6 Thermal capacities at 20 °C of some common TES materials

Material	Density (kg/m <sup>3</sup> )	Specific heat (J/kg K)	Volumetric thermal capacity (10 <sup>6</sup> J/m <sup>3</sup> K)
Clay	1458	879	1.28
Brick	1800	837	1.51
Sandstone	2200	712	1.57
Wood	700	2390	1.67
Concrete	2000	880	1.76
Glass	2710	837	2.27
Aluminum	2710	896	2.43
Iron	7900	452	3.57
Steel	7840	465	3.68
Gravelly earth	2050	1840	3.77
Magnetite	5177	752	3.89
Water	988	4182	4.17

Source: Norton (1992).

Table 3.1: Volumetric thermal capacity of various materials [49]

As it can be seen, among the materials of the list, the water is the one with highest volumetric thermal capacity. This characteristic along with the low cost and availability, and with the easiness to transport, make the water the most used material for sensible TES.

The schematics of a sensible TES system is represented in figure 3.2

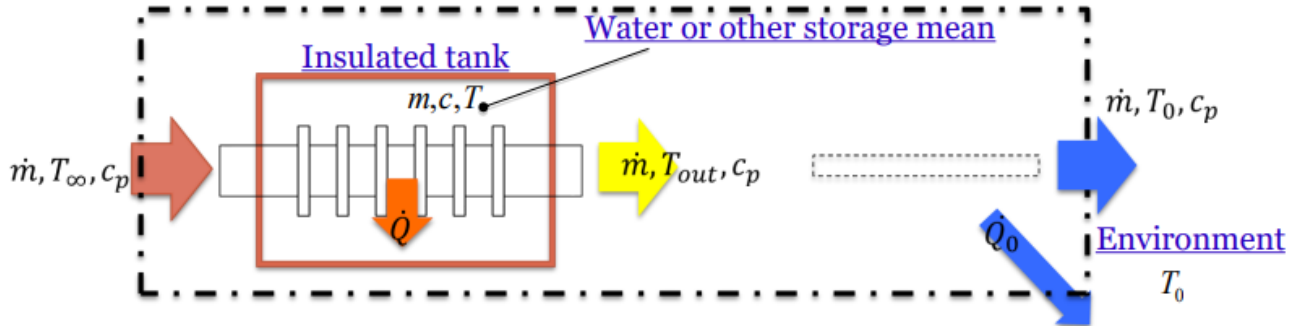


Figure 3.3: Representation of the scheme of a sensible TES system [49]

It is possible to demonstrate that the first-law efficiency of the system can be written as

$$\eta_I = \frac{m \cdot c \cdot (T - T_0)}{m \cdot c \cdot (T_\infty - T_0)} \quad (3.2)$$

Then, for the second law efficiency, it can be possible to state that it is related to a coefficient called “entropy generation number” by the following equation

$$Ns = 1 - \eta_{II} \quad (3.3)$$

It can be generally demonstrated that, in the most general case, considering the pressure losses, Ns is a function of three parameters:

$$\tau = \frac{T_\infty - T_0}{T_0}; \theta = \frac{\dot{m} \cdot c_p}{m \cdot c} \cdot t; NTU = \frac{A \cdot U}{\dot{m} \cdot c_p} \quad (3.4)$$

So, it can be written  $Ns = Ns(\tau, \theta, NTU)$  (3.5)

Krane et. al (1987) demonstrated that, in the optimal case, that corresponds to values of  $\theta_{opt} = 0.83$  and  $NTU_{opt} = 5.53$ , the minimum value obtainable for Ns is 0.734

Another important consideration regards the temperature stratification inside the system. Even if the most important characteristic of a sensible TES is the temperature of the stored liquid, generally it is possible to say that: between two tanks that have the same medium temperature, the one with higher thermal stratification has a greater exergetic content. So, the most recommendable situation is to have a tank well thermally insulated with the best possible stratification.

## Chapter 3.2: Latent TES

The latent TES is an energy storage technology that exploits the latent heat of solidification in order to save the energy.

In general, the latent heat is much greater than the sensible heat: as an example, for the water, the sensible heat is 4.2 kJ/kgK, while the latent heat is 2 MJ/kg. For this reason, the latent TES can save much more energy with respect to the sensible TES.

Typically, the Phase Change Materials (PCM) that are used for the latent TES belong to three categories: Organic PCMs, Inorganic PCMs and Eutectic mixtures.

A situation of all of the possible choices is represented in the figure 3.3, reported below

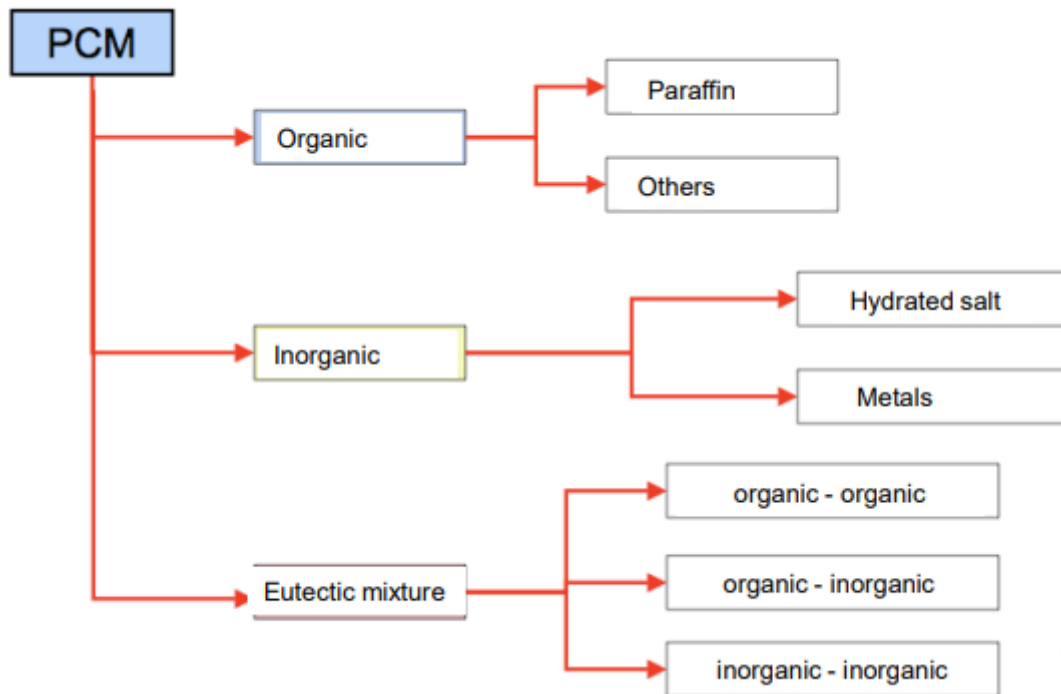


Figure 3.4: Summary of the possible materials used as PCM for latent TES [49]

### 3.2.1: Organic PCMS

As the name suggests, in the Organic PCMs, the materials used for energy storage are organic molecules.

Typically, the organic materials used can be divided in two categories:

-Paraffins

The paraffins are organic compounds that at ambient temperature have molecules with linear structure composed as:  $\text{CH}_3(\text{CH}_2)_n\text{CH}_3$ . The melting point increases with the number of carbon atoms.

-Non-paraffins: that are, materials like fatty acids, esters and alcohols are used.

The Organic PCMs present some advantages and disadvantages

For the advantages:

- They are relatively cheap materials
- They present high thermal density storage
- They are chemically inert, recyclable and with a long-life cycle.

For the disadvantages:



- Low thermal conductivity
- Low density
- Highly Flammable.

### **3.2.2: Inorganic PCMs**

The Inorganic PCMs are materials used for energy storage that are not made by organic substances.

The most important category of inorganic PCM is represented by the hydrated salts, that are salts that in during the crystallization phase include a certain number of molecules of water. The chemical formula of a hydrated salt is represented in that way:  $M \cdot nH_2O$ . For each hydrated salt, the ratio between the number of molecules of the hydrated salt and the number of molecules of water is a well-defined number and constant. The hydrated salts have a melting temperature usually around 120 °C and they are generally less expensive than the paraffines.

Other examples of Inorganic PCMs are: molten salts, metals or alloys.

The advantages of the Inorganic PCMs can be summed up as it follows:

- High storage capacity
- High density
- High thermal conductivity
- Non-flammable.

On the other hand, as disadvantages:

- Corrosive behaviour
- Suffering of the subcooling issue, that is a delay of the solidification process. If subcooling happens, some PCM remains liquid even when the temperature is below the melting point.
- Suffering of segregation, that is an irreversible process where a less hydrated salt is formed with deterioration of the thermal properties and performance of the PCM

### **3.2.3: Eutectic mixtures**

The eutectic mixtures are a mixture of two or more substances, that can be either organic or inorganic molecules. The advantage of using a eutectic PCM is that it has got a lower phase change temperature with respect to the phase change temperatures of the substances from which it is composed.

A graphical representation of a eutectic mixture is reported in figure 3.4

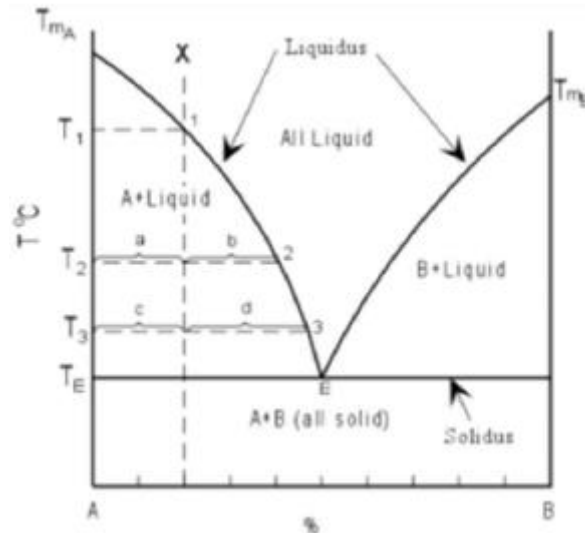


Figure 3.5: Graphical representation of a eutectic mixture [49]

### 3.2.4: Choice of the optimal PCM for latent TES

Let's represent the generic scheme of a latent TES system, as represented in figure 3.5

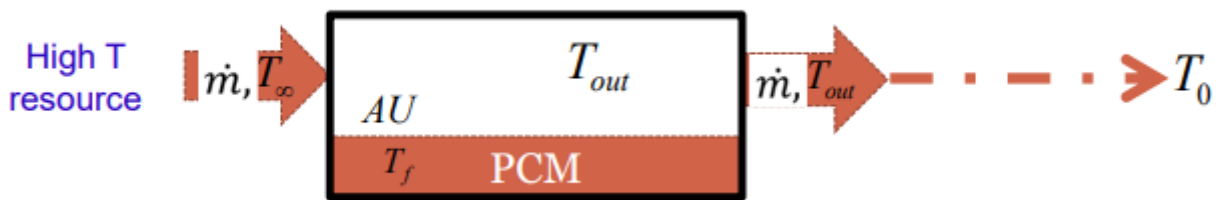


Figure 3.6: Generic scheme of a latent TES system [49]

Under the assumption of a perfectly stirred charging fluid in the storage tank, and supposing that the energy that is stored will then be used in a Carnot machine (i.e. a perfectly reversible machine), it is generally possible to demonstrate that the optimal PCM that maximizes the stored exergy is the one with a melting temperature of

$$T_{melt, optimum} = \sqrt{T_{\infty} \cdot T_0} \quad (3.6)$$

## Chapter 3.3: Reverse Thermochemical TES

Until now, the two TES technologies that have been discussed involve a direct heat exchange between the storage material and the renewable source. The direct heat exchange is generally a not optimized method because the heat flux is unavoidably coupled to an entropy flux, as represented in figure 3.6

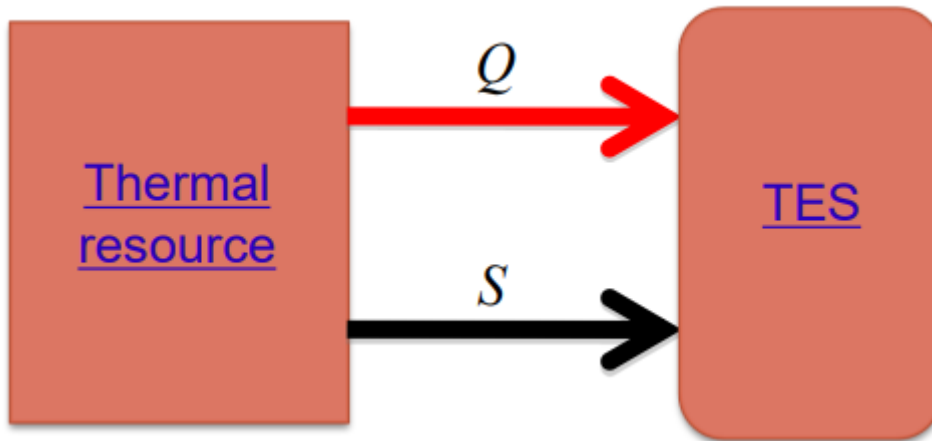


Figure 3.7: Heat and Entropy fluxes in TES technologies with direct heat exchange [49]

The idea behind the thermochemical TES is to exploit a chemical reaction in order to store the heat. So, the heat transfers between the source, the storage and the user are not direct, but indirect. In this way, the heat flux and the entropy flux can be decoupled.

As a consequence, the irreversibility that come along with the issue of the direct heat exchange (entropy flux) can be eliminated, and hence the overall energy density of the system can be increased.

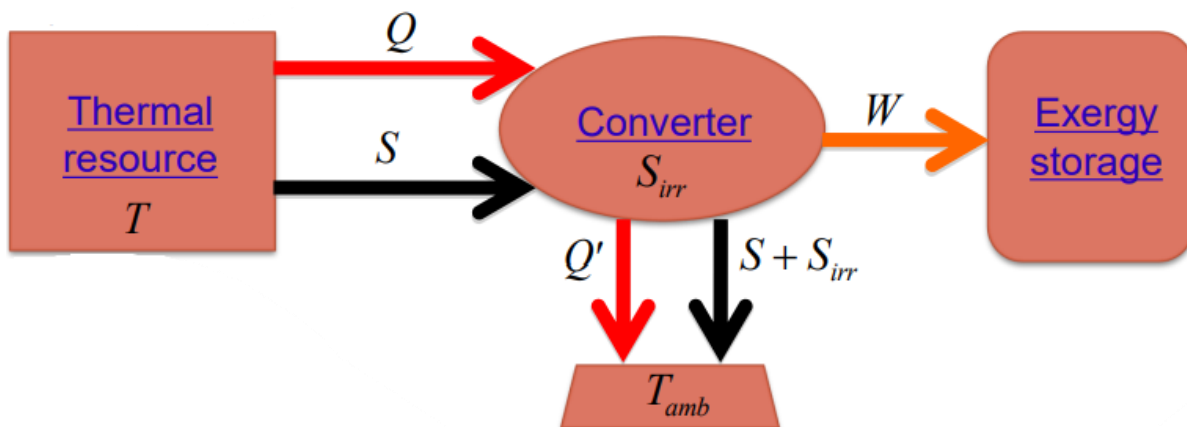


Figure 3.8: Heat and Entropy fluxes in TES technologies with indirect heat exchange [49]

Among the most modern technologies, there are the Sorption TES systems. In this kind of technology, the basic idea is to exploit reversible sorption reactions in order to obtain heat storage in an indirect way.

The sorption reaction can be either of physical nature (physi-sorption) or of chemical nature (chemi-sorption). In the physi-sorption reactions, the bonding forces are the weak Van der Waals forces, while, in the chemi-sorption reactions the bonding forces are the strong covalent or ionic bonds. For this reason, typically a chemi-sorption reaction can store much more energy that a physi-sorption reaction. Even though, in general, the physi-sorption reactions are more suitable for low-medium temperature applications, so they are most used in TES.

Let's say that there is a sorbent (A) and a sorbate (B). The chemical reaction can be written as it follows:



Since the reaction that has been written is reversible, an important role assumes the inversion temperature, that is the temperature level that decides whether will be the direction of the arrow of the reaction.

The inversion temperature can be defined considering the Gibb's free energy as:

$$\Delta G = \Delta H - T^* \Delta S = 0 \Rightarrow T^* = \Delta H / \Delta S \quad (3.8)$$

So, for temperatures  $T < T^*$  the direct reaction will take place, while, for temperatures  $T > T^*$  the inverse reaction will happen.

This basic idea is summed up in the figure 3.8, reported below

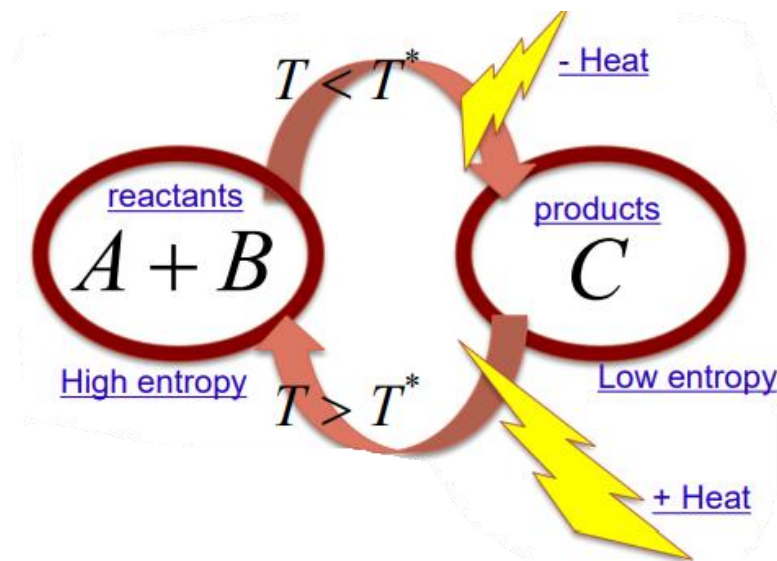


Figure 3.8: basic idea of chemi-sorption reaction [49]

As it can be seen the absorption of the sorbate by the sorbent is accompanied by heat release, while, the inverse process (desorption process) requires heat injected to be done.

So, to summarize, when coupling a sorption TES with a renewable source, the basic idea is the following: when the energy (heat) production is higher than the demand, the energy in excess is used to heat up the product (AB) in order to separate it in sorbent (A) and sorbate (B). Then, these two substances are separated in such a way that they don't interact. Then, when there is an energy demand that is bigger than the consumption, the sorbent and the sorbate are put in contact in such a way that they react, forming the product, and releasing the energy needed. It is worth highlighting that the temperature at which the thermal resource is available must be higher than the inversion temperature.

There are a lot of different solutions available in literature for the sorbent-sorbate coupling. One of the most interesting is the usage of Magnesium Sulphate ( $MgSO_4$ ) and water. The Magnesium Sulphate is interesting due to its very high energy density ( $2.8 \text{ GJ/m}^3$ ), and due to the fact that it is non-corrosive and non-toxic.

It is possible to end this brief discussion about the TES technologies by looking at the following graph, reported in figure 3.8, that highlights the different energy density of the various types of TES solutions

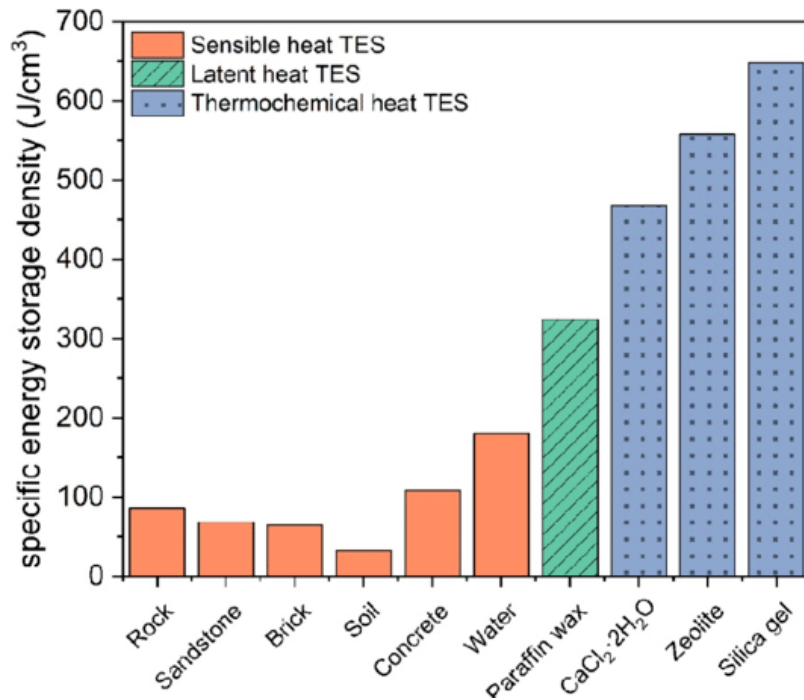


Figure 3.9: Comparison between the energy storage density of the various TES technologies [51]

Of course, it must be said that the energy density is not the only requirement to look for when deciding about the type of TES to implement. There are also other requirements to look at, such as: the average lifetime, the system size, overall cost, the type of renewable resource to exploit, the efficiency required and also, where needed, the appropriate safety aspects.

# CHAPTER 4: Modelling of an ORC on Aspen Plus

In this chapter, it has been described in detail the simulation of a system featuring a real solar collector that runs a ORC.

## Chapter 4.1: Case study introduction

In this thesis it has been decided to study the performance of an ORC by featuring solar radiation data coming from simulation made on a real solar collector and then implementing the data on a commercial software widely used in thermodynamic-related studies: Aspen Plus

### 4.1.1: Details on the solar collector

For what regards the solar collector, it has been used a Disc Solar Concentrator that has been designed and manufactured for order and account for the Politecnico di Torino for the purpose of carrying out laboratory experiments for research and temporary use.

The solar collector is represented here below in figure 4.1



*Figure 4.1: Solar collector used for the study*

The parabolic disk concentration system consists of an aluminium paraboloid coated with an internally coated with a polymer film characterised by a reflectivity with high optical efficiency.

The system is equipped with an automatic two-axis automatic tracking system with two independent axes (azimuth and elevation) for the automatic orientation of the dishes in such a way as to receive the radiation always at the best possible angle of incidence.

The biaxial solar tracker makes it possible to orientate the energy production system in the direction of the sun on an instant-by-instant basis, performing real-time calculation of solar coordinates as a function of time, date, latitude and longitude, with the maximum theoretical accuracy.

The solar tracker is biaxial, i.e. it moves the two polar axes independently, but it can easily be posted to manage only one axis (azimuth for example) while keeping the other fixed (constant tilt).

The general operating characteristics of the parabolic disk are reported below in the table 4.1

Minimum operating temperature	0 °C
Maximum operating temperature	35 °C
Relative humidity (not condensed)	95%
Maximum altitude of operation	3000 m
Maximum overall dimensions	3200 x 25800 x H3500 mm

Table 4.1: General operating characteristics of the parabolic disk

As the manufacturer handbook reports: given a capturing surface of 4.5 m<sup>2</sup> with an optical efficiency of 80% and an average direct radiation of 800 W/m<sup>2</sup>, the concentrated power under optimal conditions is approximately 2.8 kW, and at focal point the temperature can reach 1800°C

#### 4.1.2: Temperature values

For what regards the temperature reached, a simulation using the software Comsol in which it has been measured one value for each minute [52]

The results obtained for each season are reported in the graph below

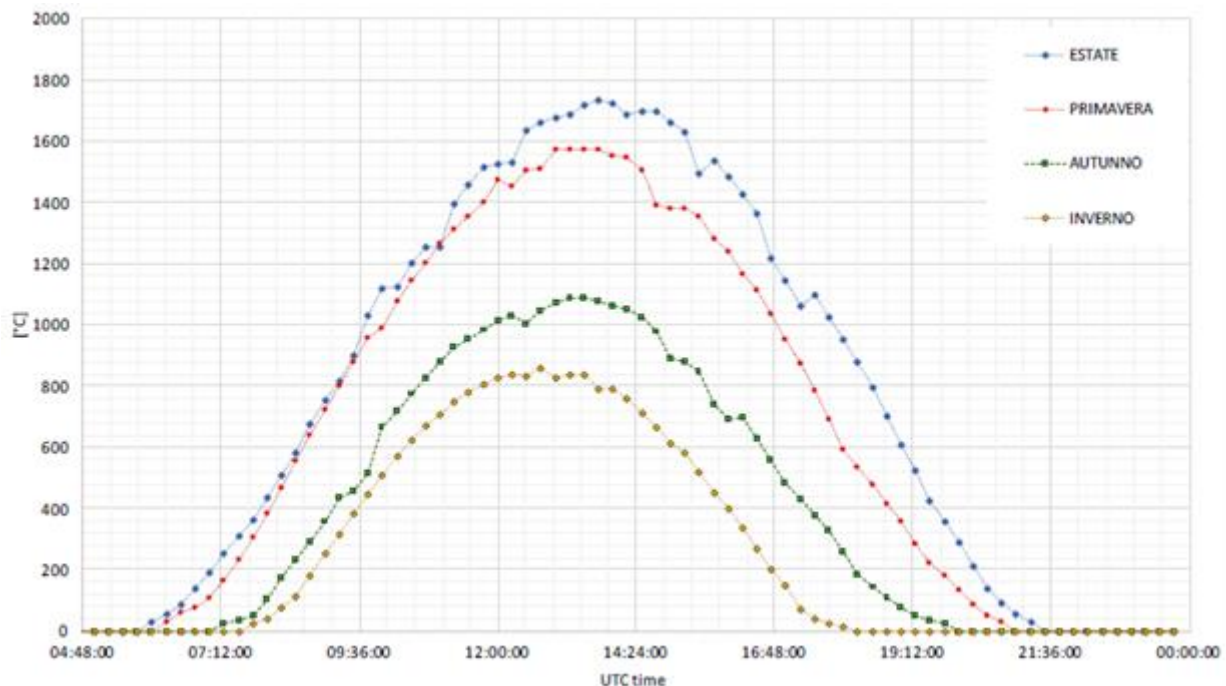


Figure 4.2: medium temperature on the solar collector as function of the time of the day for each season [52]

As it can be seen, much higher values of radiation are reached in summer and spring with respect to the autumn and winter. More in detail, the temperature reached on the collector can arrive in summer up to an average value of 1800 °C, while in winter and autumn it can be reach 1000 °C.

## Chapter 4.2: Choice of the working fluid

As previously anticipated, for an ORC, the choice of the working fluid is a very delicate matter.

To begin, it is chosen to use the R-123 fluid since in literature [53], it is said to be one of the best fluids that can be used for the ORC.

The R-123 [54], also called “2,2 dichloro-1,1,1- trifluoroethane” or Freon 123, is a fluid that presents the following chemical formula:  $\text{CHCl}_2\text{CF}_3$ .

This fluid is commonly used as refrigerant, but it is also implemented for low temperature ORC.

The R-123 was introduced as an environmentally acceptable, non-flammable replacement for chlorofluorocarbon (CFC) 11 in refrigeration and heat transfer applications. In fact, the main problem of CFC is that their stability, coupled with the presence of Chlorine content, created problems of Ozone depletion.

For what regards the R-123, even though it contains chlorine, its hydrogen containing molecules decompose primarily in the lower atmosphere before they can reach the ozone layer. As a consequence, its Ozone depletion potential is much lower if compared to the others CFC.

The T-s diagram of the R-123 has been calculated and it is represented below in figure 4.3, as it can be seen it is a Dry fluid and its critical temperature is 185 °C [55].

Moreover, it must be paid attention to the two following aspects:

- The thermal degradation temperature is 250 °C
- The auto-ignition temperature is around 770 °C

So, it will be important to remain below these temperatures

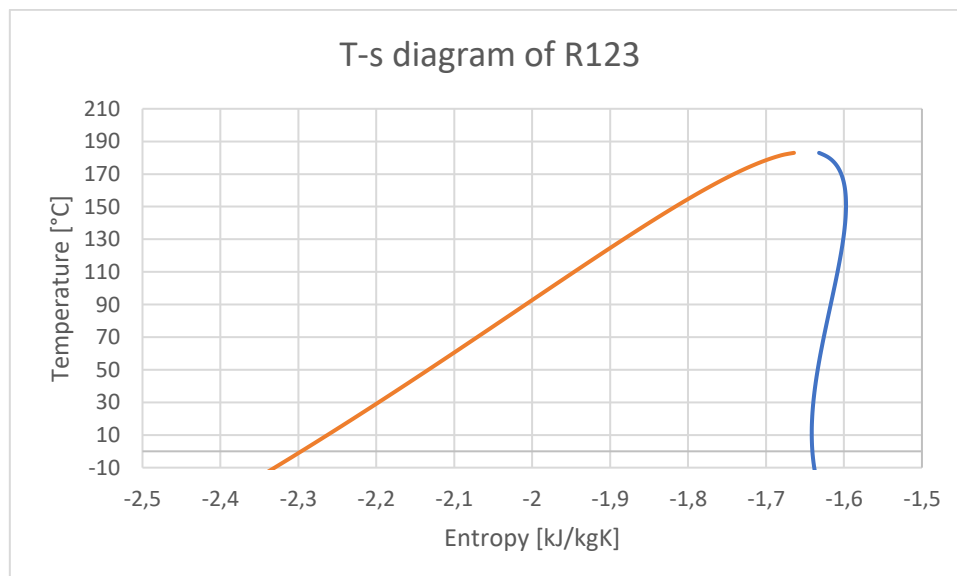


Figure 4.3: T-s diagram of R-123 calculated with Aspen Plus



## Chapter 4.3: Definition of the base components of the system

The system analysed is a base ORC cycle, that hence consists of 4 components: pump, heater, turbine and condenser

The scheme is the following, and a brief description of the implementation of the components on Aspen Plus is reported below in the figure 4.4

The plant generates as first input electricity, that is directly produced inside the turbine. Then, in order to increase the revenues, it is chosen to let the plant work in co-generation mode: the second energy vector that is produced is the waste heat produced inside the condenser, that can be used for example for district heating.

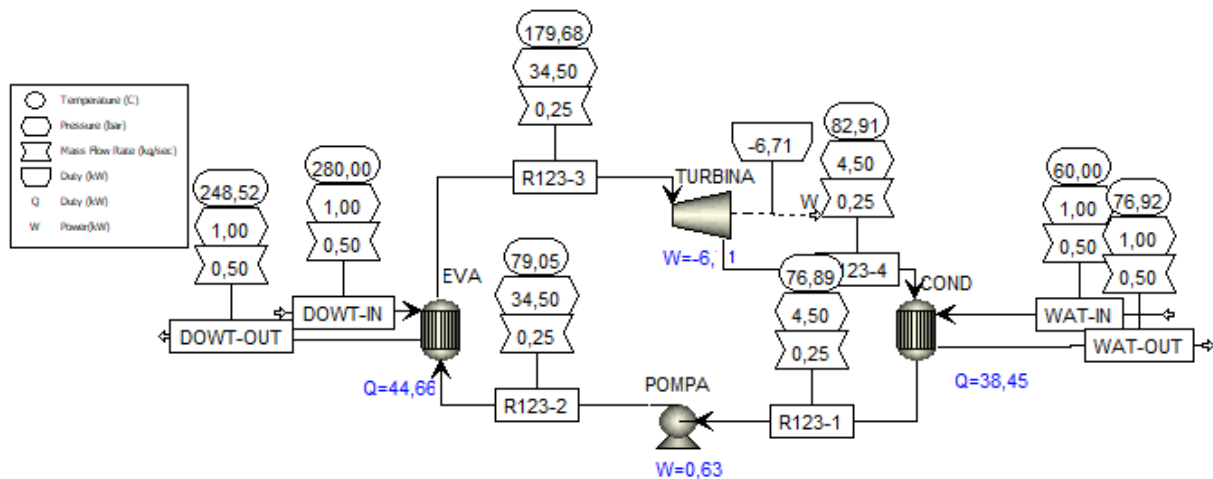


Figure 4.4: Base scheme of the ORC

### 4.3.1: Pump

The pump is the component that raises the pressure of the motor fluid leaving the condenser. The pump outlet pressure is set equal to the turbine inlet pressure.

The "Pump" component in the Aspen Plus "Pressure Changers" library is used to model the pump.

The starting point of the cycle is assumed to be the inlet of the pump. Since the pump must operate with a liquid (liquid-vapour mixtures with high percentage of vapor are forbidden in order to avoid technical problems such as cavitation), it is chosen as starting point a point of saturation on the left side of the saturation line.

As inlet pressure of the cycle it is chosen to have a pressure that has a temperature of saturation of almost 80 °C. In this way, it will be possible to heat up the water coming inside the condenser, that arrives at a temperature of 60 °C, up to similar temperature values.

So, the inlet pressure of the pump is assumed to be 4,5 bar.

To find the outlet pressure of the pump, a reasoning about the maximum temperature reached by the cycle has to be done.

Since the critical temperature of the R-123 is almost 190 °C, in order to avoid phenomenon of instability, it is supposed to work at a pressure that gives a saturation temperature of 180 °C, so more or less 10 °C lower than the critical temperature

With a temperature of 180 °C, the saturation pressure of the R-123 is 34,5 bar. This will be chosen as outlet pressure for the pump.

For what regards the isentropic efficiency of the pump, it is assumed to be 0.9. Due to the irreversibility of the pump, the outlet fluid has a slightly higher temperature than the inlet.

### **4.3.2: Evaporator**

The evaporator is the key component of the system: it allows the ORC cycle to utilise the heat from the disc concentrators.

Essentially, the evaporator is a counter-flow heat exchanger: the hot fluid gives up heat to the cold, which evaporates.

On Aspen Plus, the evaporator is modelled using the 'HeatX' component of the 'Exchangers' library.

The heat exchanger is assumed again to be of the counter-flow type.

- The hot flow is from the solar field, and as hot fluid it is chosen a commercial diathermic oil that is often used in solar fields: Dowtherm.

- The cold flow is the working fluid used in the ORC cycle. Its values correspond to the flow values obtained as an output from the pump model. It is assumed that the pressure remains constant during evaporation.

The amount of heat exchanged between the two fluids must be such that the working fluid can change state. So, the working fluid will exit in condition of saturated vapor.

In order to avoid big heat exchange areas, that will produce a steep increase of the costs, a temperature difference between inlet hot fluid and outlet cold fluid will be set as 100 °C.

Since the R-123a exits the heat exchanger at 180 °C, an inlet hot temperature of 280 °C is chosen.

### **4.3.3: Turbine (Expander)**

The expander is one of the most critical components of the ORC, indeed, a whole paragraph has previously been dedicated to this matter

The component used on Aspen Plus for modelling is a compressor from the 'Pressure Changers' library, which has been specified to work as a turbine.

As operating parameters:

- the inlet pressure of the turbine is assumed to be equal to the outlet pressure of the pump
- the outlet pressure of the turbine is assumed to be the initial pressure of the pump, equal to 5 bar.
- the Turbine inlet Temperature is assumed to be, for the R-123, 180 °C

### **4.3.4: Condenser**

Similarly to the evaporator, the condenser is a counter-current heat exchanger in which there are a hot fluid and a cold fluid that flow in opposite directions.

The hot flow corresponds to the one exiting the expander and gives up heat to the cold fluid in order to condense and return to the liquid phase; the cold flow, absorbing the condensation heat, exits at a higher temperature.

The cold fluid is assumed to be simply water, that can enter at a temperature of 60 °C.

As previously said, since the R-123 enters the condenser at a relatively high temperature, it can be used to heat up the water until it reaches a temperature higher than 70 °C. In this way, the hot water exiting from the condenser will sold for the district heating

On Aspen Plus, the condenser is modelled using the 'HeatX' component of the 'Exchangers' library.

# CHAPTER 5: Results obtained

In this section, the results obtained from the simulation of the case of the base ORC with R-123 as working fluid will be analysed.

## Chapter 5.1: Thermodynamic analysis

For what regards the power requested by the pump and the turbine, it is possible to note from the simulation that:

- The power requested for the pump is 0,63 kW
- The power produced by the turbine is 6,7 kW

Meanwhile, for the two heat exchangers it is possible to see that

- Inside the heater, there is a heat flux of 43,5 kW
- Inside the condenser, there is a heat flux of 37,7 kW

These results are reported in the table 5.1

Component	Pump	Evaporator	Turbine	Condenser
Power Flux [kW]	0,63	44,6	6,71	38,45

Table 5.1: Main power flux associated to each component

Considering that

- The solar collectors have an efficiency of 80%, with as a consequence a total thermal power input requested equal to 55,7 kW
- The alternator connected to the turbine has an efficiency that can be safely assumed equal to 98%

It is possible to calculate the total efficiency of the plant in case of single generation of electricity and combined generation of heat and power

$$- \eta_{el} = \frac{(E_{tur} - E_{pump}) * \eta_{alt}}{\frac{E_{eva}}{0,8}} = 10,67\%$$

$$- \eta_{CHP} = \frac{(E_{tur} - E_{pump}) * \eta_{alt} + E_{cond}}{\frac{E_{eva}}{0,8}} = 79,7 \%$$

To conclude, it is also possible to calculate the total hours of functioning of the plant

This number is obtained by considering, from the figure 5.1, the number of minutes per day for each season at which the temperature is higher than the one requested by the inlet of the hot fluid of the evaporator.

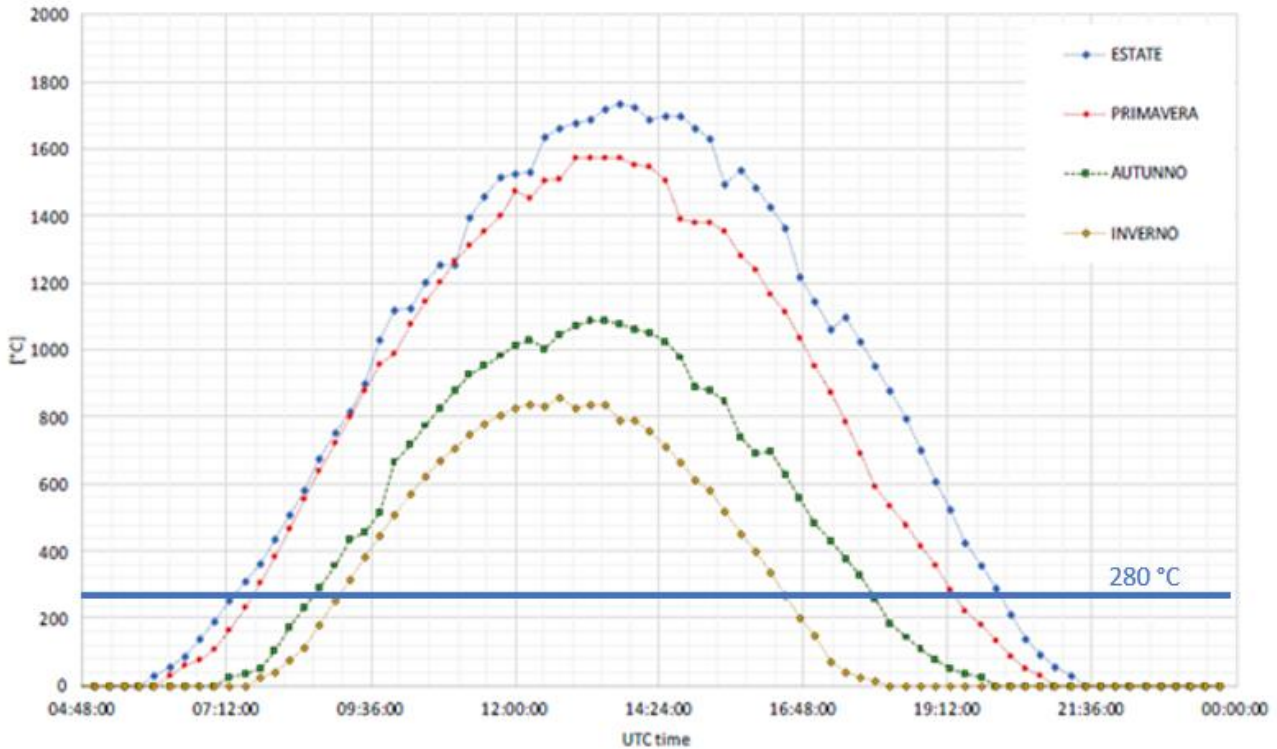


Figure 21: Average number of hours for which the temperature of the collector is equal or greater than the one requested by the inlet hot fluid of the evaporator

Season	Daily Time interval	Daily time interval converted in minutes	Number of minutes for each season
Winter	9:15-16:15	420	37800
Autumn	8:30-19:30	660	59400
Spring	7:45-19:15	690	62100
Summer	7:30-20:00	750	67500

Table 5.2: Working time of the powerplant for each season

From the data gained from table 5.2, it is possible to conclude that the powerplant works for a total of 3600 hours/year

## Chapter 5.2: Economic Analysis

The economic analysis is a crucial aspect that every project has to face.

In fact, any system may well perform from a technical-theoretical point of view, but, if this high performance has been achieved by spending a disproportionate amount of capital in terms of cost-benefit, this technology will not be considered for large-scale production until a way is found to bring the costs down.

For this reason, the economic analysis is used to understand how much any project is feasible from the economical point of view.

The expenses and the revenues for creating and running the system assume a central role, and different critical observations can be done on whether the investment is convenient or not.

### 5.2.1: Cost of the plant

The cost of each component can be computed following a standard procedure given by the NETL (National Energy Technology Laboratory), which is an association that realises guidelines about costing models [56]

This methodology defines capital cost at five levels:

- **BEC (Bare Erected Cost):** it comprises the cost of process equipment, on-site facilities, and infrastructure.

The BEC of each component can be calculated by using function called “Turton cost function” [57], that allows to estimate the purchase cost of a component for a specific base condition.

A generic cost function is expressed in the form:

$$C_{BEC} = C_p^0 \cdot F_{BEC} \quad (5.1)$$

With:

-  $C_p^0$ : purchasing cost of equipment referred to base conditions.

The purchasing cost of an equipment referred to base conditions,  $C_p^0$  may be expressed as:

$$C_p^0 = K_1 + K_2 \cdot A + K_3 \cdot (\log_{10} A)^2 \quad (5.2)$$

With:

- A is a size parameter chosen as reference for the device considered
- $K_1$ ,  $K_2$ , and  $K_3$  are three constants to fit the expression to the real cost of the device.

Deviations from these base conditions are handled by using multiplying factors that depend on the following factors:

- The specific equipment type
- The specific system pressure
- The specific materials of construction

The index that comprises all of the possible deviations is the bare erected module cost  $F_{BEC}$  is the bare erected module cost, and it is generally expressed as the product of a material factor and a Pressure factor.

$$F_{BEC} = F_M \cdot F_P \quad (5.3)$$

With:

-  $F_p$  = pressure factor.

It is a factor that considers that the component is working at a high value of pressure. The pressure factor is usually tabulated, but it can be expressed as it follows

$$F_p = C_1 + C_2 \cdot P + C_3 \cdot (P)^2 \quad (5.4)$$

With:

- P is the operating pressure
- C<sub>1</sub>, C<sub>2</sub>, and C<sub>3</sub> are three constants defined to fit the expression to the real data.
- F<sub>M</sub> material factor that is usually tabulated.

Since the capacity of the component is not included in the purchasing cost, it's necessary to adjust the formula. The most common simple relationship between the purchasing cost and an attribute of the equipment related to its capacity is given by:

$$\frac{C_1}{C_0} = \left(\frac{S_1}{S_0}\right)^n \quad (5.5)$$

With:

- S: equipment cost attribute
- C: purchasing cost
- n: cost component. In most of the cases n=0,6 in absence of other information.

The subscript 1 refers to the equipment with the required attribute and the subscript 0 to equipment with the base attribute.

The last aspect that is necessary to take into account is the effect of time on purchased equipment cost refers to a specific year

This aspect can be considered with the following equation

$$\frac{C_2}{C_1} = \frac{I_1}{I_2} \quad (5.6)$$

With:

- C: purchasing cost
- I: cost index

The subscript 2 refers to the time when the cost is desired, while the subscript 1 refers to the base time when the cost is known.

This is the last step, once that is done, the estimation of the bare erected cost of a component is done.

- **EPCC (Engineering, Procurement and Construction Cost):** it comprises the BEC plus the cost of services provided by the engineering as detailed design, contractor permitting and project/construction management costs.

- **TPC (Total Plant Cost):** it comprises the EPCC plus project and process contingencies.

- **TOC (Total Overnight Capital):** it comprises the TPC plus all other overnight costs, including owner's costs

- **TASC (Total As-Spent Capital)** it is the sum of all capital expenditures as they are incurred during the capital expenditure period including their escalation and the interest during construction.

BEC, ECC, TC, and TOC are overnight costs and are expressed in "base-year" currency (constant currency), while the TASC is expressed in current-year currency over the entire capital expenditure period.

- **Calculation of the Bare Erected Costs**

Below there are reported the procedures for the calculation of all the bare erected costs of the components of the CAES plant. The various data for the calculation are taken from an optimization study made on the ORC [58]

- **Pump**

For the pump, a radial pump is used.

The values of K1, K2 and K3 are respectively: 3.86, 0.31 and 0.12 and their range of validity is between 0,1 and 200 kW.

No Auxiliary factor for pressure and material has to be taken into account, since the maximum pressure of the cycle (24 bar) is still a low value.

With that done, the pump has a base cost of 2377 \$

- **Evaporator**

The evaporator is considered as a fixed tube type.

The values of K1, K2 and K3 are respectively: 4.32, -0.3 and 0.16.

Again, no auxiliary factor for pressure is needed.

By considering the input data, it is obtained a logarithmic mean temperature difference of 140 °C.

Supposing a coefficient of thermal transmittance of  $U= 100$  (W/m<sup>2</sup>K) , the area of thermal exchange is obtained as

$$A = \frac{\Phi_{eva}}{U * \Delta T_{ml}} = 3,38 \text{ m}^2$$

The area is very small. This is expected since from the beginning it has been chosen to maintain a high temperature difference inside the evaporator exactly for this reason.

With these data, the cost of the evaporator becomes equal to 7903 \$.

- **Turbine**

As turbine, it is chosen a radial turbine.

The values of K1, K2 and K3 are respectively: 2.24, 1.49 and -0.16

The material factor is 3.5

The cost is then 8043 \$

- **Condenser**

The condenser is assumed to be of the same type of the evaporator. For this reason, the values of K1, K2 and K3 are respectively the same.

What changes is the Area needed for the heat transfer, that is different.

The cost of the condenser is then calculated as: 17175 \$



## - Solar Collector

As previously anticipated, the solar collector has to provide to the Dowtherm fluid a thermal power equal to 44,7 kW.

Since a solar collector alone cannot give all of the desired power, more units are needed.

The calculation of the number of solar collectors needed is performed by calculating the average power produced by one solar collector and then doing the ratio with the total requested power input.

- Calculation of the average power produced by the solar collector

To calculate the power produced by a single solar collector, the following procedure is done

- As already done in table 5.2, from the data about the evolution of the temperature of the solar collector with respect to the time of the day, it is taken the reference working interval for each season.

- Then, in those time intervals, from the data about the direct normal solar radiation, it is calculated the average value of irradiance for each season

The result of this calculation is shown in table 5.3

Season	Daily Time interval	Daily time interval converted in minutes	Average value of irradiance [W/m <sup>2</sup> ]
Winter	9:15-16:15	420	497
Autumn	8:30-19:30	660	679
Spring	7:45-19:15	690	771
Summer	7:30-20:00	750	843

Table 5.3: Average daily value of irradiance for each season

- Then, an average yearly irradiance value is obtained by calculating a weighted average of the seasonal irradiance values, taking into account as a weighting factor the seasonal amount of operating time of the power plant.

By elaborating the data of the table 5.3, it has been obtained a value of average yearly irradiance equao to  $R=770 \text{ W/m}^2$

- To conclude, since the collector has respectively an optical efficiency of 80% and an area of 4,5 m<sup>2</sup>, the power is obtained as:

$$P_{collector} = R * \eta_{coll} * A_{coll} = 2,77 \text{ kW}.$$

- Calculation of the required number of collectors

As previously anticipated, the number of collectors is obtained by calculating the ratio between the total power required (44,7 kW) and the power produced by a single collector (2,7 kW)

With these data it is obtained that the required number of solar panels is equal to 17.

- Total cost for the solar collectors

Now, it is possible to obtain the total cost of the solar collectors by multiplying the number of required collectors with the cost of the single collector.

Normally one collector costs more than \$18,000. In this study case, since it is required an high number of collectors, it is possible say that the price of the single unit will be slightly lower. Therefore, by considering a relative variation of slightly less than 20%, it is assumed an average price for each collector of \$15,000.

With this price, the total expense for the collectors is equal to 255'000 \$.

In the table 5.4 it reported below there is the sum up of all the expenses for the components

PUMP	2377 \$
TURBINE	8043 \$
CONDENSER	17175 \$
EVAPORATOR	7903 \$
COLLECTORS	255000 \$

*Table 5.4: Expense of all the components*

It can be noted that the biggest expense is exactly for the solar collectors, that hence represent the bottleneck of the plant.

The effect of time will be considered by multiplying each value obtained in the table 5.4 with a conversion factor equal to 1.5

- **Calculation of the total cost of investment**

Now, the total cost of the investment can be calculated by defining the costs of the other 4 levels of capital cost

More in detail, always according to the National Energy Technology Laboratory [61], the these costs can be evaluated as it follows

- **Engineering Procurement and Construction Cost (EPCC)**

The impact of EPCCs can be calculated by adding 5% to the total cost of the components.

- **Total Plant Cost (TPC)**

The TPC can be calculated by adding 15% to the sum of total cost of the components with the EPCCs

- **Total Overnight Cost (TOC)**

The TOC can be calculated by adding 10% to the total plant cost

- **Total As-Spent Cost (TASC)**

The TASC can be calculated by adding 10% to the total overnight cost

- **Conversion of dollars to euro**

In the month of March 2024, there is a conversion factor equal to 0,92 [59].

In the end, the final value of the capital expenditures is obtained

COMPONENT	BEC	EPCC	TPC	TASC
PUMP	3595	3667	4217	4639
TURB	12167	12410	14272	15699
CONDENSER	26411	26939	30980	34078
EVA	11956	12195	14024	15426
collector	356945	364084	418696	460566
<b>TOTAL (\$)</b>	<b>411075</b>	<b>419296</b>	<b>482191</b>	<b>530410</b>
<b>TOTAL (€)</b>	<b>378189</b>	<b>385752</b>	<b>443615</b>	<b>487977</b>

Table 5.5: CAPEX of the plant

### 5.2.2: Calculation of the operating expenditures of the plant

The OPEX (OPERating EXpenditures) are the running costs of the plant, and they are calculated on yearly basis.

In the case of a solar power-driven ORC, the OPEX may coincide with the cost of the electricity to run the pump.

So, basing on that, the OPEX can be calculated as

$$OPEX = E_{pump} * h_{year} * C_{el} \quad (5.7)$$

With:

- $E_{pump}$  = power consumed by the pump = 0,63 kW
- $h$  = hours of functioning of the plant in a year = 3600
- $C_{el}$  = electricity cost = 0,20 €/kWh

The OPEX are then equal to almost 500 €/year.

It can be seen that they represent a minimal part if compared to the Capital Expenditures.

### 5.2.3: Calculation of the revenues

Since the CSP plant essentially works through co-generation, (i.e. with the simultaneous generation of electricity and thermal power), these two aspects must be considered for the calculation of the Revenue.

Moreover, also some incentives made available for co-generation by the Italian government will be considered

- **Revenue from the selling of the electrical energy**

The revenue for the selling of the electrical energy produced is simply given by the product between the electrical energy produced and the price of selling this energy.

$$R_{el} = E_{prod} * h_{year} * P_{EL} \quad (5.8)$$

Supposing that the electricity price is 0,2 €/kWh, the total revenue for the selling of electricity is equal to almost 4820 €/year.

- **Revenue from the selling of the thermal energy**

The revenue for the selling of the thermal energy produced is simply given by the product between the thermal energy exchanged and the price of selling this energy.

$$R_{th} = Q_{prod} * h_{year} * P_{th} \quad (5.9)$$

Supposing that the price of the thermal power produced is 0,1 €/kWh, the total revenue for the selling of this heat produced is equal to almost 13840 €/year.

- **Revenue from the incentives**

As previously anticipated, some incentives coming from the Italian government can be considered.

More in detail, for the co-generation, the Italian government has posed some incentives called “Certificati Bianchi” [60] which state that, for each Tonne of Equivalent Petroleum (which corresponds roughly to 11’630 kWh) not generated by conventional sources, there is an economic revenue of 260 €.

That said, the formula for the calculation of the revenue from the Italian incentives is

$$R_{inc} = \frac{\left( \left( \frac{W_{el} - W_{pump}}{\eta_{el}} + \frac{Q_{th}}{\eta_{th}} \right) * h_{year} \right)}{11630} * 260 \quad (5.10)$$

Considering that:

-  $\eta_{el}$  = average value of efficiency of single production of electricity by an Italian powerplant = 0,46

-  $\eta_{TH}$  = average value of efficiency of single production of thermal power by an Italian powerplant = 0,9

The value of Revenues coming from the incentives is equal to 4610 €/year

The total revenues are summed up in the table 5.6 reported below

Revenue from electricity generation [€]	4824
Revenue from thermal generation [€]	13841
Revenue from incentives [€]	4610
Total revenues in a year [€]	23276

Table 5.6: Total revenues

#### 5.2.4: Calculation of economic indexes

Now that the capital and operating expenditures have been calculated, it is possible to estimate some possible indexes that give information about the economic convenience of the plant.

- **Net Present Value (NPV)**

The first useful index is the NPV (Net Present Value), which is defined as follows:

$$NPV = -CAPEX + \sum_{i=1}^N \frac{F_i}{(1+r)^i} \quad (5.11)$$

With:

-  $F_i$  is the net revenue of the  $i$ -th year

$F_i$  is given by the difference between the revenue obtained from the sale of the generated energy vectors and the OPEX.

-  $r$  is the discount rate.

In this thesis, it has been assumed a reference value of discount rate equal to 1,25%

-  $N$  is the useful life of the plant (number of years)

In this thesis, it has been assumed 30 years as useful life

Using the NPV it is possible to know the total value of the revenue obtained from the investment

With all of these input data, it is obtained a final value of NPV equal to 90108 €

The trend of the NPV with respect to the year considered is reported in the figure 5.2, reported below

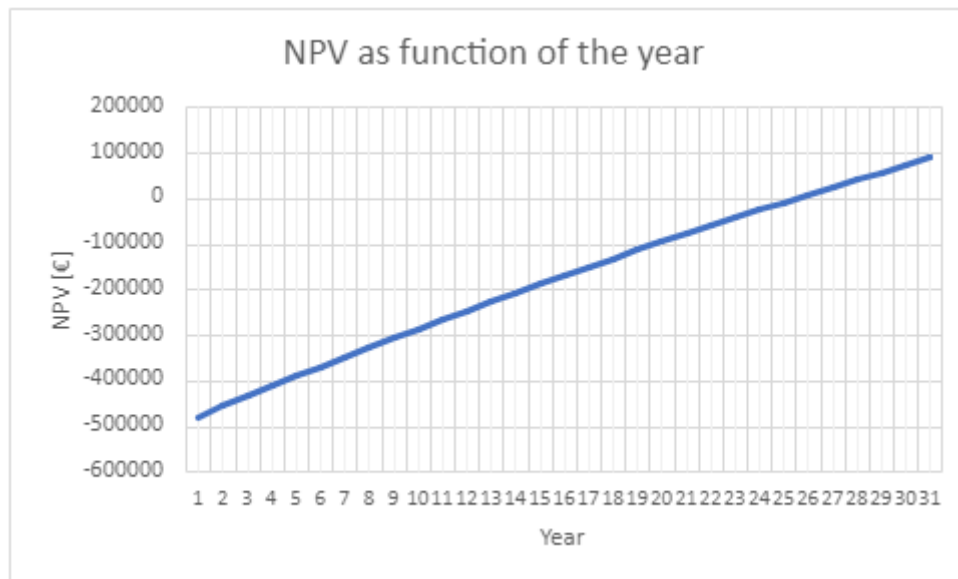


Figure 5. 2: NPV as function of the year

- **Payback Time**

The payback time (PBT) is the year in which the NPV becomes equal to zero.

In this case, PBT = 24,3 years

- **Return On Investment (ROI)**

The return on investment is simply the ratio between the NPV at the end of life of the plant and the total costs

$$ROI = \frac{\text{Net Present Value}}{\text{Total Expenses}} * 100 \quad (5.10)$$

With these input data, it is obtained a value of ROI= 17,98 %

- **Levelized Cost Of Energy**

Another useful index is the LCOE (Levelized Cost Of Energy), defined as follows:

$$LCOE = \frac{-I_0 + \sum_{i=1}^N OPEX_i * (1+r)^{-i}}{\sum_{i=1}^N E_i * (1+r)^{-i}} \quad (5.11)$$

The LCOE is usually expressed in €/kWh and indicates the minimum price at which the generated energy should be sold in order to have an NPV=0 at the end of the plant's lifetime.

This index can be used to compare different renewable technologies and determine which one allows electricity to be sold at a lower price.

In this case, since there is the co-generation, different types of LCOE can be calculated:

- Levelized cost of Electricity (LCOEI): Supposed that the ORC sells only the electricity produced, it is the price at which the electricity should be sold in order to have an NPV=0 over its entire lifetime
- Levelized cost of Heat (LCOH): Supposed that the ORC sells only the waste heat produced in the condenser, it is the price at which the heat should be sold in order to have an NPV=0 over its entire lifetime
- Levelized cost of Electricity and Heat (LCOEH): Supposed that the ORC sells the electricity and the heat at the same price, it is the price at which the energy has to be sold in order to have an NPV=0 over its entire lifetime

The results of the calculations are shown in the table 5.7, reported below

LCOEI [€/kWh]	0,81
LCOH [€/kWh]	0,14
LCOEH [€/kWh]	0,12

*Table 5.7: Levelized costs for the different types of energy considered*

As it can be seen, the Levelized cost of electricity is far from be competitive. In fact, its price is much higher than the actual price at which the electricity is sold nowadays.

For the other two indicators the situation is slightly better: the actual price of the heat is still slightly lower than the LCOH, but the difference is much reduced with respect to what it has been seen before.

# Chapter 6: Improvements

In this chapter, some improvements regarding the ORC plant are considered.

The improvements will aim mainly to improve the economical aspects of the plant, hence increasing the Net Present Value at the end life of the plant and the Return On Investment, and reducing the Payback time and the Levelized costs

## Chapter 6.1: Usage of different working fluids

The first improvement that can be considered regards the usage of other heat transfer fluids with respect to the R-123.

More in particular, two new fluids have been considered: R245fa and N-pentane.

- The R245fa, also called “1,1,1,3,3-Pentafluoropropane” is another chloro-flour-carbon (CFC) with brute chemical formula of  $C_3H_3F_5$ . Similarly to the R123, this fluid is commonly used as refrigerant, but it is also used in ORC applications [53].

The T-s diagram of the R245fa has been calculated with Aspen-Plus and reported below

Also in this case it can be seen that the fluid is dry, while the critical temperature in this case is much lower, and equal to 150 °C. Moreover, other two temperatures to which it must be paid attention are the following [61]:

- the thermal degradation temperature, that starts happening around 330 °C
- the auto-ignition temperature is equal to 412 °C

So, it will be important to remain below these values

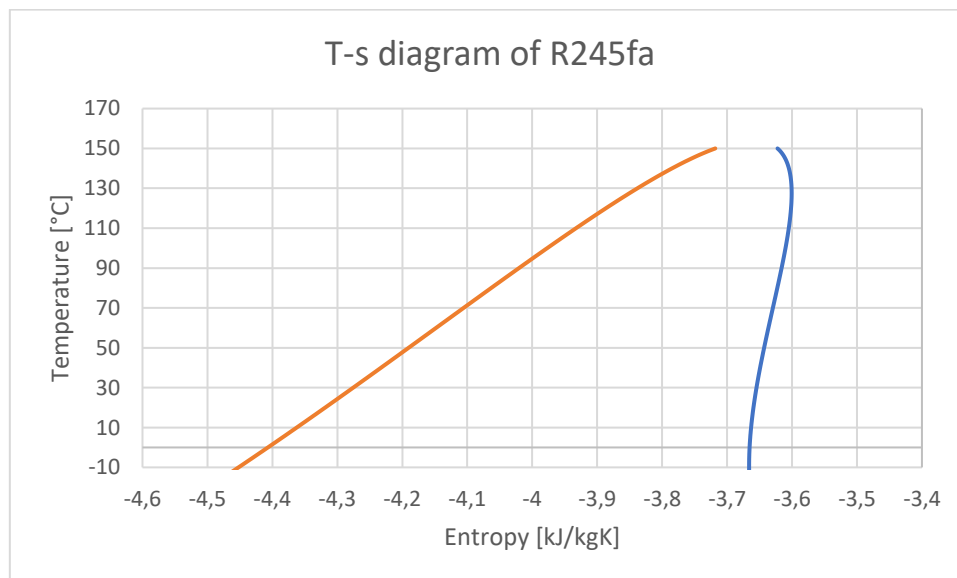


Figure 6.1: T-s diagram of the R245fa calculated with Aspen Plus

- The N-pentane, as the name suggests, is a structural isomer of the pentane, that is an alkane with the following chemical formula  $C_5H_{12}$ . Although the chemical composition is the same, the different structure of the N-pentane gives to this molecule different physical characteristics such as a different boiling point. Also the N-pentane is widely used for ORC applications.

The T-s diagram of N-pentane has been calculated with Aspen plus and reported below in figure 6.2

As it can be seen, the fluid is again dry, the critical temperature is slightly below 200 °C. Moreover, its auto-ignition temperature is around 260 °C [62], so it will be important to remain below that level of temperature.

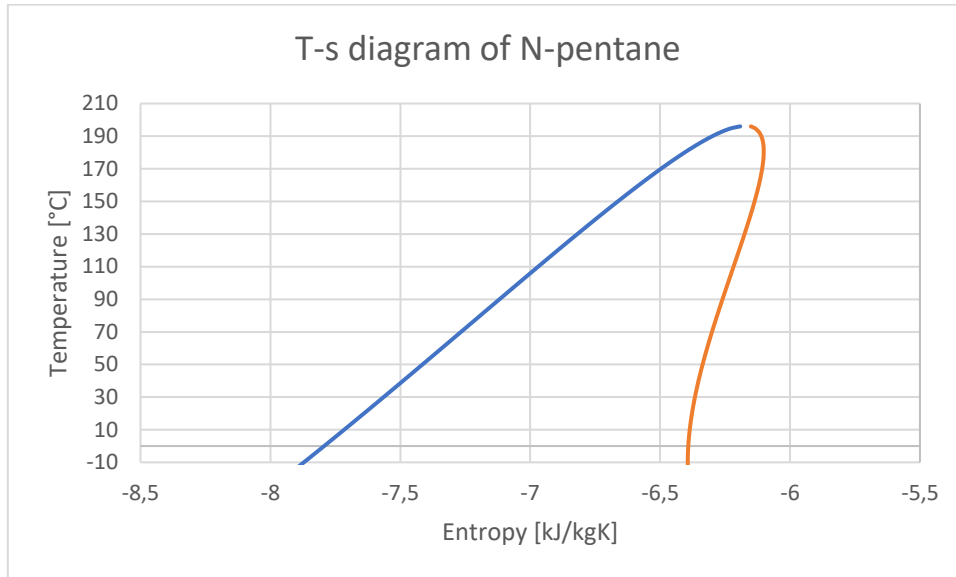


Figure 6.2: T-s diagram of N-isopentane calculated with Aspen Plus

### 6.1.1: Operational characteristics of the ORC implemented with the two fluids chosen

- **R245FA**

In the case of implementation of an ORC with R-245fa, the operational characteristics of the components have been re-adapted to the thermodynamic characteristics of this working fluid, that are similar but not equal to the one of the R-123.

The mass flows of each fluid are maintained constant in order to make a reasonable comparison between the three cases

#### - **Pump**

In this case, considering that the critical temperature of the R245fa is slightly above 150 °C, it is chosen as maximum temperature of the cycle 150 °C in order to avoid phenomenon of instability.

For this reason, as exiting pressure of the pump it is chosen the pressure of saturation at 150 °C and it is equal to 34.05 bar

#### - **Evaporator**

For the evaporator, again to contain the costs of the heat exchanger, it is chosen to use as a heat source a temperature that is 100 °C above the maximum temperature reached by the working fluid.

So, the hot stream enters at 250 °C.



### **- Turbine**

In this case, as outlet pressure of the turbine it is chosen a value for which the saturation temperature remains above 80 °C. In this way, it will be possible again to heat up the water from the condenser in order to sell thermal energy.

So, it is chosen as outlet pressure of the turbine 4,5 bar.

### **- Condenser**

In the condenser, as cooling fluid it enters water again at 60 °C and, as previously anticipated, it is said that it will be heated up until  $T > 70$  °C and the heat exchanged will be sold as thermal energy

- **N-pentane**

In the case of the N-pentane, the operational characteristics chosen for its components are the following

### **- Pump**

In this case, considering that the critical temperature of the N-pentane is slightly above 200 °C, it is chosen as maximum temperature of the cycle 146 °C in order to avoid phenomenon of instability.

For this reason, as exiting pressure of the pump it is chosen the pressure of saturation at 146 °C and it is equal to 15 bar

### **- Evaporator**

For the evaporator, again to contain the costs of the heat exchanger, it is chosen to use as a heat source a temperature that is 100 °C above the maximum temperature reached by the working fluid.

So, the hot stream enters at 250 °C.

### **- Turbine**

In this case, as outlet pressure of the turbine it is chosen a value for which the saturation temperature remains above 80 °C. In this way, it will be possible again to heat up the water from the condenser in order to sell thermal energy.

So, it is chosen as outlet pressure of the turbine 4 bar.

### **- Condenser**

In the condenser, as cooling fluid it enters water again at 60 °C and, as previously anticipated, it is said that it will be heated up until  $T > 70$  °C and the heat exchanged will be sold as thermal energy

## **6.1.2: Comparison of the Results**

In this section, it is reported a brief summary of the results obtained with the comparison of the three fluids.

- **Thermodynamic performance of the plant**

### **- Generated Electric power and Heat**

The electric power and the heat generated in the three cases varies as it follows

	Base R123	Base R245	Base n-pen
Wel (kW)	6,7	5,29	11,29
Qth (kW)	38,5	39,87	92,85

Table 6. 1: Comparison of the generated electrical and thermal power in the three cases

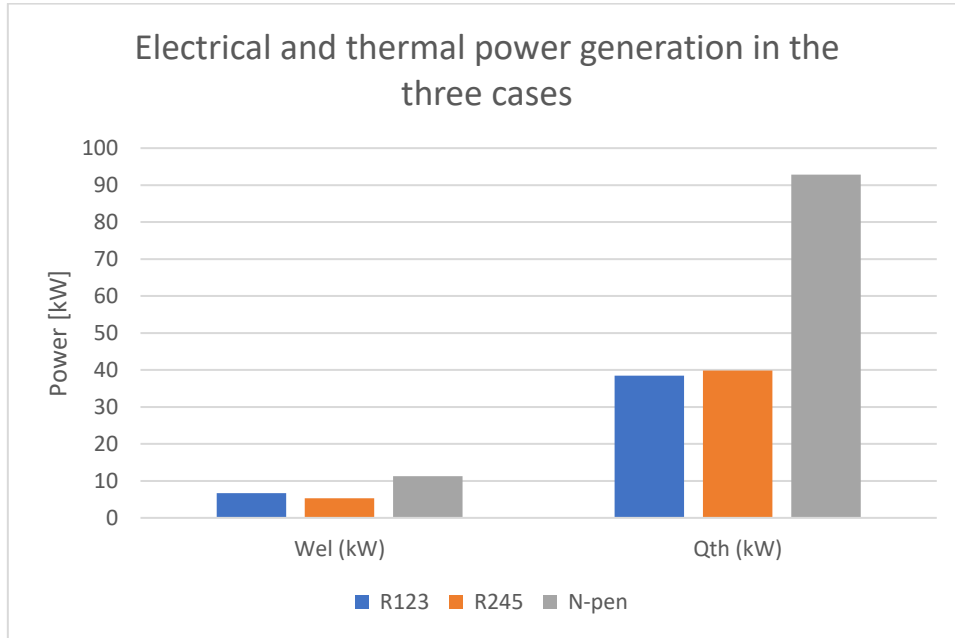


Figure 6.3: Graphic Comparison of the generated electrical and thermal power in the three cases

As it can be seen, the performance of the two CFCs are similar, while the N-pentane generated much more electric and thermal power.

#### - Electric efficiency and combined generation efficiency

The results obtained are the following

	Base R123	Base R245	Base n-pen
$\eta_{el}$ (%)	11,76	9,31	8,54
$\eta_{CHP}$ (%)	79,74	79,98	80,00

Table 6. 2: Comparison of the electrical efficiency and the efficiency of combined electrical and thermal generation for the three fluids

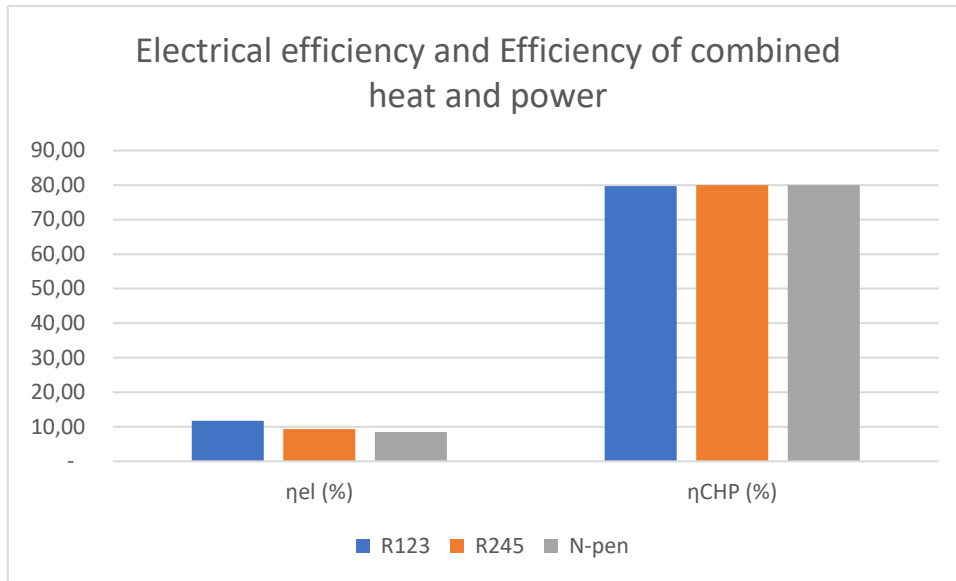


Figure 6.4: Graphic comparison of the electrical efficiency and the efficiency of combined electrical and thermal generation for the three fluids:

As it can be seen, the electrical efficiency is slightly higher for the R123, while the efficiency of combined heat and electrical generation is almost constant for all of the three cases, and equal to 80%, that is a good average value for co-generation plants.

- **Economic Performance**

Now let's take a look to the economical indicators, that represent the value of the plant in monetary terms.

- **Number of collectors**

As previously anticipated, the number of collectors is directly related to the heat required by the evaporator of the plant

The comparison between the three cases is the following

	Base R123	Base R245	Base n-pen
Number of collectors	17	16	37

Table 6. 3: Comparison of the needed number of collectors for the three different fluids

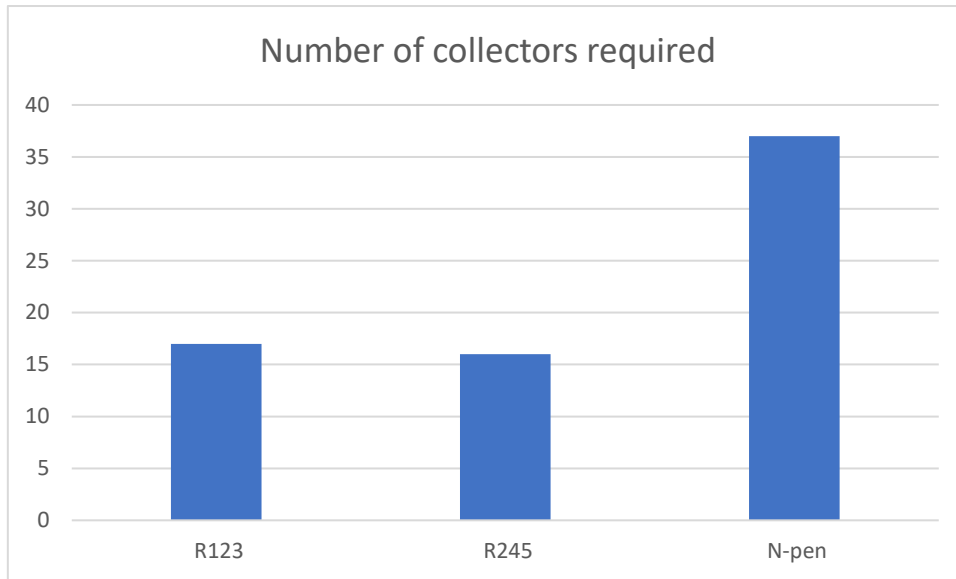


Figure 6.5: Graphic comparison of the number of collectors required for the three different fluids

As it can be seen, even if the N-pentane produces much more heat and power if compared to the two CFCs, it requires much more power exchange inside the evaporator, and this has a non-trivial impact on the number of collectors, that is almost doubled.

#### - CAPEX and OPEX

The Capital and Operational expenditures in the three cases are the following

	Base R123	Base R245	Base n-pen
CAPEX (€)	487977	480840	1068545
OPEX (€)	453	466	407

Table 6. 4: Comparison of the CAPEX and OPEX for the three different fluids

For what regards the CAPEX, as previously anticipated, due to the elevated number of collectors required, the CAPEX of the ORC working with N-pentane is much higher (it resents the million of euro).

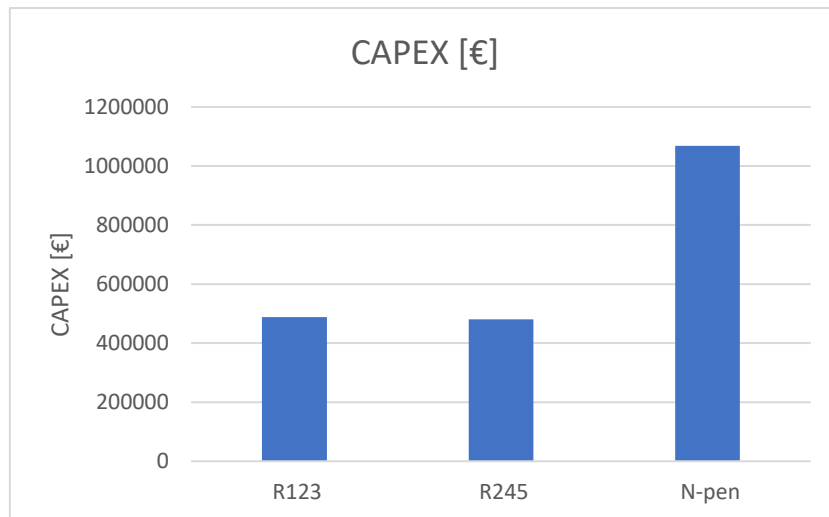


Figure 6.6: Graphical comparison of the CAPEX values for the three different fluids

For what regards the OPEX, the values are almost all the same due to the low power values required by the pump, and they always represent a minimal part of the expenses if compared to the CAPEX

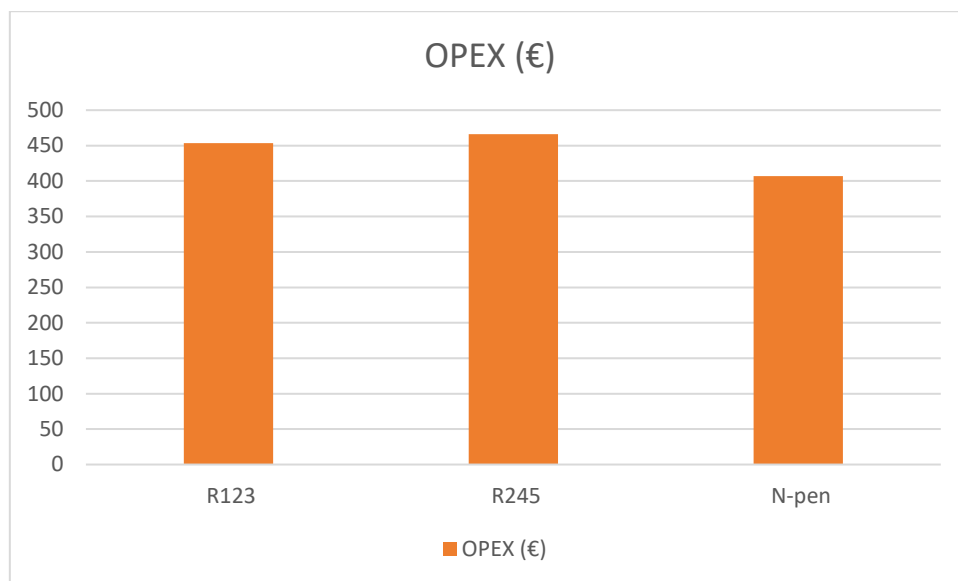


Figure 6.7: Graphical comparison of the OPEX values for the three fluids

### - Net Present Value and Payback time

The results obtained are the following

	Base R123	Base R245fa	Base n-pen
NPV (€)	90100	92402	259669
PBT (years)	24,4	24,26	23,230

Table 6. 5: Comparison of the Net Present Value and of the Payback Time for the three different fluids

For what regards the Net Present Value, it can be seen that at the end of the life of the plant the highest value is obtained with the N-pentane. Moreover, since the R123 and the R245fa have similar values of initial investment and yearly revenues, their curves are almost overlapping and therefore difficult to distinguish on the graph

So, even if the CAPEX are much higher, this choice seems to be still the most convenient.

The reason is probably related to the types of incentives that have been considered, for which: the higher the generation, the higher will be the revenues.

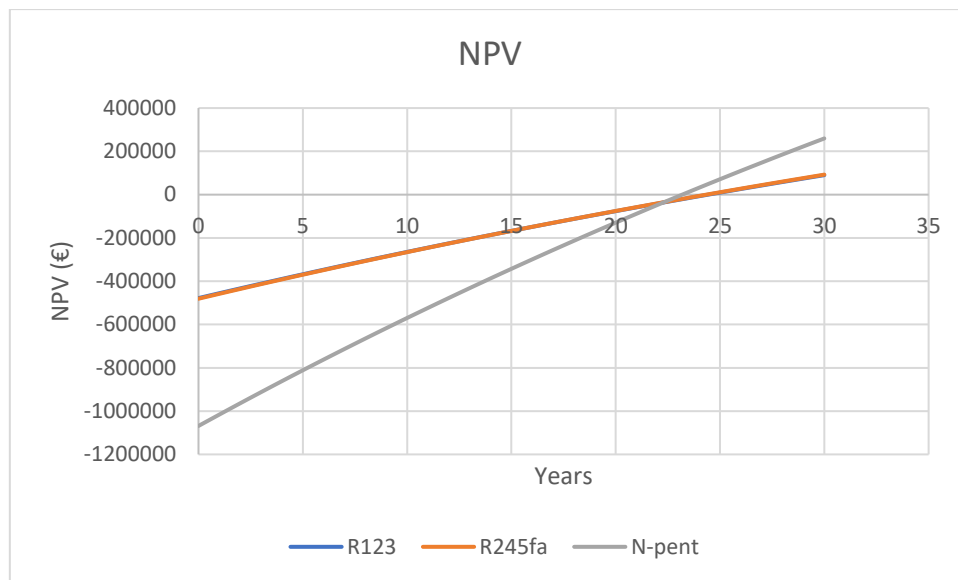


Figure 6.8: Graphical representation of the trend of the NPV along the years for the three different fluids

### - Return On Investment

The different values of ROI are reported in the table below

	R123	R245	N-pen
ROI (%)	17,98	17,60	24,04

Table 6. 6: Comparison of the values of ROI for the three different fluids

As it can be seen, the N-pentane presents also the highest values of Return On Investment

### - Levelized Costs

The results obtained for the three types of Levelized Costs considered are the following

	Base R123	Base R245	Base n-pen
LCOEI (€/kWh)	0,81	1,00	1,03
LCOH (€/kWh)	0,14	0,13	0,12
LCOE (€/kWh)	0,12	0,12	0,11

Table 6. 7: Comparison of the Levelized costs for the three different fluids

For comparison purposes, there are reported below also the levelized costs for the main technologies on the market

- For the Levelized Cost of Electricity, the most updated data on the main renewable technologies are the reported below in the table 6.8 [63]

Technology	Solar PV	Onshore wind	Offshore wind	Geothermal plants
LCOE1 (€/kWh)	0,045	0,030	0,081	0,056

Table 6. 8: Levelized cost of electricity for the different Renewable Technologies

- For the Levelized Cost of Heat, the most updated data on the main renewable technologies are reported below in the table 6.9 [64]

Technology	Biomass (domestic pellet heating)	Solar thermal heating	Offshore wind	Geothermal plants for district heating
LCOH(€/kWh)	0,067	0,093	0,081	0,059

Table 6. 9: Levelized cost of heat for the different Renewable Technologies

As it can be seen, the Levelized Cost of Electricity is always much higher than the actual price of the electricity on the market. Moreover, its value is higher, with respect to the other renewable technologies, of one order of magnitude.

For what regards the Levelized Cost of Heat, its value is competitive with the other renewable technologies.

The reason behind these results is related to the fact that the ORC plant mainly exploits its revenues with the selling of the heat power, whose Levelized Cost indeed resents the actual market prices.

## Chapter 6.2: Implementation of the Superheating strategy

As previously said in the chapter 2.5, the superheating is a technique that can be implemented in a Rankine cycle that consists in the heating of the working fluid further than its condition of saturated vapour.

So, the fluid at the inlet of the turbine becomes a superheated vapor.

The higher inlet temperature of the fluid is expected to give several benefits in the revenues for the following reasons

- The work produced for unit of mass flow, with fixed inlet and outlet pressures of the turbine, will be higher
- The outlet temperature of the fluid will be higher, and hence there will be also an higher thermal power generation
- Due to the increased electrical power and heat power generation, the revenues comes from the incentives will also be higher

### 6.2.1: Implementation of the superheating in the cycle

The implementation of the superheating is done without changing any operational condition inside the pump, turbine and condenser.

What changes is in the evaporator, that will be asked to give more heat power to the working fluid, since it has to become a superheated vapor

In the evaporator, due to the higher outlet temperature required by the fluid, also the inlet temperature of the hot fluid should increase. This would have a negative consequence on the working hours of the plant, that will be reduced.

Now, since from the economic analysis it has emerged that the main part of the costs is due to the number of collectors, the temperature difference between the inlet hot fluid (coming from the solar collector) and the temperature inlet of the turbine, can be reduced. In this case, even if the logarithmic temperature difference in the evaporator will be lower, and so the area required for the heat exchange will be higher (and so the price of the heat exchanger will increase), the number of working hours of the plant will not undergo a steep reduction and so it is expected that the higher costs required for the plant will be counter-balanced by the avoided reduction of the working hours of the plant.

So, in the following pages of this paragraph, it is considered that the temperature difference between the inlet hot fluid in the evaporator and the inlet temperature of the working fluid in the turbine is set at 10 °C.

For each fluid, two superheating temperatures will be considered.

- **R123**

For the R123, the two following superheating temperatures have been chosen: 200 °C and 220 °C. Higher temperatures are not considered because the thermal decomposition of the R123 arrives at 250 °C

So, as a consequence, the temperature of the inlet hot fluid inside the evaporator will be set respectively to 210 and 230 °C.

- **R245fa**

For the R245fa, the two following superheating temperatures have been chosen: 280 °C and 320 °C. Higher temperatures are not considered because the thermal decomposition of the R245fa happens at 330°C

So, as a consequence, the temperature of the inlet hot fluid inside the evaporator will be set respectively to 290 and 320 °C

- **N-pentane**

For the N-pentane, the two following superheating temperatures have been chosen: 220 °C and 250 °C. Higher temperatures are not considered because the N-pentane reaches the auto-ignition at 260 °C

So, as a consequence, the temperature of the inlet hot fluid inside the evaporator will be set respectively to 230 and 260 °C

## **6.2.2: Comparison of the results**

Now, for each fluid, the base case will be compared with the two chosen superheating cases, then there will be a comparison between best cases for each fluid

- **R123**

For the R123, the following results have been obtained

### **- Thermodynamic performance**



For what regards the produced electrical and thermal power, the evolution of these quantities as function of the temperature is shown in the table below

Temperature [°C]	180	200	220
Wel [kW]	6,7	8,22	9,1
Qth [kW]	38,5	45,56	50,43

Table 6. 10: Evolution of the produced electricity and thermal power as function of the turbine inlet temperature for the R123

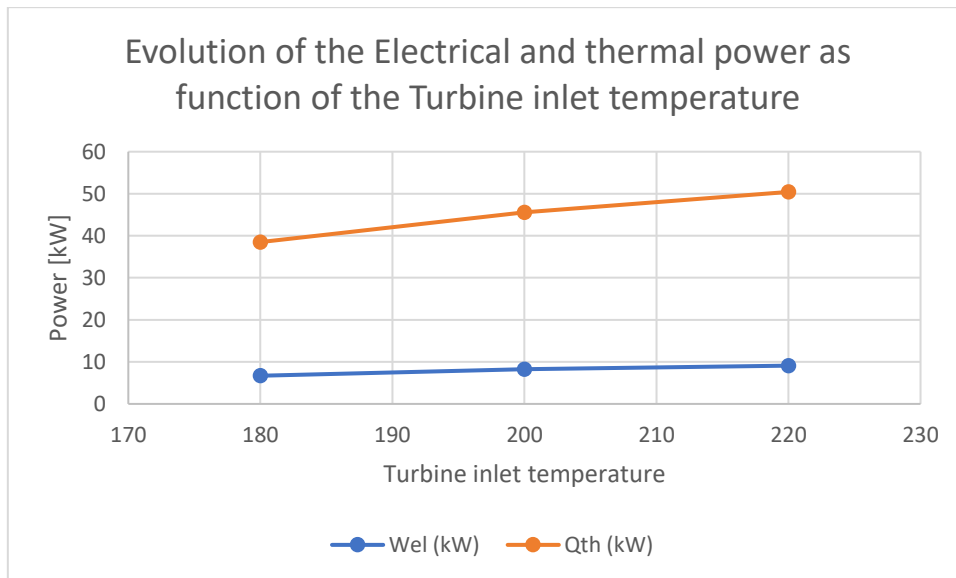


Figure 6.9: Graphic representation of the Evolution of the produced electricity and thermal power as function of the turbine inlet temperature for the R123

As expected, both the quantities increase as the temperature increase

For what regards the efficiency of electrical production and the efficiency of combined generation of heat and power the results are the following

Temperature [°C]	180	200	220
Eff el (%)	11,76	12,08	12,1
Eff th (%)	79,74	79,79	79,74

Table 6. 11: Evolution of the electrical efficiency and of the efficiency of combined generation of heat and power as function of the turbine inlet temperature for the R123

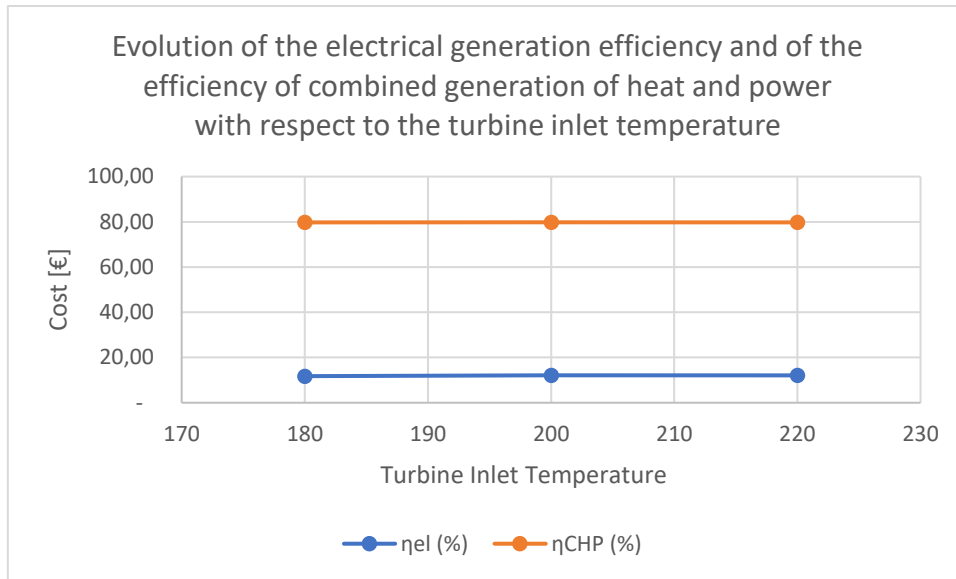


Figure 6.10: Graphic representation of the evolution of the electrical efficiency and of the efficiency of combined generation of heat and power as function of the turbine inlet temperature for the R123

As it can be seen, the efficiency of electrical power production increases, while the efficiency of combined heat and power generation remains almost constant.

#### - Economic performance

As expected, the increased heat required for the superheating has increased the number of collectors required

Temperature [°C]	180	200	220
N_coll	17	21	23

Table 6. 12: Evolution of the required number of collectors as function of the turbine inlet temperature for the R123

This aspect will produce an increase of the CAPEX, while the OPEX remain constant since the operational conditions of the pump does not change

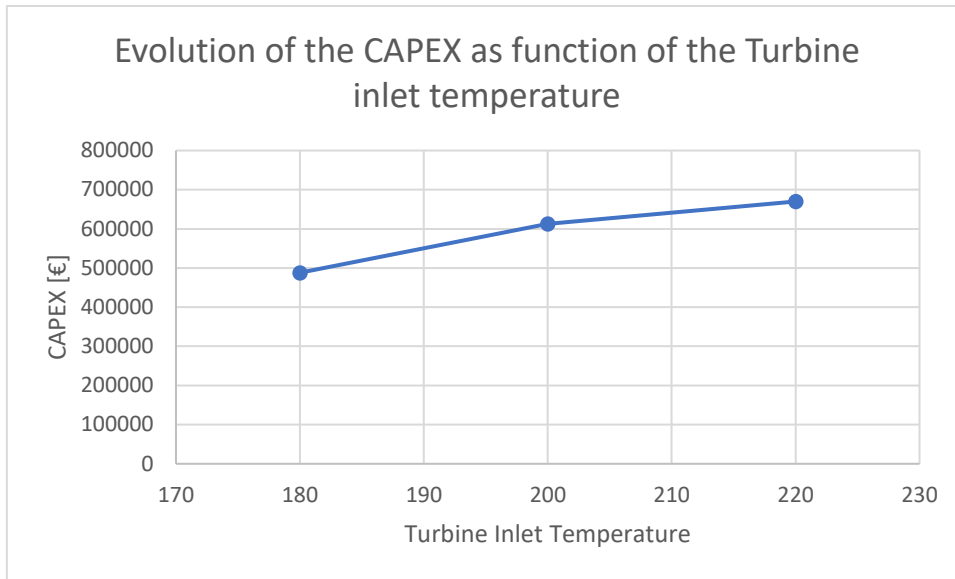


Figure 6.11: Evolution of the CAPEX as function of the turbine inlet temperature for the R123

For what regards the NPV, it increases and decrease as function of the temperature

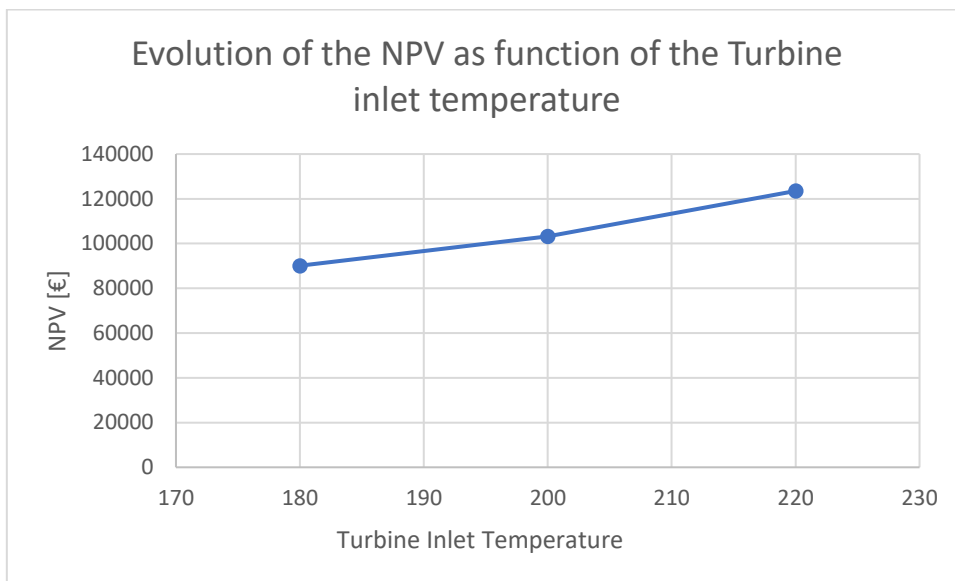


Figure 6.12: Evolution of the NPV as function of the turbine inlet temperature for the R123

For what regards the Return on the investment, it can be seen that it remains almost constant around the average value of 17%

Temperature [°C]	180	200	220
ROI [%]	18	16	18

Table 6. 13: Evolution of the Return on the investment as function of the temperature for the R123

To conclude, the evolution of the levelized costs is the following: they remain almost constant as function of the temperature

LCOEI (€)	0,81	0,81	0,80
LCOH (€)	0,14	0,15	0,14
LCOE (€)	0,12	0,12	0,12

Table 6. 14: Evolution of the Levelized costs as function of the turbine inlet temperature for the R123

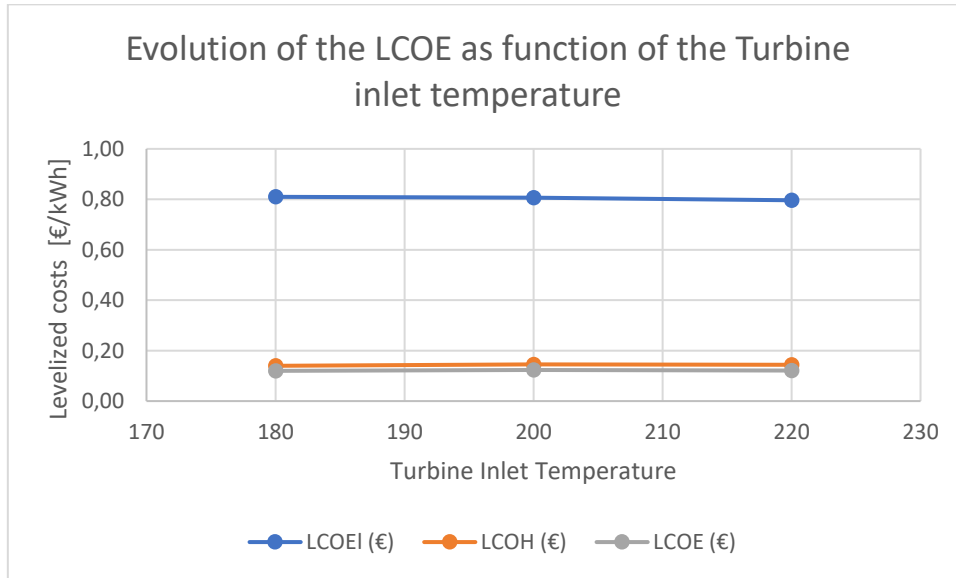


Figure 6.13: Graphical representation of the evolution of the levelized costs as function of the turbine inlet temperature for the R123

- **R245fa**

For the R123, the following results have been obtained

**- Thermodynamic performance**

For what regards the produced electrical and thermal power, the evolution of these quantities as function of the temperature is shown in the table below

Temperature [°C]	150	280	320
Wel (kW)	5,29	10,23	11,28
Qth (kW)	39,87	83,58948	96,284

Table 6. 15: Evolution of the produced electricity and thermal power as function of the turbine inlet temperature for the R245fa

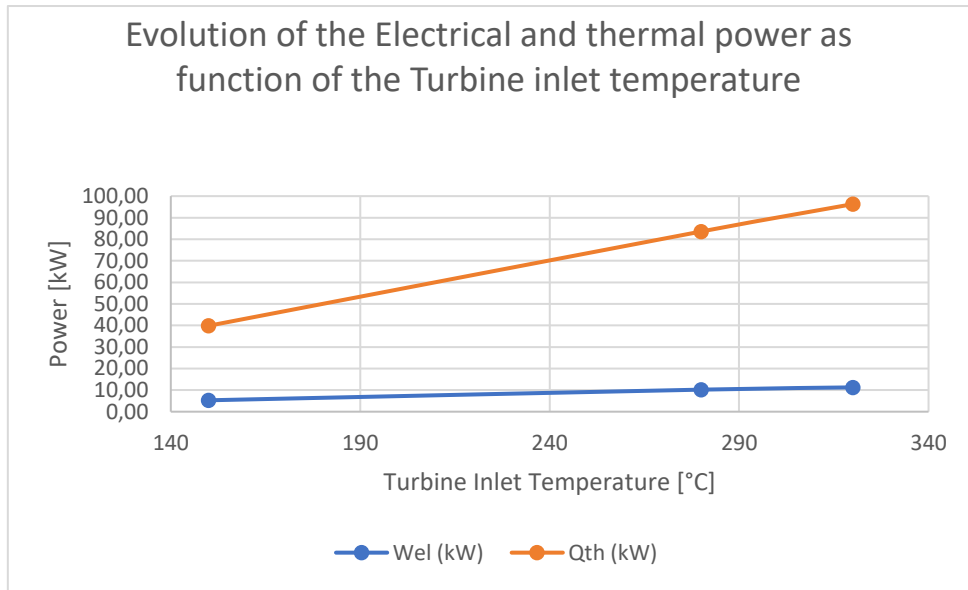


Figure 6.14: Graphic representation of the evolution of the produced electricity and thermal power as function of the turbine inlet temperature for the R245fa

As expected, both the quantities increase as the temperature increase

For what regards the efficiency of electrical production and the efficiency of combined generation of heat and power the results are the following

Temperature [°C]	150	280	320
$\eta_{el}$ (%)	9,31	8,60	8,27
$\eta_{CHP}$ (%)	79,970	80,00	80

Table 6. 16: Evolution of the electrical efficiency and of the efficiency of combined generation of heat and power as function of the turbine inlet temperature for the R245fa

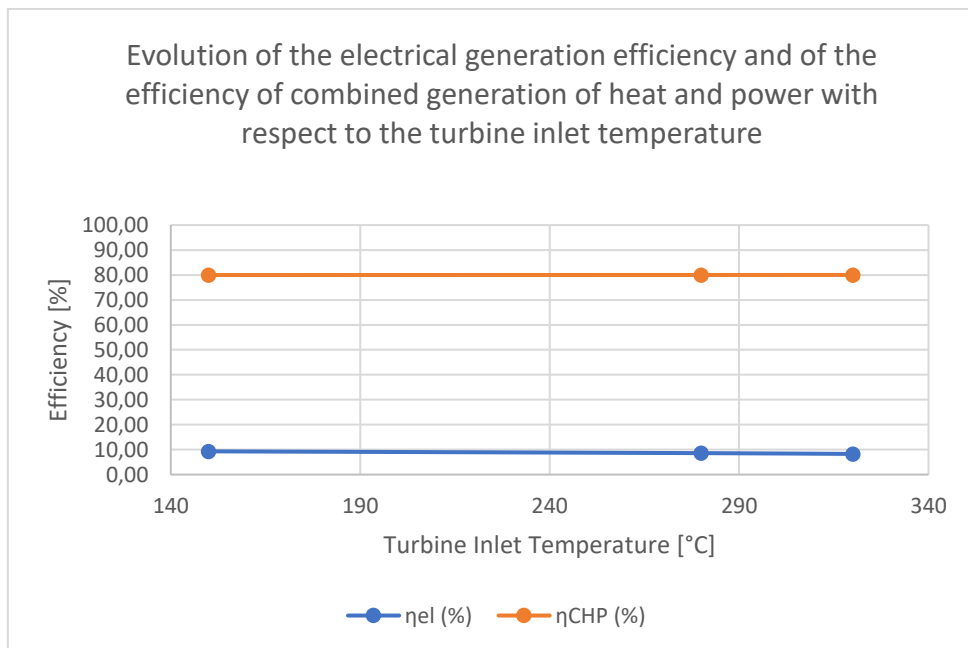


Figure 6.15: Graphic representation of the evolution of the electrical efficiency and of the efficiency of combined generation of heat and power as function of the turbine inlet temperature for the R245fa

Here it is interesting to note that the efficiency of electricity production slightly decreases, while the efficiency of combined heat and power generation remains almost constant.

**- Economic performance**

Again, as expected, the increased heat required for the superheating has increased the number of collectors required

Temperature [°C]	180	200	220
N_coll	16	34	38

Table 6. 17: Evolution of the required number of collectors as function of the turbine inlet temperature for the R245fa

So, as a consequence, there will be again an increase of the CAPEX

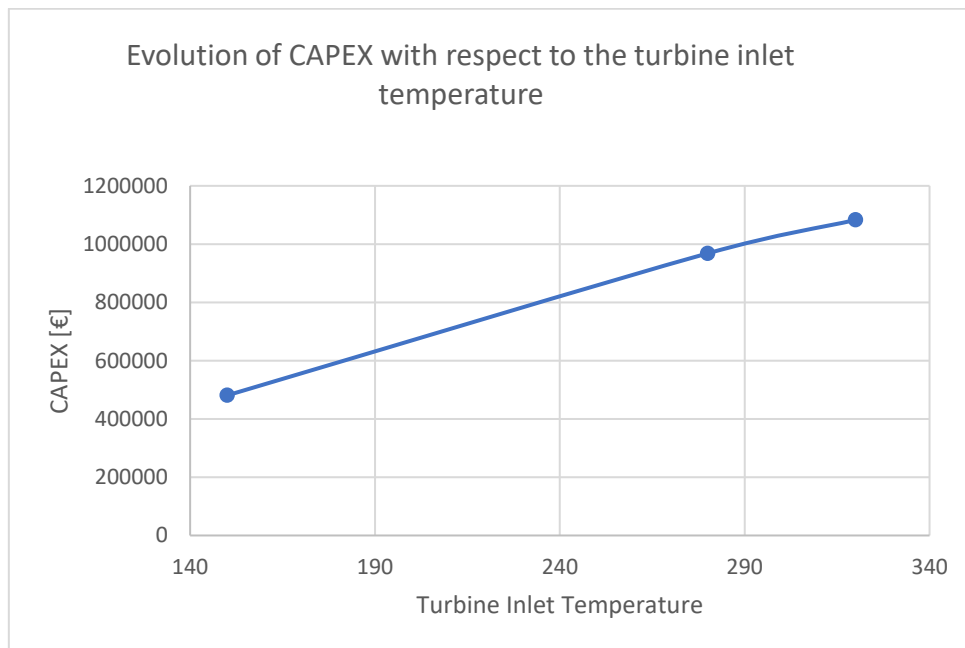


Figure 6.16: Evolution of the CAPEX as function of the turbine inlet temperature for the R245fa

For what regards the NPV and the PBT, they respectively increase and decrease as function of the temperature

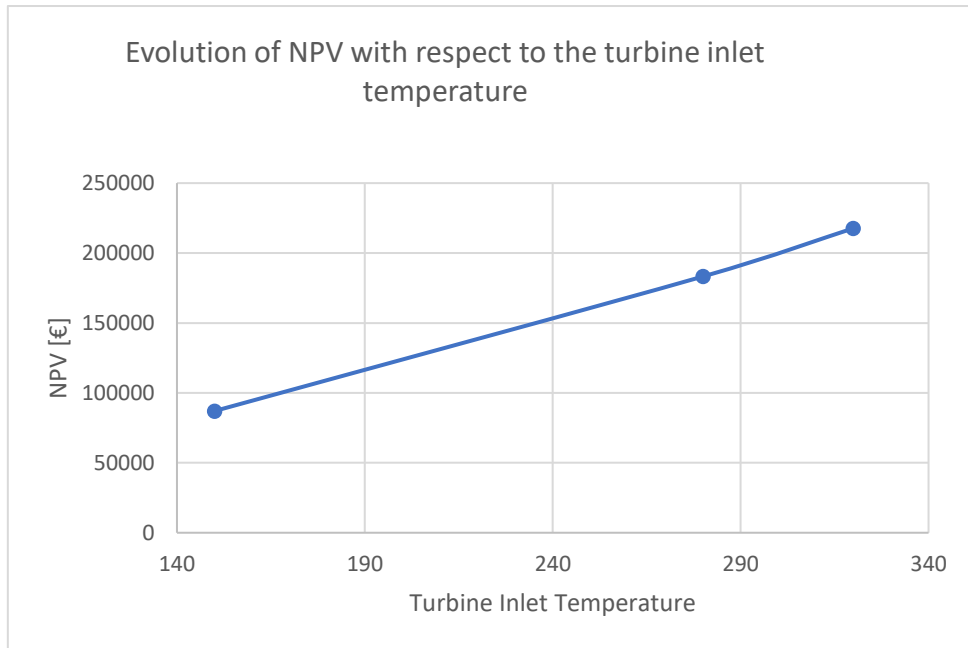


Figure 6.17: Evolution of the NPV as function of the turbine inlet temperature for the R245fa

For what regards the Return on investment, its value remains constant around 18%

Temperature [°C]	150	280	320
ROI [%]	17,6	18,6	19,8

Table 6. 18: Evolution of the Return on investment as function of the temperature for the R245fa

For what regards the evolution of the levelized cost, the one of the electricity has a slight increase while the others remain almost constant

Temperature [°C]	150	280	320
LCOEI (€/kWh)	1,00	1,07	1,10
LCOH (€/kWh)	0,13	0,13	0,13
LCOE (€/kWh)	0,12	0,12	0,11

Table 6. 19: Evolution of the Levelized costs as function of the turbine inlet temperature for the R245fa

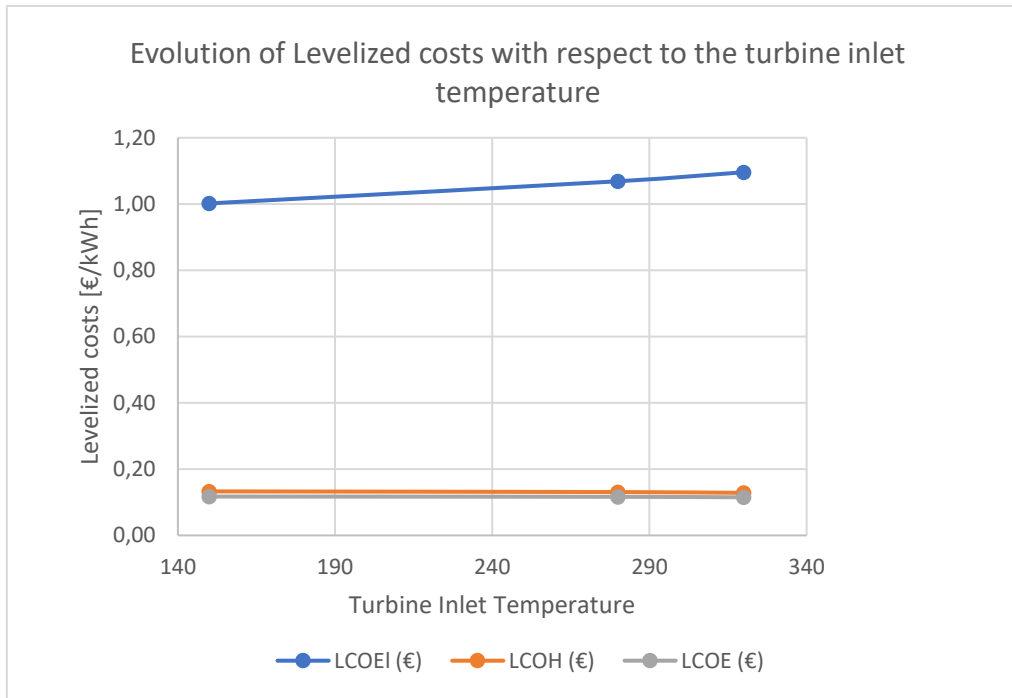


Figure 6.18: Graphical representation of the evolution of the levelized costs as function of the turbine inlet temperature for the R245fa

Again, it is possible to see that the best performance is the superheating case with the maximum turbine inlet temperature.

- **N-pentane**

For the N-pentane, the following results have been obtained

**- Thermodynamic performance**

For what regards the produced electrical and thermal power, the evolution of these quantities as function of the temperature is shown in the table below

Temperature [°C]	150	220	250
Wel (kW)	11,29	14,74	16,00
Qth (kW)	92,85	136,75	155,64

Table 6. 20: Evolution of the produced electricity and thermal power as function of the turbine inlet temperature for the N-pentane



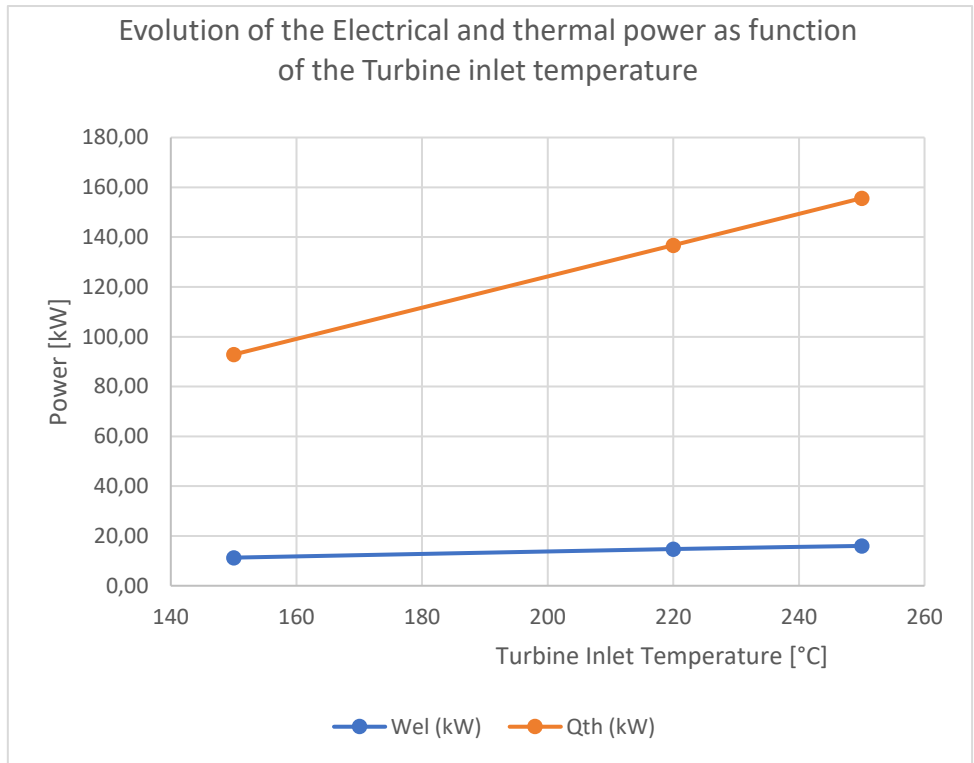


Figure 6.19: Graphic representation of the evolution of the produced electricity and thermal power as function of the turbine inlet temperature for the N-pentane

Again as expected, both the quantities increase as the temperature increase

For what regards the efficiency of electrical production and the efficiency of combined generation of heat and power the results are the following

Temperature [°C]	150	220	250
$\eta_{el}$ (%)	8,54	7,65	7,33
$\eta_{CHP}$ (%)	80,00	80	80,00

Table 6. 21: Evolution of the electrical efficiency and of the efficiency of combined generation of heat and power as function of the turbine inlet temperature for the N-pentane

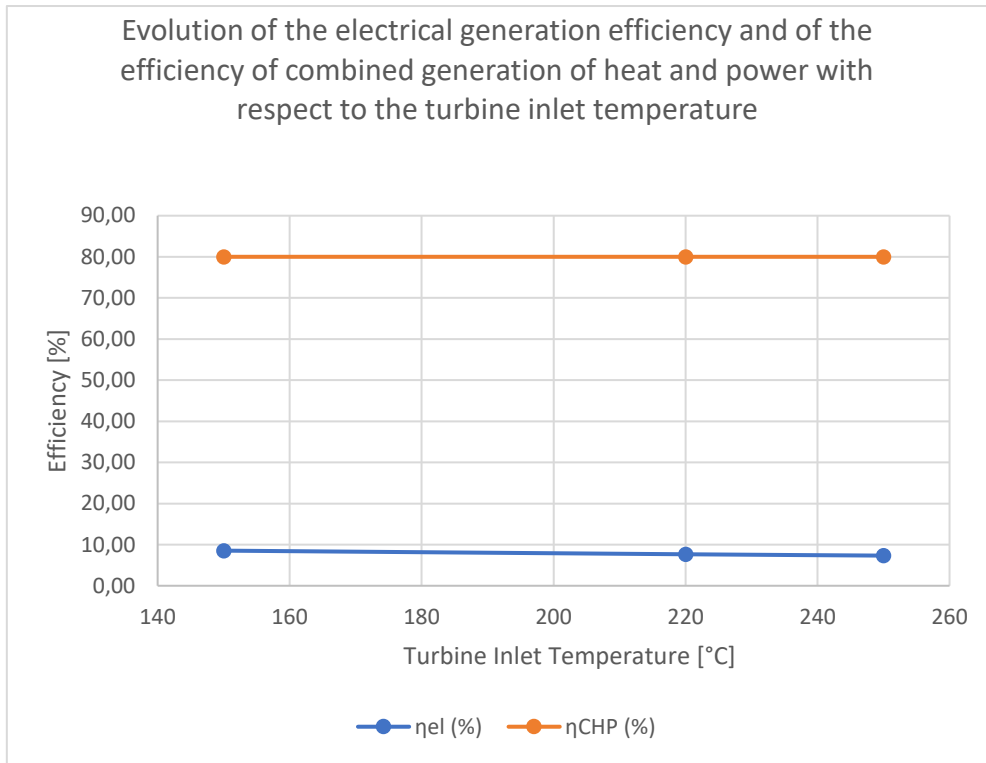


Figure 6.20: Graphic representation of the evolution of the electrical efficiency and of the efficiency of combined generation of heat and power as function of the turbine inlet temperature for the N-pentane

In the same way as the R245fa, also here it is interesting to note that the efficiency of electricity production slightly decreases, while the efficiency of combined heat and power generation remains almost constant.

### - Economic performance

Again, as expected, the increased heat required for the superheating has increased the number of collectors required

Temperature [°C]	150	220	250
N_coll	37	58	62

Table 6. 22: Evolution of the required number of collectors as function of the turbine inlet temperature for the N-pentane

So, as a consequence, there will be again an increase of the CAPEX

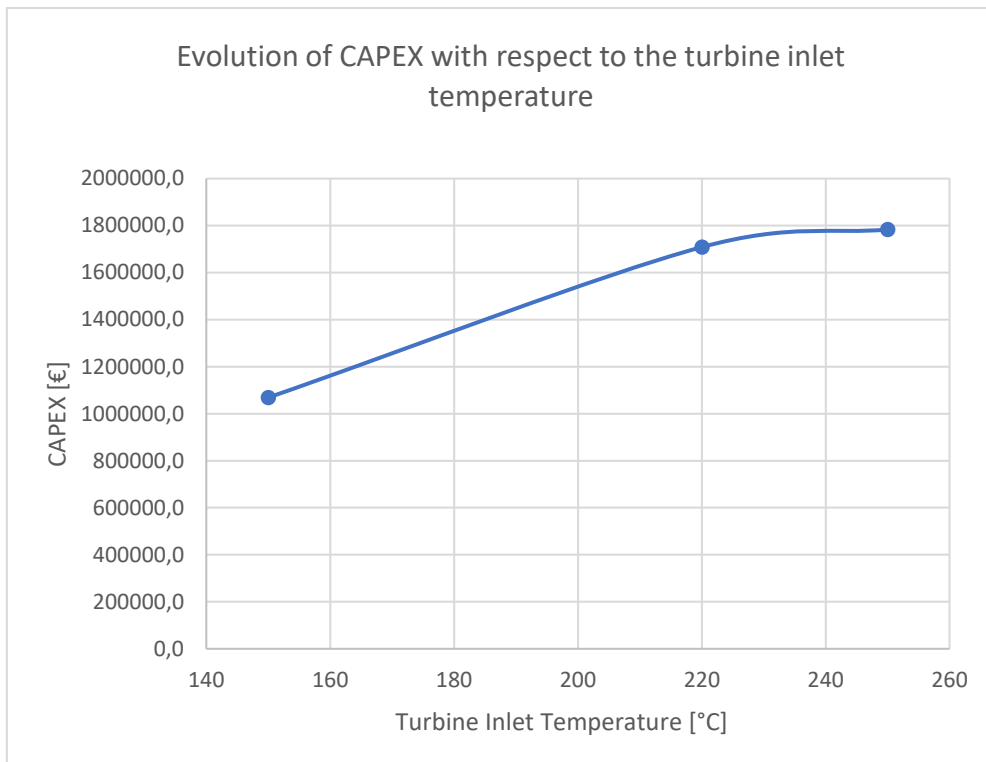


Figure 6.21: Evolution of the CAPEX as function of the turbine inlet temperature for the N-isopentane

For what regards the NPV and the PBT, this time they both increase as function of the temperature

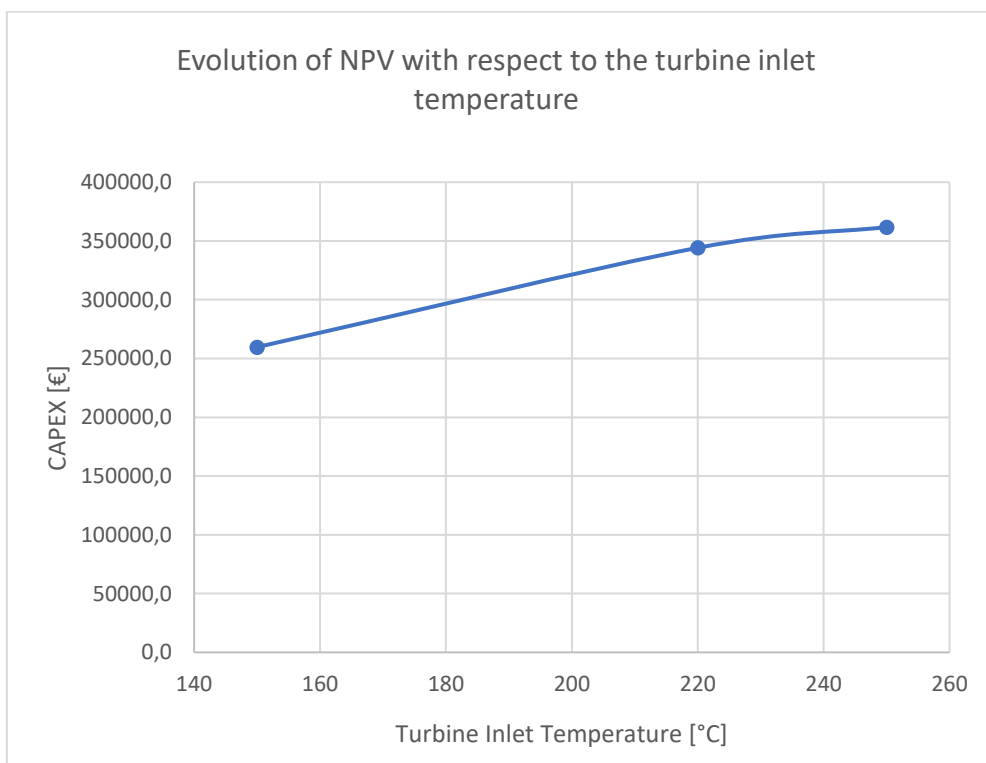


Figure 6.22: Evolution of the NPV as function of the turbine inlet temperature for the N-pentane

For what regards the ROI, it can be seen that it decreases with the temperature

Temperature [°C]	150	220	250
ROI [%]	24,03	20,05	20,14

Table 6. 23: Evolution of the ROI as function of the turbine inlet temperature for the N-pentane

To conclude, for what regards the evolution of the levelized cost, again the one of the electricity has a slight increase while the others remain almost constant

Temperature [°C]	150	280	320
LCOEI (€/kWh)	1,03	1,16	1,22
LCOH (€/kWh)	0,12	0,13	0,13
LCOE (€/kWh)	0,11	0,11	0,11

Table 6. 24: Evolution of the Levelized costs as function of the turbine inlet temperature for the N-pentane

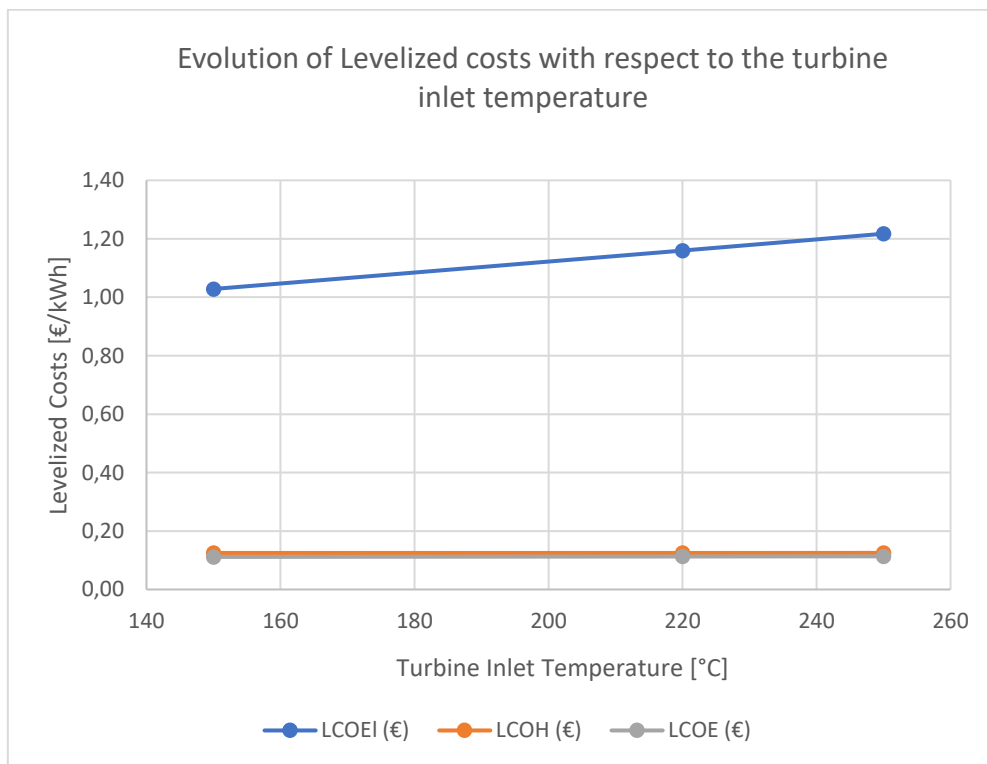


Figure 6.23: Graphical representation of the evolution of the levelized costs as function of the turbine inlet temperature for the N-pentane

Again, it is possible to see that the best performance is the superheating case with the maximum turbine inlet temperature.

- **Comparison of the best three cases**

Now, it is possible to compare the best three cases, that are respectively:

- R123 with superheating temperature of 220 °C
- R245fa with superheating temperature of 320 °C
- N-pentane with superheating temperature of 250 °C

- **Thermodynamic performance**

For what regards the electrical and thermal power generation, the highest values are for the N-pentane superheated

	R123	R245	N-pen
Wel (kW)	9,10	11,28	16,00
Qth (kW)	50,44	96,28	155,64

Table 6. 25: Comparison of the produced electricity and thermal power for the three fluids with the superheating

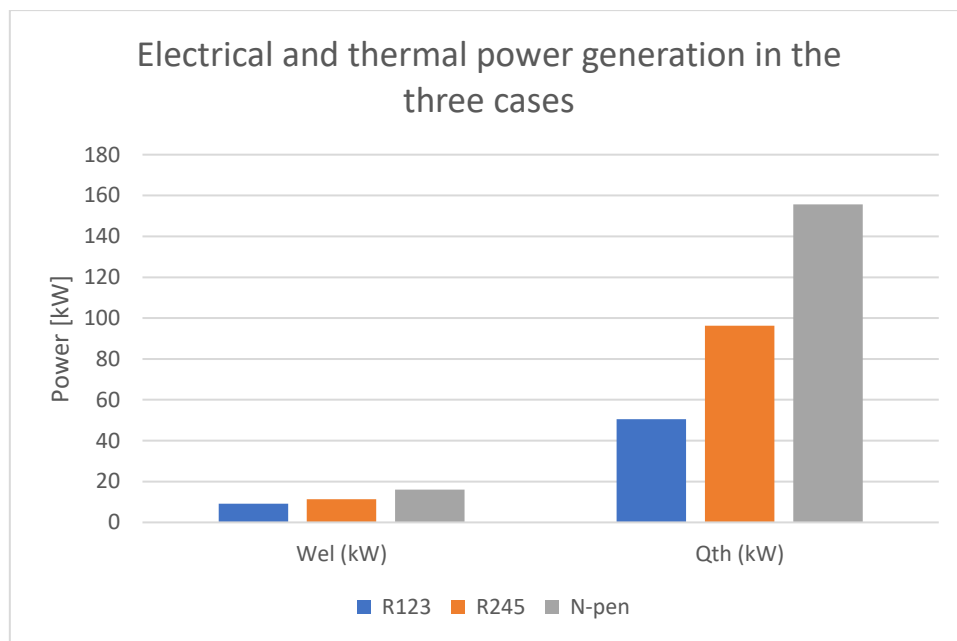


Figure 6.24: Graphical representation of the comparison of the produced electricity and thermal power for the three fluids with the superheating

On the other hand, for what regards the efficiencies, the situation is the following

	R123	R245fa	N-pen
$\eta_{el}$ (%)	12,09	8,27	7,33
$\eta_{CHP}$ (%)	79,74	80,00	80,00

Table 6. 26: Comparison of the electrical efficiency and of the efficiency of combined generation of heat and power for the three fluids with the superheating

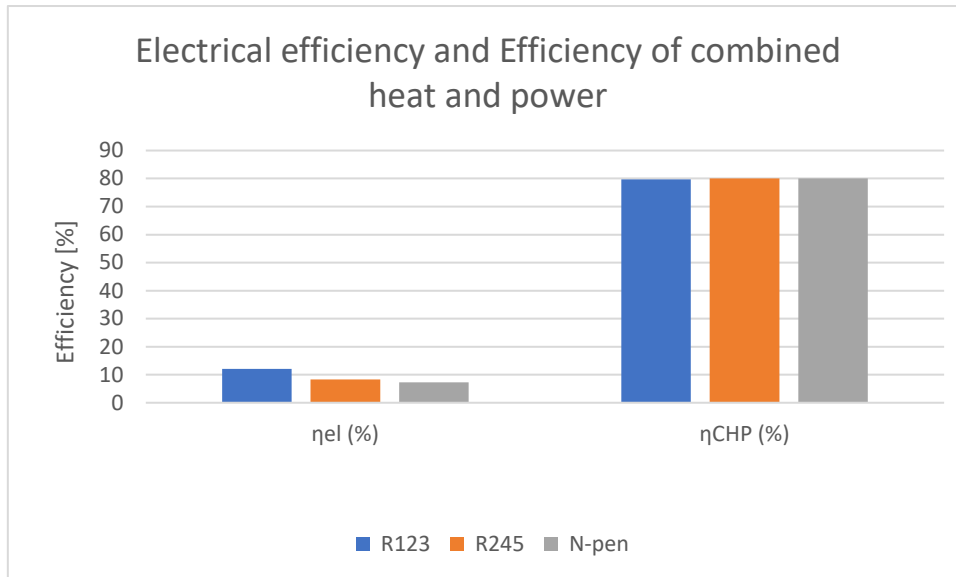


Figure 6.25: Graphic representation of the comparison of the electrical efficiency and of the efficiency of combined generation of heat and power for the three fluids with the superheating

The R123, while producing the lowest amount of heat and electrical power, is the fluid that grants the best performances in terms of electrical efficiency.

The opposite goes for the N-pentane, which has overall the lowest electrical efficiency but it gives the biggest amount of electrical power.

The efficiency of combined generation remains as always constant, with values that go around 80 %.

#### - Economic performance

As previously said, the number of collectors increased for each case due to the higher temperatures required.

The number of collectors for the R123 remains still low, while the N-pentane sees a steep increase

	R123	R245fa	N-pen
Base case	18	16	37
Superheating case	23	38	62

Table 6. 27: Comparison of the required number of collectors for the three fluids with the superheating

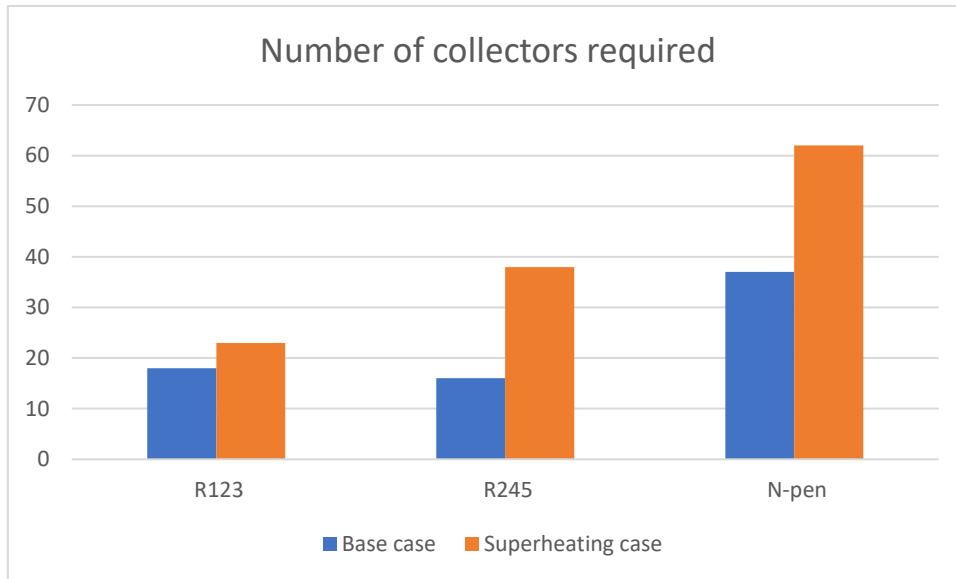


Figure 6.26: Graphic representation of the comparison of the required number of collectors for the three fluids with the superheating

As a consequence, as shown below, the CAPEX of the R123 sees a slight increase, while the CAPEX of the N-pentane steeply increases, reaching almost the 2 Million of euro.

CAPEX [€]	R123	R245fa	N-pen
Base case	487977,5	480840,5	1068545
Superheating case	669894,7	1082834	1783733

Table 6. 28: Comparison of the CAPEX required for the three fluids, with and without superheating

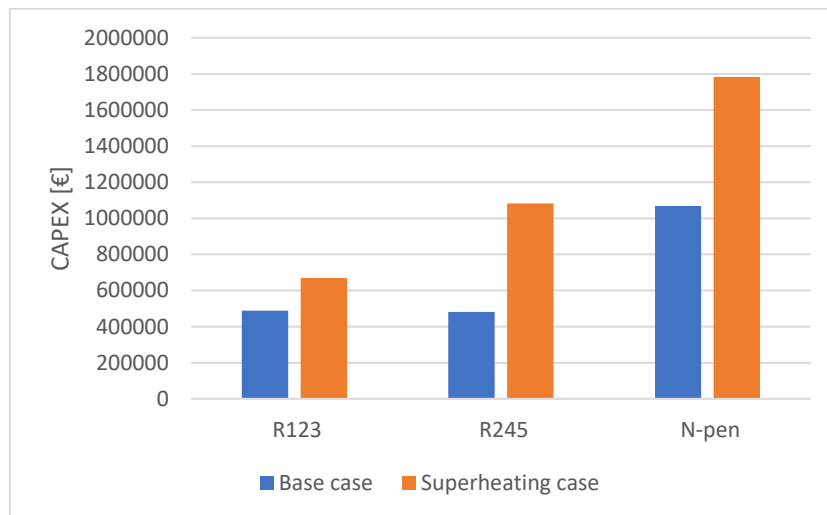


Figure 6.27: Graphic representation of the comparison of the CAPEX required for the three fluids, with and without superheating

For what regards the NPV it increases every time with the temperature.

The R245 is the fluid that most had benefits for the temperature increase, while the highest value is still obtained by the N-pentane

NPV (€)	R123	R245fa	N-pen
Base case	90100	87029,84	259669,7
Superheating case	123498	217706	361794

Table 6. 29: Comparison of the NPV for the three fluids, with and without superheating

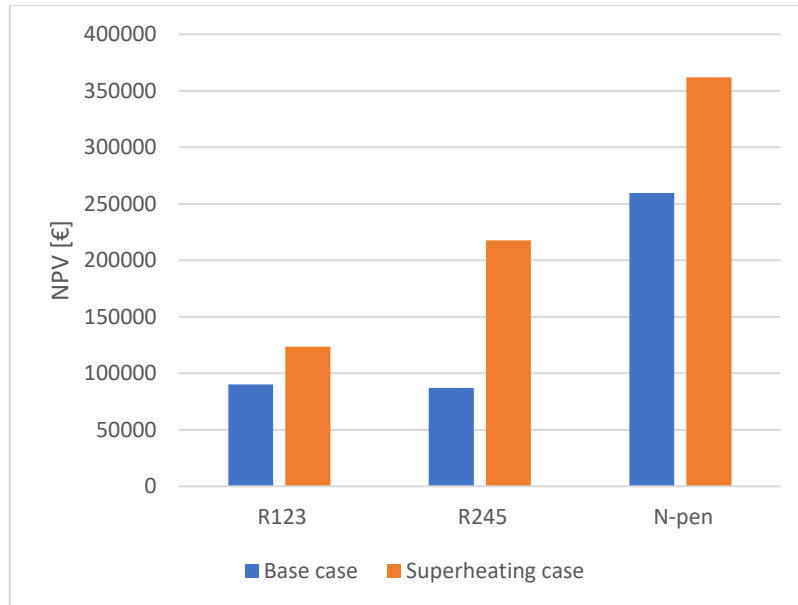


Figure 6.28: Graphic representation of the comparison of the NPV for the three fluids, with and without superheating

The payback time remained almost constant around the value of 24 years

PBT [years]	R123	R245fa	N-pen
Base case	24,3	24,2	23,2
Superheating case	24,4	24,1	24,0

Table 6. 30: Comparison of the Payback time for the three fluids, with and without superheating

For what regards the Return on the Investment, it can be said that with the implementation of the superheating the differences between the N-pentane and the two CFCs are reduced, even if the N-pentane still resists at the first place

ROI [%]	R123	R245fa	N-pen
Base case	18,0	17,6	24,0
Superheating case	18,1	19,9	20,1

Table 6. 31: Comparison of the Return on Investment for the three fluids, with and without superheating

To conclude, the Levelized costs can be seen

The levelized cost of electricity decreases only for the R123, while it increases for the other two fluids. This matter can be related to the fact that there is an increase in the electrical generation efficiency only for the R123, while for the other two fluids there is a slight decrease.

Anyway, in every case, the Levelized cost of electricity never reaches the market values, and so it testifies the fact that the CSP technology orientated for the production of electricity through an ORC does not represent, nowadays, a competitive technology for the electricity generation



LCOEL [€/kWh]	R123	R245fa	N-pen
Base case	0,81	1,00	1,02
Superheating case	0,79	1,09	1,21

Table 6. 32: Comparison of the Levelized cost of electricity for the three fluids, with and without superheating

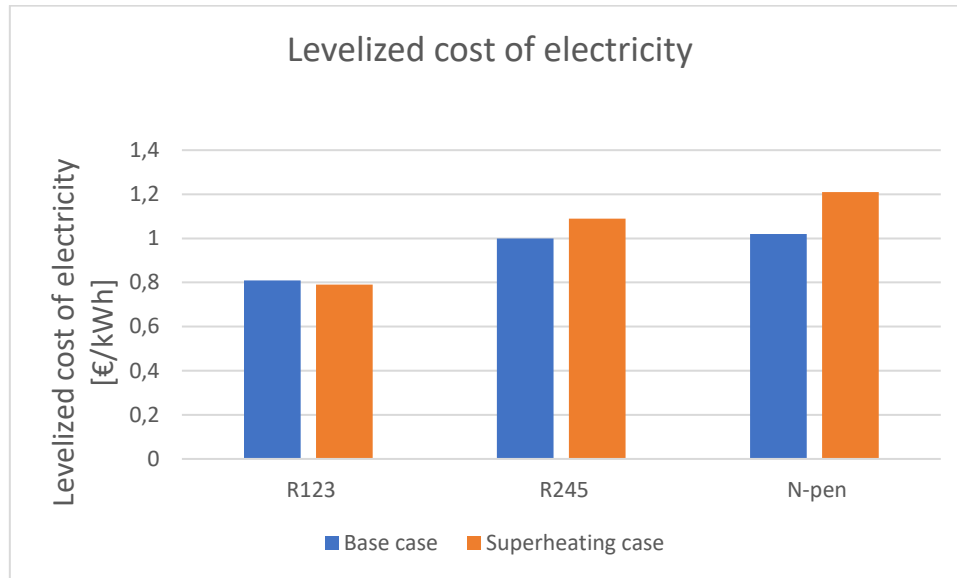


Figure 6.29: Graphic representation of the comparison of the Levelized cost of electricity for the three fluids, with and without superheating

The Levelized Cost Of Heat, in the same way as the combined generation of heat and power, remains almost constant for every technology and the values are all near to each other

LCOH [€/kWh]	R123	R245fa	N-pen
Base case	0,14	0,13	0,12
Superheating case	0,14	0,12	0,12

Table 6. 33: Comparison of the Levelized cost of heat for the three fluids, with and without superheating

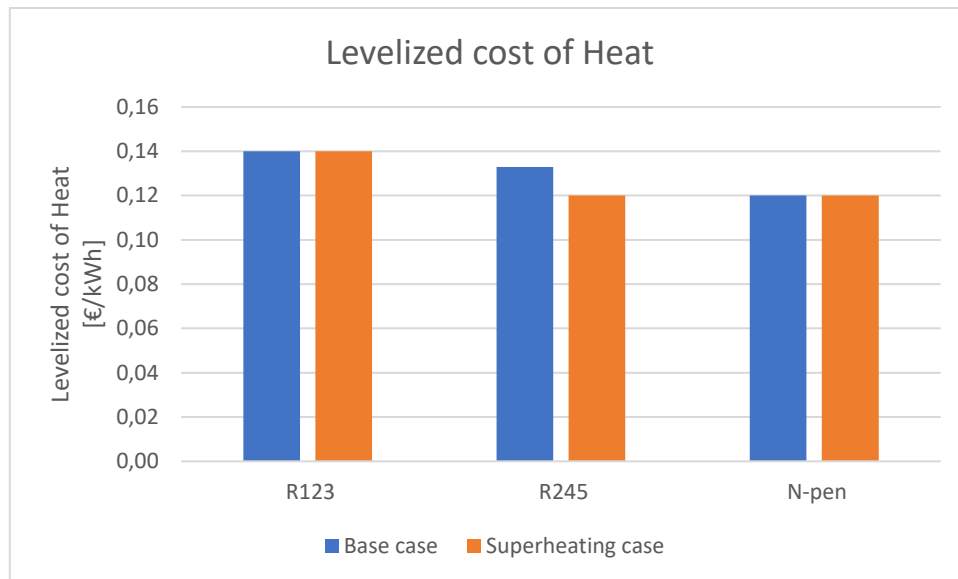


Figure 6.30: Graphic representation of the comparison of the Levelized cost of heat for the three fluids, with and without superheating

To conclude, the Levelized Cost Of Energy slightly decreases for the R123 while it remains constant for the other two cases. The reason might be related to the fact that the biggest part of the energy produced is the thermal power in the condenser, and so its part is the one that mostly impacts the LCOE.

LCOE [€/kWh]	R123	R245fa	N-pen
Base case	0,12	0,12	0,11
Superheating case	0,12	0,11	0,11

Table 6. 34: Comparison of the Levelized cost of energy for the three fluids, with and without superheating

### Chapter 6.3: Implementation of the Heat recuperation strategy

Until now, one of the main results that has been obtained is the fact that the principal bottleneck of the ORC powered by CSP is the cost related to the solar collectors, that might represent much more than 50 % of the total CAPEX.

The power that has to be given by the solar collector is directly related to the heat that is required by the working fluid in order to reach the turbine inlet temperature. For this reason, one of the possible ways to reduce the CAPEX is to implement a third heat exchanger, called “recuperator” that is placed after the turbine outlet and that pre-heats the fluid coming from the pump in order to reduce the amount of thermal energy requested for the phase change and eventual superheating.

Normally, this strategy increases the electrical production efficiency since there is a direct reduction of thermal power needed, while maintaining as constant the inlet and outlet conditions of the turbine (and so, the electrical power produced).

In this case, since the plant is working in co-generation mode, the efficiency of co-generation might not increase because part of the products is given by the thermal power exchanged in the condenser, which decreases due to the presence of the recuperator because the working fluid, before entering the condenser, is colder due to the heat given off for the superheating.

Now, in this last part of the improvements, it will be seen how the presence of a recuperator will affect all of the thermodynamic and economic performances analysed until now.

Since it has been previously seen that the superheating strategy is the most convenient, the recuperated cycle will be applied for each fluid only at its configuration with the superheating.

What it is expected is that the presence of the recuperator, that causes an additional cost since another heat exchanger is needed to be installed, will be counter-balanced by the reduced number of solar collectors.

### **6.3.1: Implementation of the recuperator**

For each working fluid, it has been searched for the configuration that gave the maximum amount of power exchanged inside the recuperator

- For the R123, it has been seen that in the evaporator the maximum temperature difference between inlet hot fluid (that is, the working fluid exiting from the turbine) and outlet cold fluid (that is, the working fluid that is exiting the recuperator and entering the evaporator) is equal to 25 °C.

This means that the working fluid enters the evaporator no longer at 79 °C, but at 118 °C, and as a consequence the power saved is equal to 11,1 kW

- For the R245fa, it has been seen that in the evaporator the maximum temperature difference between inlet hot fluid and outlet cold fluid is equal to 110 °C

This means that the working fluid enters the evaporator no longer at 80 °C, but at 165 °C, and as a consequence the power saved is equal to 53,1 kW

- For the N-pentane, it has been seen that in the evaporator the maximum temperature difference between inlet hot fluid and outlet cold fluid is equal to 100 °C

This means that the working fluid enters the evaporator no longer at 80 °C, but at 117 °C, and as a consequence the power saved is equal to 23,3 kW

### **6.3.2: Comparison of the results**

Now, in this last section, it will be analysed the difference between the superheating case (that is the best configuration seen until now for each fluid) and the recuperated case

#### **- Thermodynamic results**

For what regards the electrical power produced, since both the mass flows and the thermodynamic conditions at the inlet and outlet of the turbine are still constant, the values are the same

On the other hand, for what regards the thermal power produced, there is a reduction because, as previously anticipated, the working fluids are entering at lower temperatures inside the condenser, and so less thermal power is exchanged. This matter will influence the costs.

Thermal power produced [kW]	R123	R245fa	N-pen
Superheated case	50,44	96,28	155,64
Recuperated case	39,31	43,19	132,3

Table 6. 35: Comparison of the thermal power produced for the three fluids, with and without recuperator

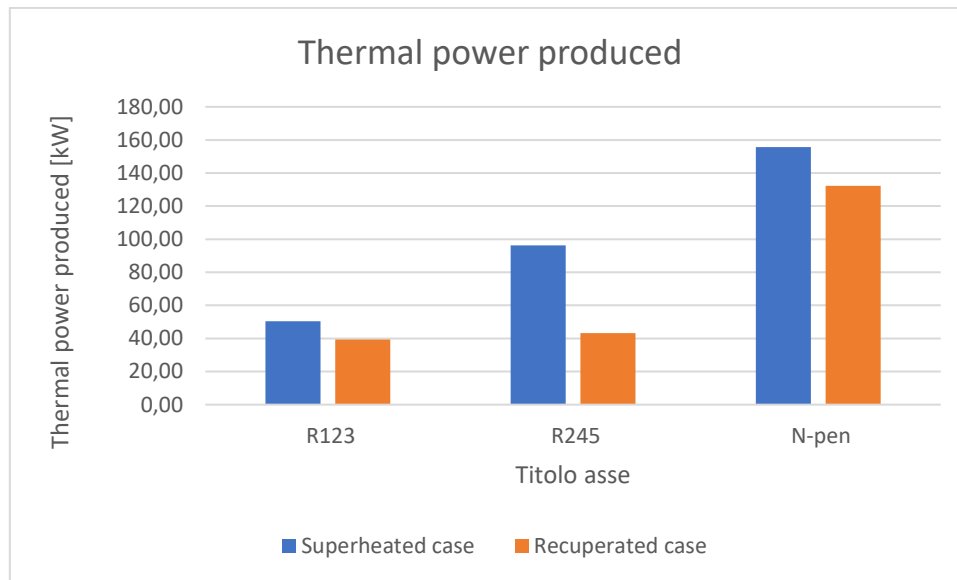


Figure 6.31: Graphic representation of the comparison of thermal power produced for the three fluids, with and without recuperator

The biggest reduction is for the R245fa, where there is the biggest amount of energy saved in the recuperator.

For what regards the electrical efficiency, as previously anticipated, the presence of the recuperator permits to reduce the required thermal input inside the evaporator, and so, with the same electricity produced, the values increase.

Electrical efficiency [%]	R123	R245fa	N-pen
Superheated case	12,09	8,27	7,33
Recuperated case	15,24	16,45	8,50

Table 6. 36: Comparison of the electrical efficiency for the three fluids, with and without recuperator

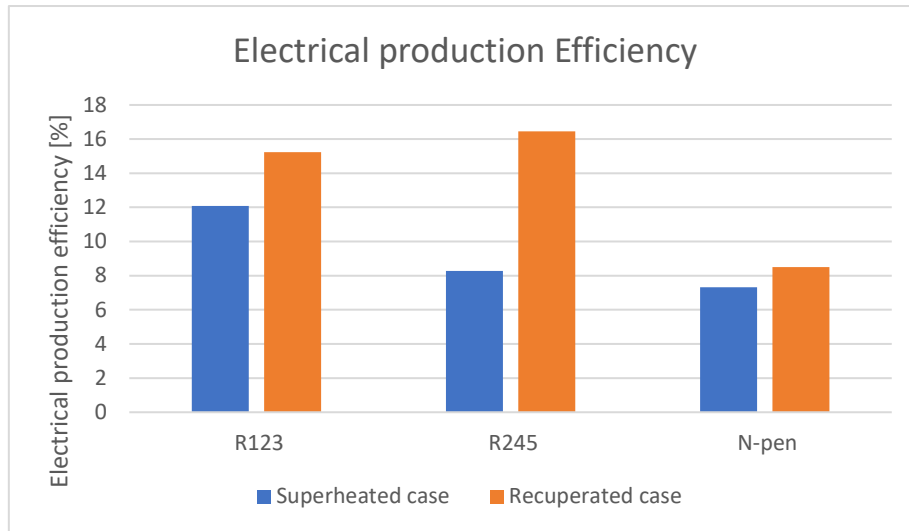


Figure 6.32: Comparison of the electrical efficiency for the three fluids, with and without recuperator

For what regards the efficiency of combined production of heat and power the situation is a bit less trivial: on one side, there is the reduction of thermal input produced inside the evaporator, but, on the other side, there is also the reduction of thermal power produced inside the condenser.

In the end of the story, it can be seen that the values remain once again constant around the value of 80 %

Efficiency of combined production of heat and power [%]	R123	R245	N-pen
Superheated case	79,74	80	80,00
Recuperated case	79,73	80	79,92

Table 6. 37: Comparison of the efficiency of combined generation of heat and power, with and without recuperator

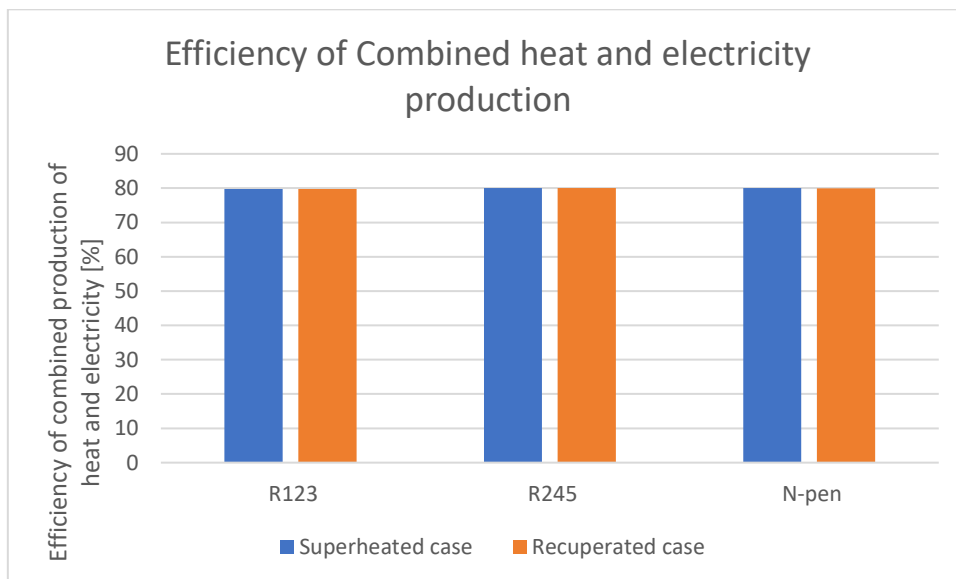


Figure 6.33: Graphic representation of the comparison of the efficiency of combined generation of heat and power for the three fluids, with and without recuperator

## - Economic performance

As previously anticipated, the number of collectors decreased for each fluid used

The biggest reduction in absolute terms come for the R245fa

Number of collectors	R123	R245fa	N-pen
Superheating case	23	38	62
Recuperator case	18	20	53

Table 6. 38: Comparison of the number of collectors for the three fluids, with and without recuperator

As a consequence, every configuration will face a reduction of the CAPEX.

Graphically it can be seen, according to what it has just been stated, that the biggest CAPEX reduction come for the R245fa

CAPEX [€]	R123	R245fa	N-pen
Superheating case	669894	1082834	1783733
Recuperator case	561006	599926,7	1499037

Table 6. 39: Comparison of the CAPEX for the three fluids, with and without recuperator

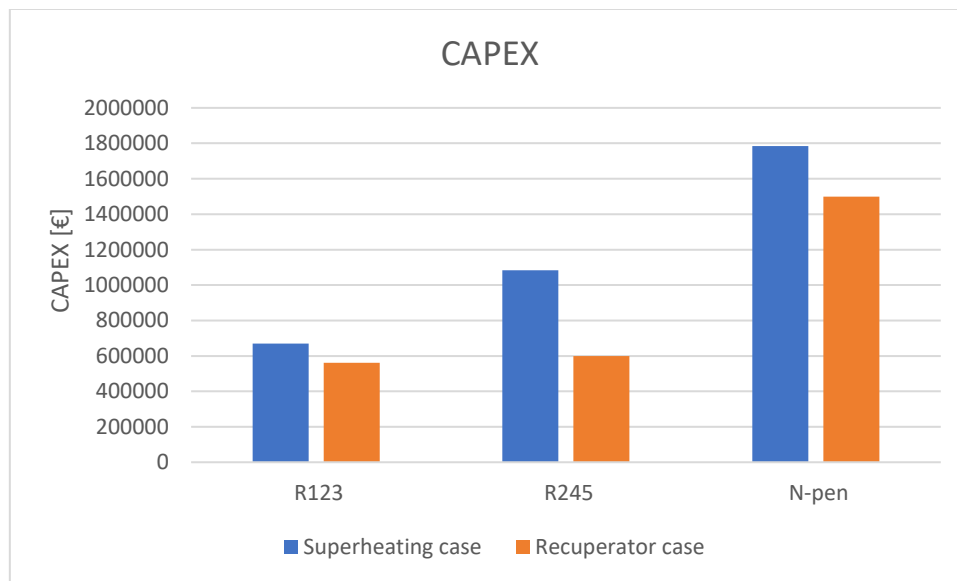


Figure 6.34: Graphic representation of the comparison of the variation of the CAPEX for the three fluids, with and without recuperator

Now, the results for the NPV and PBT can be seen.

According to what it is reported in the table below, it can be seen a non-trivial result: even though there is a reduction of CAPEX, the NPV at the end of the life of the plant is smaller for the R123 and for the R245fa, while it increases for the N-pentane.

Net Present Value [€]	R123	R245fa	N-pen
Superheating case	123498	217706	361794
Recuperator case	99721	123304	384664

Table 6. 40: Comparison of the Net Present Value for the three fluids, with and without recuperator

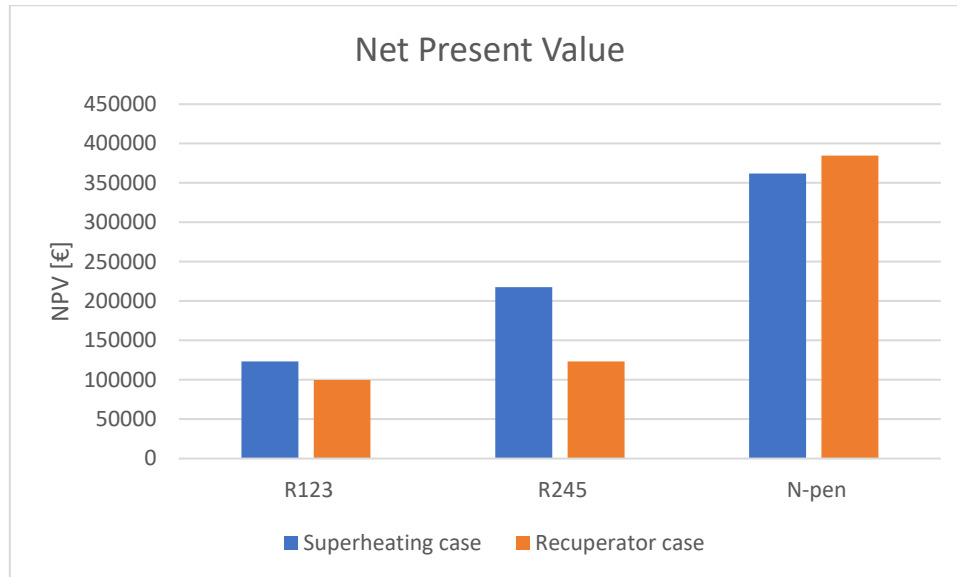


Figure 6.35: Graphic representation of the comparison of the Net Present Value for the three fluids, with and without recuperator

The reason behind this result is probably to attribute to the reduced thermal power produced in the condenser.

In fact, every detail on the analysis performed until now suggests that the biggest responsible for the revenues is the selling of the thermal power. With the recuperator case, since there is a reduction in the power output from the condenser, part of these revenues is inevitably lost. Moreover, since the incentives that have been considered depend linearly from the power production, the damage done by the reduction in the power output are even bigger. Another proof comes from the table that reports the thermal power variation between the superheating case and the recuperator case: the R245fa is the fluid that has faced the biggest reduction of thermal power produced, and now it can be seen that it is the fluid that has faced the biggest reduction in the NPV

The values of the Payback Time remain almost constant and around the 24 years. The only exception is given by the N-pentane with the recuperator case, in which the value is decreased to a bit less than 23 years.

PBT	R123	R245fa	N-pen
Superheating case	24,4	24,1	24,0
Recuperator case	24,6	23,9	22,9

Table 6. 41: Comparison of the PBT for the three fluids, with and without recuperator

Then, for what regards the Return on investment, it can be seen that for the R123 there is a slight decrease, even if the value is always still around the 18 %, while for the N-pentane there is a steep

increase. The reason for this last result might be that the N-pentane case is the only one that has seen both the decrease of CAPEX and the increase of the NPV with the usage of the recuperator

ROI [%]	R123	R245	N-pen
Superheated case	18,1	19,9	20,1
Recuperated case	17,4	20,0	25,5

Table 6. 42: Comparison of the Return on Investment for the three fluids, with and without recuperator

To conclude, the Levelized costs can be seen

For what regards the Levelized cost of Electricity, it can be seen that it increases with the presence of the recuperator in each case. The reason is probably related to the enhanced electrical efficiency that comes from the reduced thermal input: with less collectors (and so, a lower CAPEX), the electricity produced is the same, so the increase of this levelized cost was unavoidable.

Even though there is this decreasing trend, it can be seen that the values are still not enough to be competitive with the production coming from other technologies.

LCOEL [€/kWh]	R123	R245	N-pen
Superheating case	0,79	1,09	1,21
Recuperator case	0,66	0,60	1,02

Table 6. 43: Comparison of the levelized cost of electricity for the three fluids, with and without recuperator

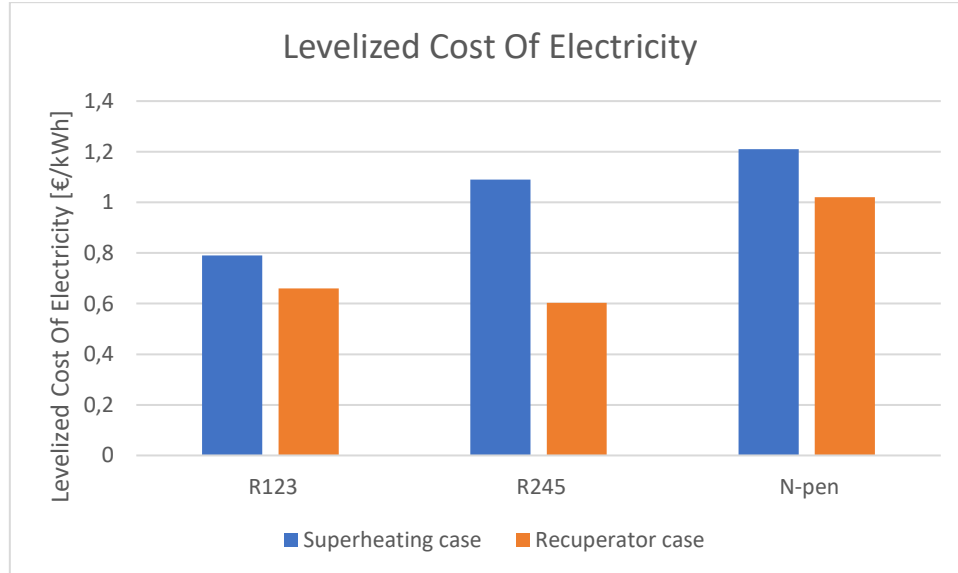


Figure 6.36: Graphic representation of the Comparison of the levelized cost of electricity for the three fluids, with and without recuperator

On the other hand, it can be seen that the Levelized cost of heat increases with the presence of the recuperator. This matter indicates that the CAPEX reduction is not enough to face the reduction of thermal power produced.



LCOH [€/kWh]	R123	R245	N-pen
Superheating case	0,14	0,12	0,12
Recuperator case	0,15	0,15	0,12

Table 6. 44: Comparison of the levelized cost of heat for the three fluids, with and without recuperator

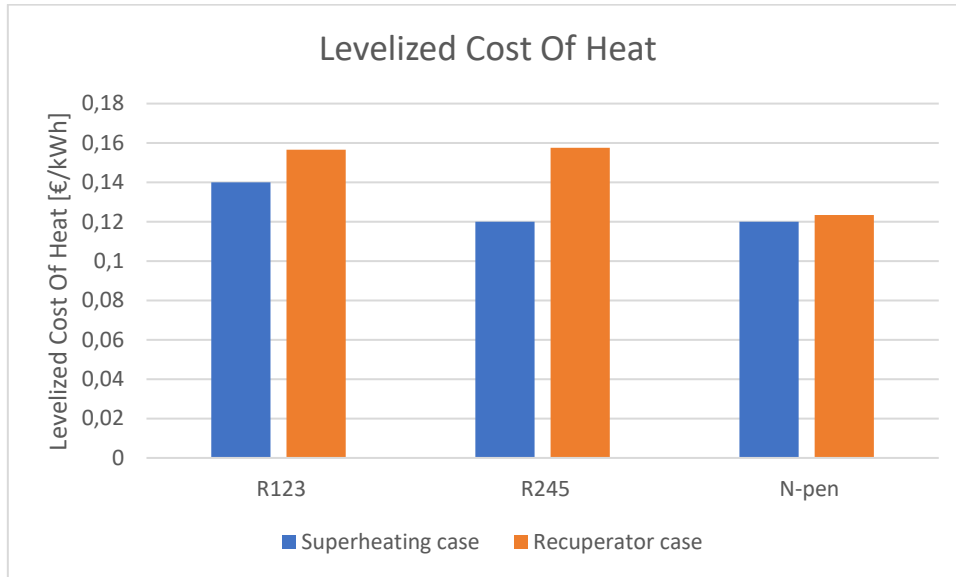


Figure 6.37: Graphic representation of the comparison of the levelized cost of heat for the three fluids, with and without recuperator

To conclude, the levelized cost of energy slightly increases for the R123 and for the R245fa, while there is a slight reduction for the N-pentane

LCOE [€/kWh]	R123	R245	N-pen
Superheating case	0,12	0,11	0,11
Recuperator case	0,13	0,12	0,11

Table 6. 45: Comparison of the levelized cost of energy for the three fluids, with and without recuperator

## Chapter 7: Conclusions

In this thesis, the functioning of an Organic Rankine Cycle feed with the usage of a Solar collector of the type “Parabolic Dish” has been analysed.

From all of the data that have been elaborated, some crucial points can be summed up.

First of all, it has to be said that up to this day, this type of technology is still not ready to be competitive on the market for the production of electricity and heat. In any case, the final net present value is very small if compared to the dimensions of the investment that has to be done, while the payback times arrive usually very late, at some years of distance from the end of life of the plant.

Among all of the fluids that have been considered, the best one has been always the N-pentane, that is an isotropic form of the pentane. This fluid does not have the best thermodynamic performances, but at the end it gives the best results in economic terms.

- If considering a base ORC, from the data taken inside the energy center in Turin, it appears that this technology always gives positive values of Net present value at the end of the life of the plant, but, as previously said, their value is contained. As a proof to that, the values of return of investment are very low, never above 25%

- Then, it can be said that the implementation of the superheating, if coming also with a considerable optimization of the thermal exchange inside the evaporator, is always convenient. The thermodynamic performance of the plant may increase or decrease with respect to the fluids used and their operating conditions, but, in any case the Net present value increases

- Then, it can be said that the implementation of the recuperator along with the superheating can produce contrasting results. The electric production efficiency always increases, due to the lower thermal power requested in the evaporator, while the co-generation efficiency remains always almost constant and at a relatively high value, comparable with other co-generation plants.

Among all of the cases, the best one that has been analysed is the implementation of an ORC with N-pentane as working fluid, and with superheating at 250 °C and with the usage of a heat recuperator. In this case, the thermal efficiency is still relatively low (around 8,5 %), but still higher than the case involving only the superheating at 250 °C. The NPV is not far from 400'000 euros at the end of the life of the plant, and the payback time comes after “only” 23 years, so with more than 1 year with respect to the average of the other results obtained. Moreover, this case also presented the highest value of return on the investment, equal to 25,5%.

In the end, to conclude, by analysing the Levelized costs, some other consideration about the competitiveness of the plant can be deducted

- For what regards the Levelized cost of electricity, it can be said that its values almost never reach the actual values of the market. The reason is probably to attribute at the low temperatures at which the ORC works, that certainly do not help the efficiency and the electricity production. This furtherly means that the ORC, at the working temperatures analysed in this thesis, in order to be economically convenient and competitive it must always work in co-generation and not with the single production of electricity.

To conclude, it can be said that the presence of the superheating can either increase or decrease the value of this levelized cost, while the presence of the recuperator helps partially its decrease, even if this effect is still not sufficient to be taken alone.

- For what regards the Levelized cost of heat, it can be said that its values are always slightly higher than the market prices, even if its difference is much more contained with respect to the ones of the Levelized cost of electricity. This furtherly confirms that, at these working temperatures (lower than 350 °C), the ORC can gain more from the selling of the waste heat with respect to the selling of the electricity produced.

In this case, the presence of the superheating always helps this levelized cost, while the presence of the recuperator negatively influences its values.

- For what regards the Levelized cost of Energy, its values are almost competitive with respect to the market prices. In general, its values can either increase or decrease, depending on the type of fluid and on the operational characteristics chosen for the plant

To conclude, two last observations can be done:

- The presence of economically convenient incentives is essential for the growth of this technology. In this sense, much more effort have to be done for the government in order to make investments in the concentrated solar power technology more convenient.

- All of this study has been conducted by choosing Turin, in Piedmont, as operational base. Certainly, the implementation of a solar power based ORC technology will result more convenient if as working point it is selected a more sunny location, for example the southern Italy, that receives much higher values of solar radiation, or even other countries around the equator line, such as the African countries. Anyway, in these cases other problems related to the very high temperatures of exercise have to be considered.

## Bibliography

- [1] Hannah Ritchie, Max Roser and Pablo Rosado (2022) - "Energy". Published online at OurWorldInData.org. Retrieved from: '<https://ourworldindata.org/energy>' [Online Resource]
- [2] <https://www.terna.it/it/sistema-elettrico/statistiche/pubblicazioni-statistiche>
- [3] [https://www.gse.it/documenti\\_site/Documenti%20GSE/Rapporti%20statistici/Rapporto%20Statistico%20GSE%20-%20FER%202021.pdf](https://www.gse.it/documenti_site/Documenti%20GSE/Rapporti%20statistici/Rapporto%20Statistico%20GSE%20-%20FER%202021.pdf) pp.37
- [4] Islam, Rabiul, ABM Noushad Bhuiyan, and Md Wali Ullah. "An overview of Concentrated Solar Power (CSP) technologies and its opportunities in Bangladesh." *International Conference on Electrical, Computer and Communication Engineering (ECCE) IEEE*, 2017.
- [5] Paul Heller, "The Performance of Concentrated Solar Power (CSP) Systems: Analysis, Measurement and Assessment", Paesi Bassi: *Elsevier Science*, 2017.
- [6] Enescu, Diana & Chicco, Gianfranco & Porumb, Radu & Seritan, George. (2020). Thermal Energy Storage for Grid Applications: Current Status and Emerging Trends. *Energies*. 13. 340. 10.3390/en13020340.
- [7] Ahmed Amine Hachicha, Bashria A.A. Yousef, Zafar Said, Ivette Rodríguez, "A review study on the modeling of high-temperature solar thermal collector systems", *Renewable and Sustainable Energy Reviews*, Volume 112, 2019, Pages 280-298, ISSN 1364-0321, <https://doi.org/10.1016/j.rser.2019.05.056>.
- [8] Matthias Günther, Michael Joemann, Simon Csambor "Advanced CSP teaching materials" Chap.5, pp.13-55, *EnerMENA*
- [9] Analysis and reduction of models using Persalys - Scientific Figure on ResearchGate. Available from: [https://www.researchgate.net/figure/An-example-of-PTSC-Source-Tagle-Salazar-et-al-2020\\_fig1\\_354810878](https://www.researchgate.net/figure/An-example-of-PTSC-Source-Tagle-Salazar-et-al-2020_fig1_354810878)
- [10] Matthias Günther, Michael Joemann, Simon Csambor "Advanced CSP teaching materials" Chap.6, pp.4-21, *EnerMENA*
- [11] Antonio Famiglietti, Antonio Lecuona, "Small-scale linear Fresnel collector using air as heat transfer fluid: Experimental characterization", *Renewable Energy*, Volume 176, pp. 459-474, 2021
- [12] [LF20: Linear Fresnel Solar Collector - Solar Impulse Efficient Solution](#)
- [13] [Solar process heat for paintshops | Article | Automotive Manufacturing Solutions](#)
- [14] Matthias Günther, Michael Joemann, Simon Csambor "Advanced CSP teaching materials" Chap.6, pp.30-36, *EnerMENA*
- [15] Matthias Günther, Michael Joemann, Simon Csambor "Advanced CSP teaching materials" Chap.8, pp.9-70, *EnerMENA*
- [16] <https://medium.com/@allison.df10/concentrating-solar-power-can-improve-the-efficiency-of-solar-energy-3d8fcee20480>
- [17] Analysis and Design of Organic Rankine Cycle based Power Plants (initial draft) - Scientific Figure on ResearchGate. Available from: [https://www.researchgate.net/figure/16-Point-focus-parabolic-mirror-with-Stirling-engine-at-its-focus-Solar-tracker\\_fig10\\_335661943](https://www.researchgate.net/figure/16-Point-focus-parabolic-mirror-with-Stirling-engine-at-its-focus-Solar-tracker_fig10_335661943)
- [18] W. B. Stine, and R. W. Harrigan, "Solar Energy Fundamentals and Design: With Computer Applications". Hoboken, NJ, USA: *Wiley*, 1985.
- [19] B. Hoffschmidt, S. Alexopoulos, C. Rau, J. Sattler, A. Anthrakidis, C. Boura, B. O'Connor, R.A. Chico Caminos, C. Rendón, P. Hilger, "Comprehensive Renewable Energy" (Second Edition), *Elsevier*, Vol.3, pp.670-724, 2022.

- [20] Pye e M. Simonetti, Dispense per il corso di "Technology for renewables energy sources" - Politecnico di Torino.
- [21] B. Hoffschmidt, S. Alexopoulos, C. Rau, J. Sattler, A. Anthrakidis, C. Boura, B. O'Connor, R.A. Chico Caminos, C. Rendón, P. Hilger, 3.18 - Concentrating Solar Power, Editor(s): Trevor M. Letcher, *Comprehensive Renewable Energy (Second Edition)*, Elsevier, 2022, Pages 670-724, ISBN 9780128197349
- [22] BIERMAYR, Peter. "Potential of Solar Thermal in Europe", *Studie im Auftrag der European Solar Thermal Industry Federation ESTIF*", AEE–Institute for Sustainable Technologies, Vienna University of Technology, Brüssel, 2009.
- [23] Veera Gnanaswar Gude, "Renewable Energy Powered Desalination Handbook", *Butterworth-Heinemann*, Chap.4, pp.141-176, 2018
- [24] S. Kalogirou, "Seawater desalination using renewable energy sources", *Progress in Energy and Combustion Science*, Vol.31, pp. 242-281, 2005.
- [25] AQUA-CSP concentrating solar power for desalination. *Final Report by German Aerospace Center (DLR)*. Stuttgart, Germany, November 2007.
- [26] Alexopoulos, S., Hoffschmidt, B. (2022). Concentrating Receiver Systems (Solar Power Tower). In: Alexopoulos, S., Kalogirou, S.A. (eds) *Solar Thermal Energy. Encyclopedia of Sustainability Science and Technology Series*. Springer, New York, NY. [https://doi.org/10.1007/978-1-0716-1422-8\\_677](https://doi.org/10.1007/978-1-0716-1422-8_677)
- [27] S. Alexopoulos, B. Hoffschmidt, "Solar tower power plant in Germany and future perspectives of the development of the technology in Greece and Cyprus", *Renewable Energy*, Vol.35 (7), pp. 1352-1356, 2009.
- [28] I.P. Jain, "Hydrogen the fuel for 21st century", *International Journal of Hydrogen Energy*, Vol. 34, pp. 7368-7378, 2009.
- [29] A. Giaconia, "Advances in hydrogen production, storage and distribution", *Woodhead Publishing*, pp.263-280, 2014
- [30] <https://diren.mines-paristech.fr/Sites/Thopt/en/co/centrales-vapeur.html>
- [31] Alhwayzee, Mohammed & Jawad Kadhim, Hayder & Rashid, Farhan. (2021). Aspen Plus Simulation for Performance Improving of Al-Khayrat Power Plant Using Heat Recovery Steam Generation (HRSG) System. *Journal of Mechanical Engineering Research and Developments*. 44. 400-411.
- [32] Brahim Dincer, Yusuf Bicer, "Integrated Energy Systems for Multigeneration", *Elsevier*, Chap.4, pp.143-146, 2020.
- [33] <https://www.slideshare.net/hashimhasnainhadi/ideal-rankine-cycle>
- [34] Brahim Dincer, Yusuf Bicer, "Integrated Energy Systems for Multigeneration", *Elsevier*, Chap.4, pp.147-148, 2020.
- [35] Ennio Macchi, Marco Astolfi, "Organic Rankine Cycle (ORC) Power Systems: Technologies and Applications", *Elsevier*, pp.6, 2016.
- [36] Li, G. Organic Rankine cycle environmental impact investigation under various working fluids and heat domains concerning refrigerant leakage rates. *Int. J. Environ. Sci. Technol.* **16**, 431–450 (2019). <https://doi.org/10.1007/s13762-018-1686-y>
- [37] Ennio Macchi, Marco Astolfi, "Organic Rankine Cycle (ORC) Power Systems: Technologies and Applications", *Elsevier*, pp.6-16, 2016

- [38] Xiaojun Zhang, Lijun Wu, Xiaoliu Wang, Guidong Ju, Comparative study of waste heat steam SRC, ORC and S-ORC power generation systems in medium-low temperature, *Applied Thermal Engineering*, Vol. 106, pp.1427-1439, 2016.
- [39] A. Corsini, "Cicli Rankine a fluido Organico", Aerospace and mechanical engineering department, university "La Sapienza". Source free available online: [http://www.ingmecc.uniroma1.it/attachments/2300\\_Lez%20SE%20ORC.pdf](http://www.ingmecc.uniroma1.it/attachments/2300_Lez%20SE%20ORC.pdf)
- [40] A. Hromádka and Z. Martínek, "Overview of the organic Rankine cycles and their current utilization: Verification of several current ORCs utilization by the software Dymola," *2017 18th International Scientific Conference on Electric Power Engineering (EPE)*, Kouty nad Desnou, Czech Republic, 2017, pp. 1-6, doi: 10.1109/EPE.2017.7967272.
- [41] Capata, Roberto & Toro, Claudia. (2014). Small-Scale ORC Energy Recovery System for Wasted Heat: Thermodynamic Feasibility Analysis and Preliminary Expander Design. 10.3390/ece-1-b001.
- [42] A. Fakeye Babatunde and O. Oyedepo Sunday 2018 IOP Conf. Ser.: Mater. Sci. Eng. 413 012019
- [43] Henrik Ö & Per L, "Comparison and analysis of performance using Low Temperature Power Cycles", *Applied Thermal Engineering*, Vol.52, pp.160-169, 2013.
- [44] "Cicli ORC- Energetica applicata" [Online]: [https://elearn.ing.unipi.it/pluginfile.php/96784/mod\\_resource/content/1/ORC.pdf](https://elearn.ing.unipi.it/pluginfile.php/96784/mod_resource/content/1/ORC.pdf).
- [45] F.Alshammari, M. Usman and A. Pesyridis, Expanders for Organic Rankine Cycle Technology. Organic Rankine Cycle Technology for Heat Recovery, InTech, 2018. Available at: <http://dx.doi.org/10.5772/intechopen.78720>.
- [46] Luo, X.; Wang, J.; Krupke, C.; Xu, H. Feasibility Study of a Scroll Expander for Recycling Low-Pressure Exhaust Gas Energy from a Vehicle Gasoline Engine System. *Energies* **2016**, *9*, 231. <https://doi.org/10.3390/en9040231>
- [47] Cryogenics for Particle Accelerators and Detectors - Scientific Figure on ResearchGate. Available from: [https://www.researchgate.net/figure/Schematic-view-of-a-piston-expander\\_fig10\\_44216049](https://www.researchgate.net/figure/Schematic-view-of-a-piston-expander_fig10_44216049) [accessed 13 Feb, 2024]
- [48] Gang Li, Organic Rankine cycle performance evaluation and thermoeconomic assessment with various applications part I: Energy and exergy performance evaluation, *Renewable and Sustainable Energy Reviews*, Volume 53, 2016, Pages 477-499, ISSN 1364-0321.
- [49] E. Chiavazzo, Dispense per il corso di "Energy Storage" - Politecnico di Torino.
- [50] <https://blog.sintef.com/sintefenergy/thermochemical-energy-storage-the-next-generation-thermal-batteries/>
- [51] Multifunctional structural composites for thermal energy storage - Scientific Figure on ResearchGate. Available from: [https://www.researchgate.net/figure/Comparison-of-specific-energy-storage-density-values-of-different-sensible-latent-and\\_fig2\\_346205001](https://www.researchgate.net/figure/Comparison-of-specific-energy-storage-density-values-of-different-sensible-latent-and_fig2_346205001) [accessed 13 Feb, 2024]
- [52] E. Montà, «Realizzazione di processi di chemical looping e produzione di gas sintetico mediante solare termico a concentrazione,» 2020.
- [53] Abrar Sobhan Chowdhury, M Monjurul Ehsan, A Critical Overview of Working Fluids in Organic Rankine, Supercritical Rankine, and Supercritical Brayton Cycles Under Various Heat Grade Sources, *International Journal of Thermofluids*, Vol.20, 2023.

- [54] <https://www.freon.cn/-/media/files/freon/freon-123pushbulletin.pdf?rev=b5fb1eba89d946d898997fea881b03b2>
- [55] [http://www.frigoristes.fr/static/telechargement/abaques/diagramme\\_enthalpiqueR123.pdf](http://www.frigoristes.fr/static/telechargement/abaques/diagramme_enthalpiqueR123.pdf)
- [56] “NETL-National Energy Technology Laboratory”. Available: [https://netl.doe.gov/projects/files/QGESSCostEstMethodforNETLAssessmentsofPowerPlantPerformance\\_090119.pdf](https://netl.doe.gov/projects/files/QGESSCostEstMethodforNETLAssessmentsofPowerPlantPerformance_090119.pdf)
- [57] R. Turton, S. J. A., B. Debangsu e W. W. B, “Analysis, synthesis, and design of chemical processes”, Pearson Education, 2018
- [58] Song Jian, Loo Ping, Teo Jaime, Markides Christos N, “Thermo-Economic Optimization of Organic Rankine Cycle (ORC) Systems for Geothermal Power Generation: A Comparative Study of System Configurations”, *Frontiers in Energy Research*, Vol.8, 2020.
- [59] <https://mercati.ilsole24ore.com/strumenti/converti-valute>
- [60] <https://www.ri-esco.it/cogenerazione-incentivi-previsti/>
- [61] Dai, X.-Y & An, Qingsong & Shi, L, “Experiment research for the thermal stability of isobutene and isopentane”, *Kung Cheng Je Wu Li Hsueh Pao/Journal of Engineering Thermophysics.*, Vol.34, pp. 1416-1419, 2013.
- [62] [ICSC 0534 - n-PENTANE \(ilo.org\)](https://www.ilo.org/publications/2023/Aug/Renewable-Power-Generation-Costs-in-2022)
- [63] <https://www.irena.org/Publications/2023/Aug/Renewable-Power-Generation-Costs-in-2022>
- [64] <https://www.ipcc.ch/site/assets/uploads/2018/03/Annex-III-Recent-Renewable-Energy-Cost-and-Performance-Parameters-1.pdf>